



Dynamic Control of Light Direction Enabled by Stimuli-Responsive Liquid Crystal Gratings

Rafael S. Zola, Hari Krishna Bisoyi, Hao Wang, Augustine M. Urbas, Timothy J. Bunning, and Quan Li*

The ability to control light direction with tailored precision via facile means is long-desired in science and industry. With the advances in optics, a periodic structure called diffraction grating gains prominence and renders a more flexible control over light propagation when compared to prisms. Today, diffraction gratings are common components in wavelength division multiplexing devices, monochromators, lasers, spectrometers, media storage, beam steering, and many other applications. Next-generation optical devices, however, demand nonmechanical, full and remote control, besides generating higher than 1D diffraction patterns with as few optical elements as possible. Liquid crystals (LCs) are great candidates for light control since they can form various patterns under different stimuli, including periodic structures capable of behaving as diffraction gratings. The characteristics of such gratings depend on several physical properties of the LCs such as film thickness, periodicity, and molecular orientation, all resulting from the internal constraints of the sample, and all of these are easily controllable. In this review, the authors summarize the research and development on stimuli-controllable diffraction gratings and beam steering using LCs as the active optical materials. Dynamic gratings fabricated by applying external field forces or surface treatments and made of chiral and nonchiral LCs with and without polymer networks are described. LC gratings capable of switching under external stimuli such as light, electric and magnetic fields, heat, and chemical composition are discussed. The focus is on the materials, designs, applications, and future prospects of diffraction gratings using LC materials as active layers.

the duality consolidation, the idea of controlling light and how it interacts with matter has always been an exciting topic. Visible light, as we perceive it, is a small portion of the electromagnetic spectrum composed of mutually perpendicular oscillating electric and magnetic fields that propagate through space and presents wave-like and particle-like behavior. Since the elements comprising matter possess dynamic electron clouds, the electromagnetic nature of light prompts different responses when it interacts with different materials, depending on its intensity, frequency, the arrangement of molecules, and so on. Whenever light interacts with matter, it might be absorbed, re-emitted, scattered, or transmitted. Although these effects are well known, the combination of them with new, innovative materials pushes optics forward. In fact, advances in optics have often occurred through the development of materials with improved optical properties, thus creating remarkable applications that tremendously influence our daily lives. These exciting applications include image processing and recording, lasing, data storage, display devices, detector systems, propulsion systems, and optical tweezers, which have enabled remote micromanipulation of colloidal particles and promising applications in various biomedical and biological

applications.^[1–3] There is, however, one component that stands out: the diffraction grating. It is generally regarded as one of the most important devices in the development of several fields of science.^[4] Such importance comes from the fact that a diffraction grating is a device with a periodic structure capable of changing the propagation and splitting the spectrum

1. Introduction

The development of optics has occurred through centuries of studies on the basic properties of light and how it interacts with matter. From the initial assertions of modern science that light could be comprised either of particles (rays) or waves to

Prof. R. S. Zola, Dr. H. K. Bisoyi, H. Wang, Prof. Q. Li
Liquid Crystal Institute and Chemical Physics Interdisciplinary Program
Kent State University
OH 44242, USA
E-mail: ql1@kent.edu

The ORCID identification number(s) for the author(s) of this article can be found under <https://doi.org/10.1002/adma.201806172>.

DOI: 10.1002/adma.201806172

Prof. R. S. Zola
Departamento de Física
Universidade Tecnológica Federal do Paraná
Rua Marclio Dias, 635, 86812-460 Apucarana, Paraná, Brazil
Dr. A. M. Urbas, Dr. T. J. Bunning
Materials and Manufacturing Directorate
Air Force Research Laboratory
Wright-Patterson AFB
OH 45433, USA

of light. Among the many applications, spectroscopy enabled by diffraction gratings is used in chemistry to determine the presence and concentration of a certain species in a sample; in astrophysics as a way to determine the presence of certain elements in planets, stars, and other objects in the universe; and in telecommunications to increase the capacity of optical fibers.^[5] Nonetheless, modern applications demand for controllable gratings that can be readily and facilely tuned by external stimuli drives further innovation. Such devices should be robust to work under diverse conditions, capable of operating in the mesoscale, diffract in more than one dimension, and, most importantly, have as few components as possible. To this end, liquid crystals (LCs) have arisen as potential candidates to serve as diffraction gratings. LCs are structured dynamic soft materials that can be controlled by several external stimuli and they assume several different textures depending on their geometric confinement condition and applied external stimuli. Furthermore, LCs are birefringent, meaning there are multiple distinct refractive indices associated with the medium and different propagation directions and polarizations within, so light can exhibit the so-called double refraction phenomenon, in which light is split into two rays, traveling at different speeds. These properties and indices can be controlled in direction and magnitude by external stimuli resulting in dynamic optical properties such as switchable birefringence. As a result, LCs might be thought of as light valves. Such remarkable property of LCs enables their use in a plethora of display and nondisplay applications including electro-optical devices, optics, and photonics. The remarkable optical characteristics of LCs qualify them as great candidates for employment as diffraction gratings.

In this review, we summarize the research and development on controllable diffraction gratings and beam steering by using LC materials as the active optical layers and directed by different stimuli. We review ways of fabricating diffraction gratings with different chiral and achiral LCs. We focus our discussion on the design principles and characteristics of the LC gratings.

2. Fundamentals

2.1. Diffraction Gratings

In science and engineering, ways of steering and separating light's wavelengths have long been pursued and accomplished. The first well-documented study about optics is attributed to Isaac Newton, whose main discovery was that light could be separated into, what he called, "an infinite number" of colors as it passes through a prism.^[4] This fascinating phenomenon is known as dispersion, and it arises because light of different wavelengths exhibits distinct refraction angles while propagating through a prism. Another way of splitting light has also been discovered in 1785 by the astronomer David Rittenhouse, who built a simple version of what is now known as diffraction grating after the observation from Francis Hopkinson that light from a lamp passing through a fine French silk handkerchief produces multiple images.^[6] Rittenhouse quickly figured out that the observed effect was due to diffraction of light, a phenomenon associated with electromagnetic waves scattering from obstacles creating multiple scattered waves interfering



Rafael S. Zola received his B.S. and M.S. degrees in physics from Maringá University, Brazil, in 2006 and 2007, respectively. In 2012, he obtained his Ph.D. degree from Kent State University, at the Liquid Crystal Institute, USA. He is currently a professor in the Physics Department of the Federal University of Technology-Paraná, Brazil. His current research interests are the physics of liquid crystals, surfaces and interfaces, diffusion process, and photodriven liquid crystal materials/process.



Hari Krishna Bisoyi is a Research Associate in the group of Professor Quan Li at the Liquid Crystal Institute of Kent State University. He obtained his B.Sc. Honors (2001) and M.Sc. (2003) in Chemistry from Berhampur University, Odisha. Subsequently, he received his Ph.D. degree (2010) from Jawaharlal Nehru University, India, working at the Raman Research Institute, Bangalore, under the guidance of Professor Sandeep Kumar. His current research interests include chiral liquid crystals, supramolecular liquid crystals, liquid crystal nanoscience, and stimuli-responsive soft materials.



Hao Wang is a Ph.D. student in the group of Professor Quan Li at the Liquid Crystal Institute of Kent State University. He obtained his B.Sc. degree (2011) from the Department of Macromolecular Materials and Engineering, Beijing University of Chemical Technology, China. His research mainly focuses on soft matter, light-driven chiral molecular switches or motors, functional halogen-bonded materials, as well as their emerging applications in diverse fields ranging from dynamic photonics to energy.

with themselves.^[7] In 1803, Thomas Young noticed that red light passing through a grating could be observed along four different directions.^[8] However, it was Joseph von Fraunhofer who got credit for fabricating the first diffraction grating with high accuracy after developing the ruling engine and investigating its properties. With his great devotion to optical elements and the

grating itself, Fraunhofer accurately measured the absorption lines in the solar spectrum, now known as the Fraunhofer lines,^[9] and compared them to other stars, thus giving birth to stellar spectroscopy.^[4] Nobert and Rutherford pushed the fabrication and development of diffraction gratings further forward, with better fabrication methods and precision. It was H. A. Rowland however who became the father of modern spectroscopy by establishing the diffraction grating as the primary optical element in spectrophotometers. Rowland's success in fabricating gratings as large as 7.5 in. essentially supplied gratings for the scientific community for nearly 50 years.^[10]

Nowadays, diffraction gratings are fabricated using various sophisticated methods including interference lithography and are widely used in several fields across science and engineering. In a few words, a diffraction grating is a set of periodically disposed elements separated by a distance comparable to the wavelength of light. Such periodic disposition might be, for example, a distribution of thin glass lines separated by air, thus causing the refractive index to change across the "grooves." It can either reflect or transmit light, depending on the desired application, that is, it can act as a set of slits or a set of reflection grooves where each feature acts as a diffracting element. Diffraction gratings have been classified based on many different criteria. They can be phase, amplitude, phase relief, holographic, lithographic, ruled, transmission or reflection, blazed, and so on. Such a long list of classifications is in part due to historic reasons. Other classification schemes of diffraction gratings are based either on the way they operate, their structural features, or how they are fabricated.^[4] For example, phase gratings, where refractive index varies in space, are supposed to modulate the phase of light whereas amplitude gratings should modulate amplitude only. For amplitude diffraction gratings, a binary structure with alternate low and high transmission of incident light enables a regular amplitude modulation, thus appearing light diffraction. The most important fact about phase diffraction gratings is that the refractive index is regularly modulated, thus causing light with a given wavelength to be reflected (or transmitted) only along certain directions. Both phase and amplitude gratings can be fabricated by holography, lithography, or ruled (mechanically written by a diamond pen on a solid substrate) technique and can operate by reflecting (if the background is a metal for example) or transmitting light (transparent background). Based on their structural features, gratings can be classified as surface relief grating (where a surface relief structure separates two media of different refractive index), symmetrical grating (the grooves are symmetric, so equal efficiencies are delivered into the symmetrical orders), or blazed gratings (the groove has a triangular shape, so the diffraction efficiency is maximized for a certain diffraction order). An important parameter to characterize the performance of a diffraction grating is the diffraction efficiency, which is a measure of how much power is diffracted in a certain direction when compared to the input power. In general, most of the gratings are produced either by the ruling process, which results in higher diffraction efficiency due to their blaze angle or holographic gratings, in which a photoresist is exposed to interfering laser beams to create the grating-like pattern. The holographic gratings, usually, have smaller errors leading to higher diffraction efficiency and reduced scattered light.

The classification of gratings into Bragg type and Raman–Nath type is an important but subjective distinction and is directly relevant to the discussions in this review article. In a Bragg-type grating, only a few orders can propagate, which are usually associated with the so-called thick or volume gratings.^[4,11] Usually, Bragg-type gratings are fabricated to have relatively weak periodic variation of the refractive index and extended thickness, so it reflects light in a certain wavelength (bandgap) that satisfies the Bragg condition, $\lambda = 2\Lambda n \cos \theta$, where λ is the reflected wavelength, n is the average refractive index, Λ is the grating periodicity, and θ is the angle of propagation direction relative to the grating's normal. Other wavelengths are, in general, weakly affected by the grating. Bragg-type gratings can be applied as couplers for laser diodes, in optical fibers (to reflect light in the fibers or for mode coupling in multimode fibers), for data storage and many others. Raman–Nath-type gratings have a stronger periodic variation of index and yield, in general, several diffracted orders. This type is often referred to as a thin grating.^[11] LC phases can be used to obtain both Bragg-type and Raman–Nath-type diffraction gratings. In this review, our primary focus is on the Raman–Nath kind, although a few examples of the Bragg grating are explored, e.g., Bragg diffractions in chiral LCs.^[12,13]

Figure 1 depicts the general principle behind a diffraction grating. When a ray of white light (Figure 1A) strikes on a grating with groove spacing d and making an angle θ_i with the grating normal, it is successively diffracted by the grooves at angles θ_m . The remarkable feature of the diffraction grating is that each diffracted ray will suffer constructive interference only when the geometrical difference traveled by each diffracted ray is an integer multiple of the wavelength of light. Thus, for a given wavelength of light and a grating with period d , there is a unique set of angles at which the diffracted orders can be seen. In a reflective grating, the so-called zeroth order means the specular reflection whereas the other orders are a result of the diffracted light by the grooves. In a Raman–Nath transmissive grating, the zeroth order represents the refracted beam. From simple geometrical considerations, one can easily determine the relationship between the incident angle, the diffracted angles (for each order, with $m = 0, \pm 1, \pm 2, \pm 3, \dots$), the groove spacing, and the wavelength of light as $\sin \theta_i \pm \sin \theta_m = m\lambda/d$. This equation indicates that each wavelength of a polychromatic light is diffracted at a different angle within a diffraction order which results in dispersion of light. Other interesting aspect of this equation is that longer wavelengths (such as red) diffract at higher angles than shorter wavelengths (such as blue), thus the resulting dispersion pattern exhibits reverse wavelength distribution compared to light dispersion by prisms. In other words, the dispersion order of light wavelengths upon passing through a diffraction grating is opposite to that observed through a prism. This dispersive aspect of diffraction gratings is the key to their utility since atoms and molecules have unique spectra associated with their emission, thus precisely separating the wavelengths from a certain sample allows the detection, identification, and quantification of elements present in a material. Furthermore, gratings can be used for beam steering (light deflection from its original transmission path), depending on the desired applications. Figure 1B shows an illustration of a monochromatic ray incident on an amplitude grating. The black arrow shows the so-called grating

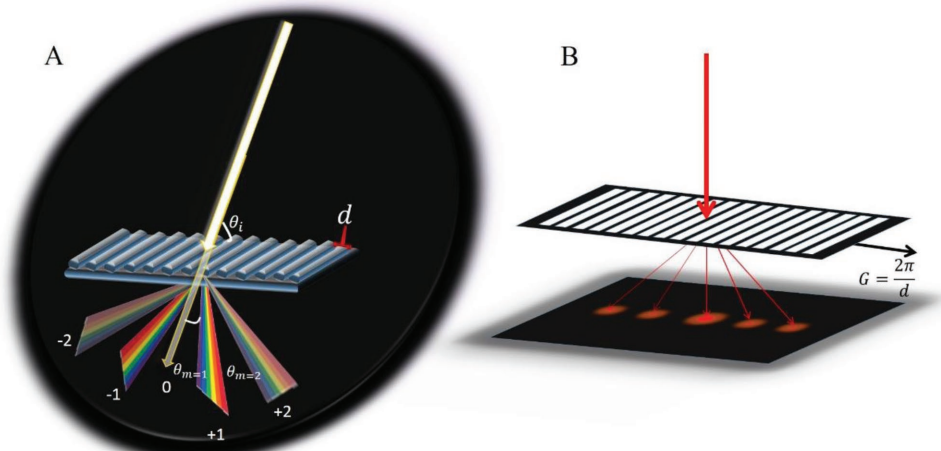


Figure 1. Illustration of a typical transmission, phase diffraction grating causing the A) diffraction and dispersion of incident white light and B) diffraction of monochromatic incident light on an amplitude grating. The black arrow in (B) represents the grating vector.

vector, given by $G = 2\pi/d$. The grating vector is a very important quantity in the context of this article since in the switchable LC gratings either the amplitude or the direction (or both) of G can be changed. If only amplitude is changed, the diffracted pattern lies on the same line before and after being switched, but since the spacing d changes, the diffraction angle of light changes. When the direction of G changes, i.e., the grating vector reorients, the whole diffracted pattern will exhibit in-plane rotation or even direction switching. As we shall see here, both changes are desired in LC gratings.^[14]

The structures that cause light diffraction occur in several places in nature.^[15–21] Indeed, grating-like structures (periodic structures) are very common in nature, such as the periodicity of gene segments in biological body which leads to the

diversity of biology; distribution periodicity of energy band determines the transportation of electrons and thereby influences the conductivity and dielectricity of the materials. Similarly, as a periodic modulation of light amplitude or the phase is generated, a specific propagation of photons appears, i.e., diffraction. A few general examples of such periodic arrangements that are found in nature are shown in **Figure 2**. The Bobtail Squid (*Euprymna scolopes*) is a versatile cephalopod with a unique ability to control their coloration and their glow and adjusting themselves with the brightness of the moonlight. Recently, it was discovered that their tissues are composed of an abundance of an unusual protein called reflectin, which assembles in a periodic fashion, thus acting as a diffraction grating.^[15] Another well-known example of naturally

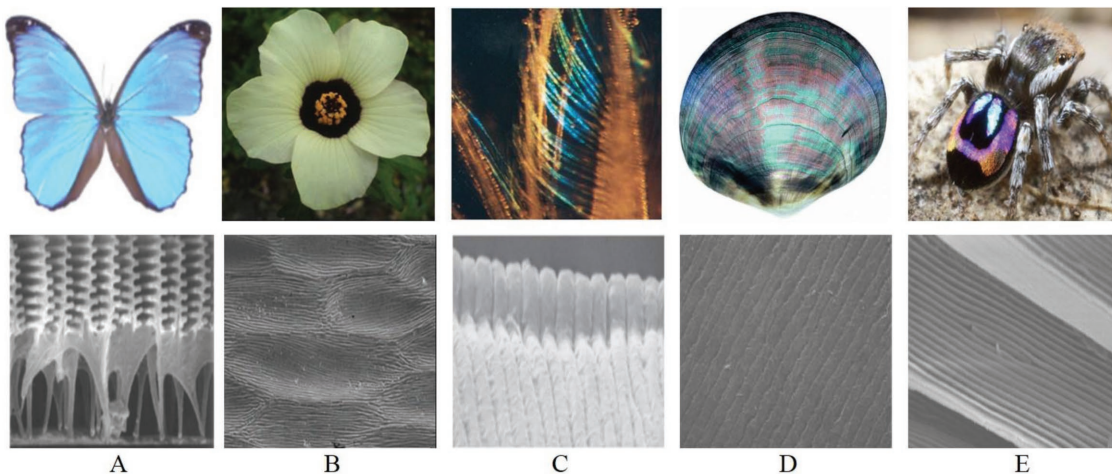


Figure 2. Examples of natural diffraction gratings. A) Photograph of a morpho butterfly and the scanning electron microscope (SEM) image of its wing. Adapted with permission.^[17] Copyright 2008, American Physical Society. B) Photograph of a *Hibiscus trionum* flower and SEM image corresponding to its pigmented epidermis. Adapted with permission.^[18] Copyright 2009, American Association for the Advancement of Science. C) The first antenna of the seed-shrimp (ostracod crustacean) *Azygocypridina lowryi* and SEM of the diffraction grating found in the hair of the seed-shrimp. Adapted with permission.^[19] Copyright 2004, The Royal Society of Chemistry. D) The iridescence color of a polished shell of the mollusk *Pinctada margaritifera* from the Tuamotu Archipelago of French Polynesia and the reflecting grating structure of the shell as observed by SEM. Adapted with permission.^[20] Copyright 1999, Optical Society of America. E) A miniature peacock spider *Maratus robinsoni* with rainbow iridescence and SEM of its iridescent scales. Adapted with permission.^[21] Copyright 2017, Springer Nature.

occurring grating is striated muscle.^[16] The *morpho* butterflies possess equidistant ridges whose space acts as diffraction gratings, conferring them beautiful colors (Figure 2A).^[17] Some of the other naturally occurring diffraction gratings in plants, sea creatures, and insects are shown in Figure 2B–E.^[18–21]

In our daily life, diffraction gratings are encountered in compact disks, which are made of grooved-like substrates that are “burned,” i.e., laser written in a specific sector to store information.^[22]

Modern technology demands highly accurate equipment at the lowest possible cost. An example applied to our context is the use of laser light for fast sampling of the environment, or, for light detection and ranging, which can be used in a rover exploring a planet or even for assisting drivers to overcome safety issues. For accomplishing

this, the device has to steer the direction of light. It is required that the steering device (the grating) is small and low cost. There has been an intense effort toward developing such devices, with silicon photonic chips capable of 1D and 2D steering.^[23–26] Recently, a remarkable, fully integrated 2D steerable laser chip was developed.^[26] However, in order to produce such result, it needs 164 components. Although it is a breakthrough, it is rather complicated to fabricate. So, it is highly desirable to obtain reversible wide-range 2D beam steering and spectrum scanning in a simple and efficient way.

A possible candidate to simplify the aforementioned light steering device would be using LC gratings, especially in situations where less space is available and some degree of tunability is required. Indeed, LCs are remarkable materials that have found many applications beyond display devices,^[27] such as in optics and photonics,^[28] biophysics,^[29] nanoscience,^[30–33] and in many other domains.^[34–36] In the next section, we introduce some of the basics of LCs and how they can be made into a diffraction grating.

2.2. Liquid Crystals

LCs are intermediate phases (also referred to as mesophases) occurring between the ordered solid crystal and the disordered isotropic liquid. They are classified according to the way they transit from one phase to the other: by varying the concentration of amphiphilic molecules in a solvent, they are called lyotropic LCs, where the molecules self-assemble into molecular aggregates such as micelles. Lyotropics are particularly important for biological applications.^[37] If, on the other hand, the phase transition occurs by variations of temperature, they are called thermotropic LCs, generally composed of organic molecules with anisometric shapes such as cylinders (calamitic), discs (discotic), or banana shaped (bent cores).^[38] Due to the anisometric shape of the molecules, thermotropic LC materials organize themselves in such a way that orientational order and, in some cases, short-range positional order

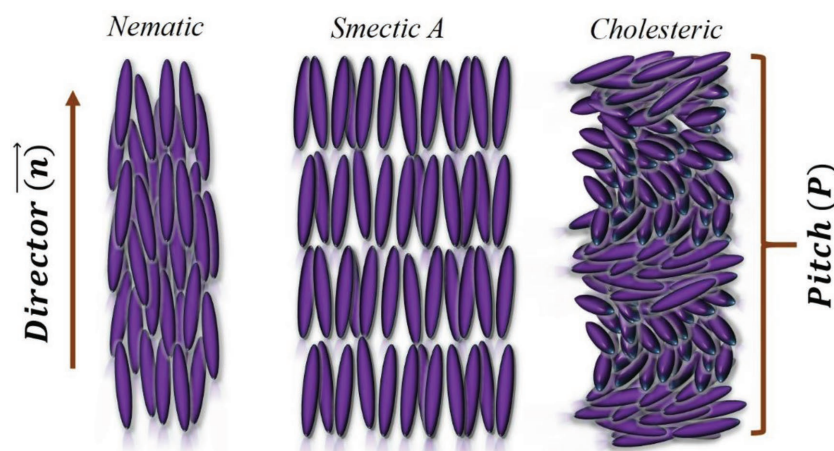


Figure 3. Schematic representations of molecular organizations in common LC phases. From left to right, nematic, smectic A, and cholesteric LC phase. The arrow on the left side indicates the average direction of the molecules, represented by the director \vec{n} . On the right-hand side, the pitch (distance to complete a 360° rotation) of the cholesteric phase is depicted.

are present. When temperature is raised, the process of losing order (from the solid crystal) usually occurs through one or more mesophases, classified according to their symmetry. In some materials, as the solid is heated, the positional order is partially lost by forming smectic (Sm) LCs. They are organized in layers where at least 1D positional order exists. The most common is the smectic A (SmA) LC, having 1D positional ordering of layers but molecules do not possess any positional ordering within the layers.^[38]

If the material is further heated, the positional order is completely lost and only orientational order of the molecules, represented by a vector called director \mathbf{n} , remains and a nematic phase results. Therefore, in the nematic LC phase, the constituent molecules possess only orientational ordering. The nematic LC can be made chiral by adding a small amount of a chiral dopant which results in a cholesteric LC (CLC) phase. CLCs are essentially nematics but possess a self-organized helical superstructure where the director rotates, completing a 360° rotation along a length called pitch (P). **Figure 3** illustrates the molecular organizations in the three most common LC phases, i.e., nematic, smectic A, and cholesteric phases. The peculiar shape of the constituent molecules exhibiting LCs confers them with anisotropies in every physical property, such as electrical and optical, besides presenting elastic responses to any stress that disturbs the order. The strong anisotropies, elastic response, and lack of symmetry of LCs yield certain characteristic textures to each LC phase. They also limit the number of ways the molecules can organize, and, therefore, the material presents a number of patterns that can be formed under several stimuli and constraints.^[39,40] Interestingly, these patterns can be driven in such a way that an LC cell can be turned into a diffraction grating. For example, a CLC under an applied electric field may assume a configuration called lying helix, in which the helix (heretofore characterized by a direction named helical axis) lies on the plane of the limiting substrate surface. Since the CLC is a periodic structure with periodic variation of refractive indices, in this situation it resembles a diffraction grating. In fact, if the pitch length is about the wavelength of light, it

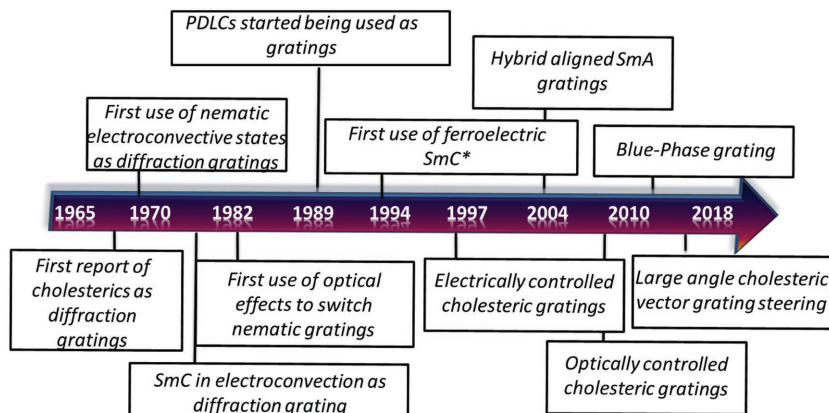


Figure 4. A timeline showing the evolution and important discoveries in the LC diffraction grating field. Although the first report appears to be for a CLC, the initial uses focused primarily on the nematic LC including polymer-dispersed LC gratings. A few examples were reported for the smectic C phase before 1980 but most of the applications of smectics did not occur until the 1994 with the chiral smectic C phase. The first report of electrically controlled CLCs occurred only in 1997 while blue phase LC gratings did not occur until a few years ago. In the recent years, several works using CLCs have reported wide-angle nonmechanical beam steering in one and two dimensions as well as stimuli-directed orthogonal switching of the grating vector.

can be used for such purpose. However, the CLC is just one example of diffraction grating. Indeed, LCs have been used as diffraction gratings in several applications for nearly 50 years, but very condensed and specific accounts covering very limited aspects have been published to date. **Figure 4** shows a timeline depicting the chronological order of the main discoveries (and when each LC phase started being used) of LC gratings. In the following sections, nematic, smectic, cholesteric, and the beautiful blue phase (BP) LCs are explored and their many facets in the application as diffraction gratings are presented.

3. LCs as Diffraction Gratings

3.1. Nematic LCs

3.1.1. Surface Template and Electric Field–Driven Gratings

Nematic phase is, as previously stated, the simplest kind of LC phase. For this reason, many of the development made in the LC field involves nematic LCs first. It is also the case with the LC gratings. One of the first evidences that LCs could be used as gratings arose when it was discovered that a low-frequency electric field applied to some nematic LCs (with the correct dielectric and conductivity anisotropies) could present distinct hydrodynamic instabilities in which the material organizes itself as a periodic lattice of domains (or stripes).^[41–43] It is difficult to pin point the very first work that studied nematic LCs as gratings since several of them did not focus on the diffractive characteristics. Nevertheless, researchers started paying attention to it by the end of the 1960s. The existence of diffraction was first mentioned during scattering studies of nematics in hydrodynamic motion.^[44] In 1970, Lu and Jones reported on the diffraction patterns that were observed when a 25 µm thick, planar oriented *N*-(4-methoxybenzylidene)-4-butylaniline (MBBA) sample was subjected to a 60 Hz frequency.^[45]

Several different patterns were found as the field amplitude was swept from 36 to 90 V, passing through what is today known as Williams domains and Chevrons.^[46] **Figure 5A** shows some of these patterns that evolve from simple diffraction spots to more complicated patterns as the voltage is increased. At 36 V, they observed the well-known Williams domains, a series of convective rows that yield a grating pattern and under monochromatic illumination results in a pattern of intensity maxima, from which the grating periodicity was calculated, matching the distances measured under polarized optical microscope (POM). As the voltage was increased, passing through Chevron domains, the well-defined spots of diffraction pattern gradually turned into a herringbone-shaped pattern, as a result of the loss of alignment of the grating. They also discovered that the diffraction occurs only if the light beam is polarized perpendicularly to the rubbing direction of the sample. A 2D pattern was measured in the field range where the striped pattern starts to change to a dynamic scattering mode (DSM), proving that the domains are not randomly distributed but instead organized in a rectangular shape.^[47] Through optimizing cell design, high diffraction efficiency was achieved.^[48] Carroll was the first to identify and name the hydrodynamic pattern as a diffraction grating.^[49] He also observed that diffraction patterns would change the intensity maximum distances upon change in voltage and frequency, which can be associated with the change in the diffraction order that these two parameters cause. A mathematical model is also provided for predicting the diffraction intensities.^[49] Later, new features at the onset of instabilities (Williams and Chevron) were discovered,^[50] corresponding to contributions to the diffraction pattern at half of the expected grating periodicity, which was associated with the nonorthogonal traversals of the phase grating. Therefore, there is a contribution to the diffracted pattern with periodicity Λ associated with the uniaxial characteristic of the medium and a contribution with spatial frequency $\Lambda/2$ caused by variation in birefringence. Similar results were later reported by inducing instabilities in nematics by repeated shear flow.^[51] In a few years, the observed diffraction patterns ceased to be seen exclusively in negative dielectric materials^[52] and the diffraction patterns began to be used as a way of characterizing the instabilities.^[53] Instabilities patterns arising in bent-core nematic LCs have been described and explored for its use as gratings. The diffraction patterns were used as ways of characterizing, among others, instabilities called flexodomains.^[54,55] Recently, such flexodomains were shown to act as adjustable gratings that respond to an applied field.^[56,57] The diffraction patterns and the corresponding LC textures for several voltages are shown in **Figure 5B**.

The use of electric field induced instabilities has, however, its drawbacks. Since it relies on charges diluted in the sample, it is difficult to control, reproduce, and the dynamic patterns might give poor diffraction orders. Therefore, it did not take long until

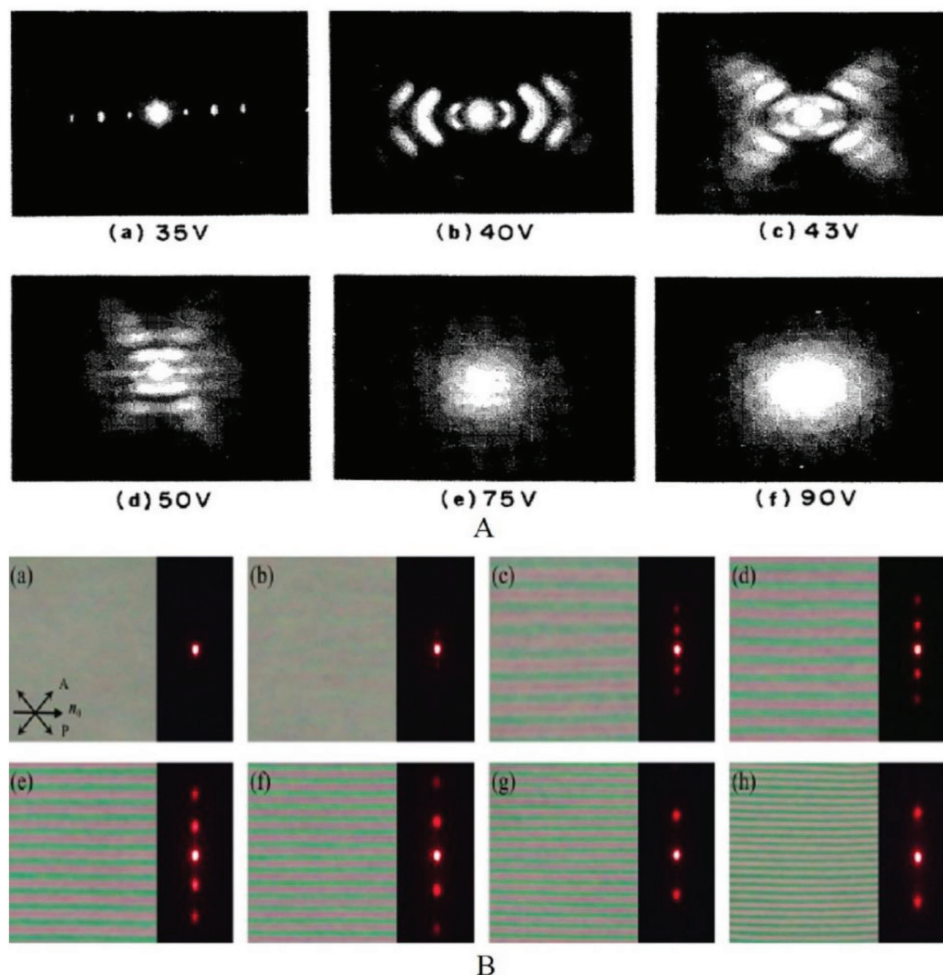


Figure 5. Examples of the data reported in the pioneer works on nematic gratings. Panel (A) shows some patterns measured when a laser light is diffracted while passing through a nematic sample (MBBA) that changes the electroconvective modes as the voltage is increased. Adapted with permission.^[45] Copyright 1997, American Institute of Physics. Panel (B) shows the adjustable diffraction patterns and the flexodomains in a nematic bent-core material under different applied voltages. Reproduced with permission.^[56] Copyright 2018, Optical Society of America.

new approaches started to emerge. In 1979, a special cell was designed with periodically arranged electrodes capable of modulating the director orientation.^[58] As a result, a diffraction grating was developed that was controlled by field with diffraction intensities controlled by the amplitude of the applied electric field. Analogous results were reported by Soffer et al. in several works where a photoconductive layer, periodically arranged, was used to control the distribution of DC voltage across the cell under light illumination, resulting in a grating whose periodicity changed with the amplitude of the field.^[59–61] Such devices are called variable grating-mode (VGM) LC devices.

Researchers soon realized that diffraction gratings could be used for color filtering in the zeroth diffraction order.^[62] The idea is simple and relies on the fact that gratings split polychromatic light (as previously discussed) into its constituent wavelengths. If appropriately designed, it may diffract one wavelength as the zeroth order and the other wavelengths as higher order which can then be blocked. In this sense, LCs are highly desirable because they can be tuned by external fields and are birefringent, so the filtered color is readily tuned. The proof of

concept was demonstrated when a nematic LC grating was fabricated by grooving poly(methyl methacrylate) (PMMA) by means of photolithography and inserting the LC into the periodically arranged array with red, green, blue, and yellow colors obtained in a range of 5 V of applied voltage.^[63] Other uses of LC gratings rapidly developed, as in tunable waveguide systems.^[64,65]

For the simplicity and great reduction in the number of components needed for operating an LC grating in comparison with standard grating systems, numerous ways of fabricating these systems started to develop. One clever way of making them is by using interdigitated electrodes, which consists of periodically spaced electrodes on one of the substrates, while the opposite bounding glass is used for applying field. Such scheme is well known and widely used in in-plane switching schemes. If the substrates are treated for inducing homeotropic alignment (so no light passes through a set of crossed polarizers), a periodic structure is generated when an electric field is applied for a positive dielectric anisotropy material (molecules orient parallel to the applied field) such as 4-cyano-4'-pentylbiphenyl (5CB). The first work using such a cell and describing the diffraction

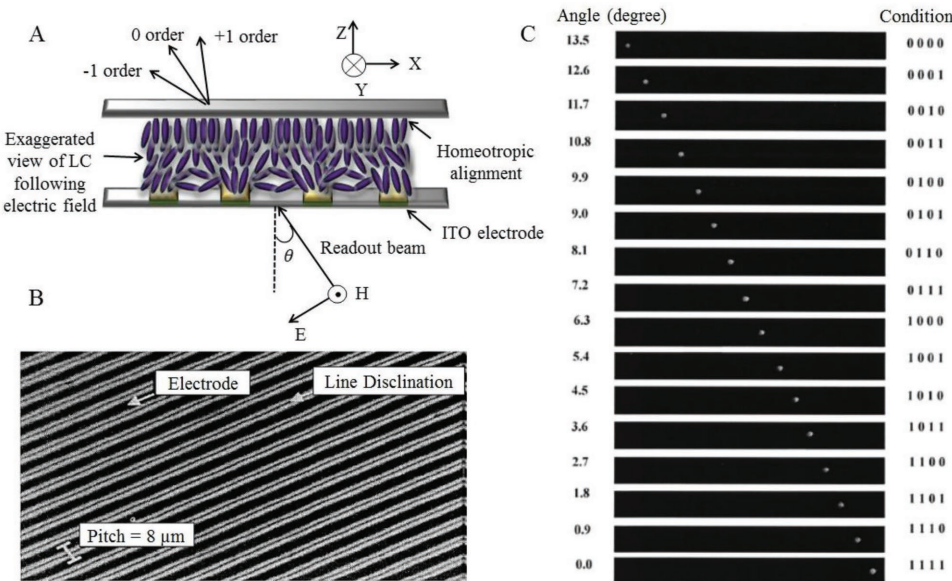


Figure 6. A) An illustration of a homoetropically aligned nematic sample in a cell with interdigitated electrodes and the spatially distributed director configuration. B) The photomicrograph of the cell. A,B) Adapted with permission.^[67] Copyright 1994, Optical Society of America. C) The 16 angles where a diffracted spot is subjected as four stacked gratings are field tuned. Adapted with permission.^[70] Copyright 2000, Optical Society of America.

of light is attributed to Prost and Pershan.^[66] However, their focus was on the flexoelectric effect rather than light control as a grating. Almost 20 years later, in 1994, a detailed study on lateral electric field induced LC gratings was performed.^[67] A nematic LC was injected into a homeotropic cell with interdigitated electrodes and electric field was used to drive the grating. Figure 6A shows the illustration of the cell and the spatially varying director formed when field is applied while Figure 6B shows the photomicrograph of the phase grating between crossed polarizers. Periodicity of $0.8\text{ }\mu\text{m}$ was produced and diffraction efficiency of up to 30% reported for the -1 order. On the other hand, positive orders had a lower efficiency, a characteristic of blazed gratings (diffraction gratings optimized for high efficiency of a determined diffraction order). A few years later, a similar cell design was used but instead of indium tin oxide (ITO) the interdigitated electrodes were made of aluminum.^[68] Since aluminum is not transparent, it forms an amplitude modulation grating. Both the intensity and the polarization state of light could be controlled electrically, the intensity being symmetrical (1st and -1st order) and the polarization state asymmetrical with respect to 90° rotation of the analyzer. The interdigitated arrangement may be one alternative for beam steering devices. In fact, blazed gratings have been proposed as small-angle beam steering devices.^[69] Accordingly, a plane wave is tilted as it passes through a stair step ramp phase delays, so the steered angle is given by $\sin \theta = \lambda/m d$, where λ is the designed wavelength, m is the number of steps, and d is the width of the step. The steps are produced by patterned electrodes that control the change in birefringence for each part of the wave front by applying different voltages to the LC sample. The steering effect can be observed for spatial light modulators (SLMs) or even TV panels.^[70] However, if the desired application needs large steering angles, the LC-phased array^[71] presents problems since the diffraction efficiency drops

considerably as the steered angle increases.^[72] For example, beam steering device consisting of an array illuminator and an LC grating was reported to have 76% efficiency; however, the steered angle is less than 1°.^[73] In contrast, when using a stack of cells,^[74] a blazed grating was fabricated with e-beam photolithography on PMMA and it was shown to have 16 different steering angles (when four gratings with different periodicity are stacked) and a contrast ratio of 18 and high diffraction efficiency. The 16 angles are shown in Figure 6C along with the condition (on and off) of each of the stacked gratings. A model and way of optimizing phased arrays was presented aiming high efficiency beam steering devices.^[72] Further development is currently undergoing, and more information about designs and fabrication process is often obtained, including that for some kinds of gratings, even the side of incidence of light matters for the beam steering efficiency.^[75] Large-angle steering devices have been well documented.^[76,77] Recent results using newly designed nematic phased array (called vernier optical phased array) have been shown to have fine steering precision without affecting the steering range.^[78] In addition, nematic gratings using the field fringe effect have been shown recently to diffract large angles with high efficiency^[79] and are tunable by low voltage fields.^[80]

The use of interdigitated electrodes has, however, a few problems. With no grounding electrodes, the fringe electric field destroys the square wave distribution of the orientation of LC molecules resulting in loss of diffraction efficiency. Furthermore, the electrodes are complicated to design and fabricate, and the diffraction efficiency has strong polarization dependence, meaning at least 50% of light is lost. One alternative way of producing LC gratings is by using patterned alignment layers. Accordingly, a photoresponsive alignment was produced by mixing the silicone polyimide copolymer SPI2000^[81] with 33 wt% diazodiamine and spin coating it to an ITO glass

to make the bounding substrates of the LC cell.^[82] The substrates were then exposed to linearly polarized Argon laser, so the LC molecules orient homogeneously and perpendicular to the laser polarization. The cells were then assembled (11 μm cell gap) and mounted on motorized, computer controlled x-y translation stage where a laser beam writes a grating structure by designing areas with perpendicular orientation to the background, previously designed. Linear and chirped (line space varies as a function of distance from the center) gratings were designed. **Figure 7A,B** shows POM images of the linear and chirped gratings, respectively. For the linear grating, zeroth- and first-order diffraction beams are measured against voltage, showing tunability and low dependence on the input polarization. The chirped grating acts as a focusing lens, which can be readily tuned with electric field and shows, as the linear grating, low dependence on the input polarization. A similar idea where an alternating stripe configuration was fabricated with hybrid aligned nematic LC has been employed.^[83] The hybrid alignment is produced by coating the top substrate with a homeotropic alignment layer and the bottom substrate coated with a planar aligning agent. The planar side, coated with the polyimide PI7311,^[83] passed through a double-rubbing processing in which after the first rubbing (used for the direction of the planar aligned LC), a photolithography process for the grating pattern is used and then it was rubbed again perpendicularly to the first rubbing direction. As a result, the hybrid aligned stripes are perpendicular to each other. This procedure yields a fine aligned periodic structure that achieves nearly 100% diffraction efficiency and has no dependence on beam input polarization. Furthermore, the fabrication is straightforward and convenient for mass production. The same group proposed another double-rubbed cell with adjacent twisted-nematic domains to fabricate a reflective (aluminum coated lower substrate) grating,^[84] which also displayed about 100% efficiency, polarization independence and voltage tunability.

As mentioned earlier, one very straightforward way of fabricating LC gratings is by having patterned surfaces capable

of modulating the nematic orientation. Molecularly designed surfaces were produced by adsorption of alkanethiols on a thin gold film for this purpose.^[85] Depending on the number of methylene groups in the alkanethiols, a nematic LC can anchor homogeneously and perpendicular to the deposition direction if the number is odd or parallel to this direction in case of even number. Furthermore, if long and short alkanethiols are deposited together, the LC anchors homeotropically. The authors used microcontact printing to prepare the grating structure (alternating regions of planar and homeotropic alignment regions for example). The opposite substrate of the cell, used to confine the nematic, had uniform anchoring direction. Depending on the way the film is patterned (homeotropic, planar parallel or planar perpendicular), and upon assembling into an LC cell filled with 5CB, polarization sensitive or insensitive with high resolution gratings are demonstrated. **Figure 7C** shows the grating formed by planar anchoring on the top substrate and bottom substrate formed by two mutually perpendicular planar zones. **Figure 7D** shows the diffracted pattern. **Figure 7E,F** shows the other two arrangements as proposed.^[85]

Other ways of making nematic gratings include methods for photopatterning the alignment layer of the cell. A sinusoidal surface relief structure has been fabricated by photopolymerization through the interference of two lasers, resulting in a grating structure.^[86] A demixing process of binary blends of mutually incompatible polymers during coating to produce nano and micro structures,^[87] which could be used to produce surface relief structures for LC gratings. Other ways of manipulating the surface for making LC gratings include scribing the alignment layers with an atomic force microscope to create polarization gratings^[88] and holographically (polarization holography) patterned alignment layers.^[89] Polarization-sensitive azo dye-doped polyimide films have also been used as aligning layers.^[90] Two coated substrates were assembled to form a cell and exposed to two interfering polarized beams before filling the cells with a nematic LC. The two aligning substrates nearly replicate the grating written on the surfaces on the bulk LC,

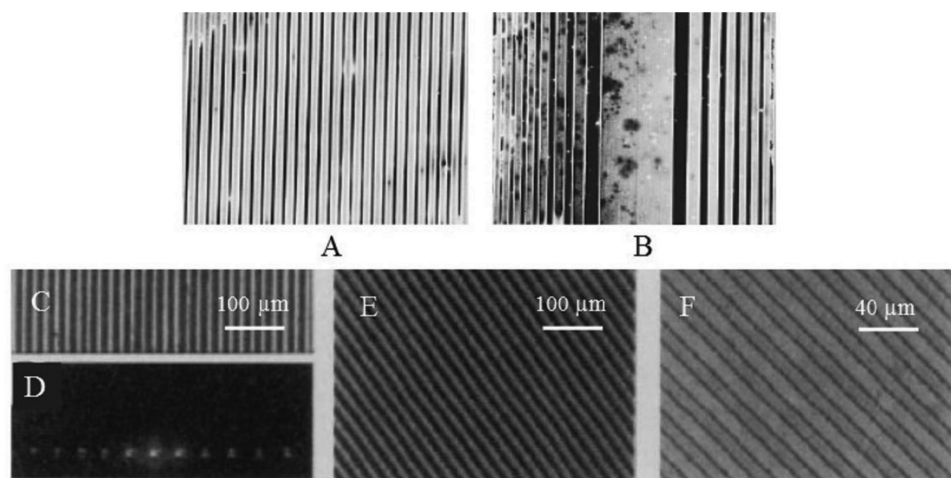


Figure 7. Panels (A) and (B) show the linear and chirped gratings fabricated with a nematic LC. Adapted with permission.^[82] Copyright 1994, American Institute of Physics. Panels (C)–(F) show different gratings (and one diffraction pattern) formed by patterned surfaces with alkanethiols on a thin gold film that acts as an alignment layer to produce the nematic grating. Adapted with permission.^[85] Copyright 1997, American Association for Advancement of Science.

achieving up to 98% diffraction efficiency. More recently, alternating semicircular microgrooves were imprinted on a UV curable polymer which was combined with another glass coated with a material imposing vertical alignment to form an LC cell.^[91] Such configuration yields a continuous grating with high efficiency and electric field tunability. A similar approach toward continuous grating has been described,^[92] where a twisted nematic was chosen as the LC material and the alignment was produced through a microrubbing process, yielding highly efficient gratings.

A remarkable LC grating capable of phase and amplitude modulation has been demonstrated.^[93] It consists of alternating regions of parallel aligned and twist nematic regions in a cell placed between two crossed polarizers. The grating, which is fabricated through a photoalignment technique, is capable of displaying four distinct optical states, 1D and 2D capabilities, fast switching at low voltages, high efficiency and high contrast ratio, unique features arising from the combined effects of the parallel and twisted nematic zones. **Figure 8A** shows four different states of the grating while **Figure 8B** shows the behavior

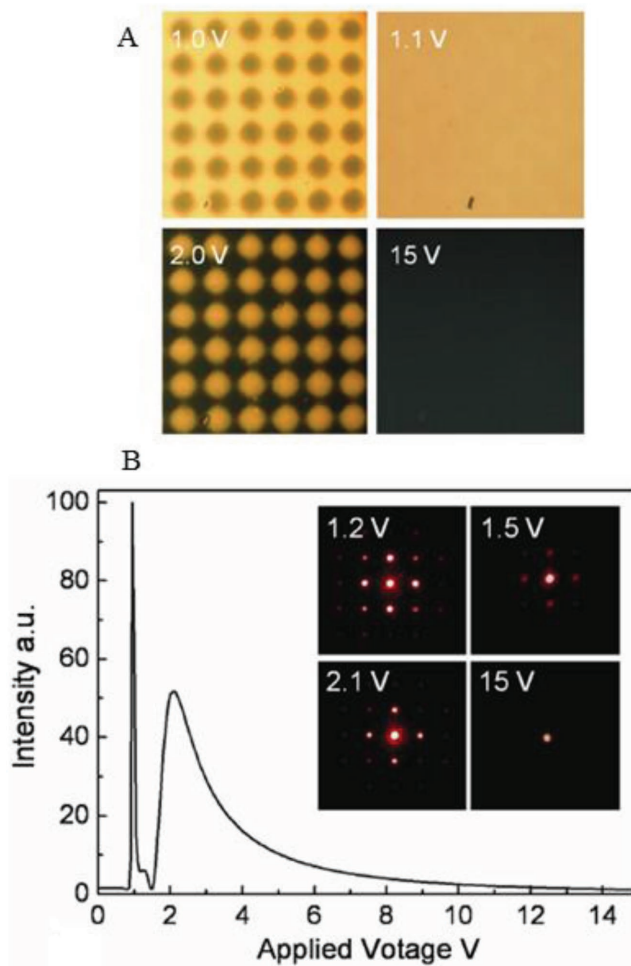


Figure 8. Alternating regions of parallel aligned and twist nematic regions as a diffraction grating. A) Four states of the grating; B) the intensity versus applied voltage profile of the first order while the insets show the diffraction patterns for different voltages. Adapted with permission.^[93] Copyright 2012, Optical Society of America.

of the first-order diffraction versus voltage. The insets show the diffraction pattern at different voltages. Recently, published results also demonstrate LC gratings through surface modification,^[94] where an array of carbon nanotubes were patterned on a substrate, thus inducing defects on the nematic organization, acting as a 2D grating.

In another work, azo-dye alignment layers were exposed to two interfering laser beams with opposite circular polarizations, resulting in a circular pattern of periodicity equal to 20 μm .^[95] Upon assembly of two substrates, and by orienting the patterned substrates with the wave vectors of the polarization grating orthogonal to each other, an array of twisted nematic structures, once the nematic material is filled into the cell, is formed. This results in a 2D diffraction pattern that can be electrically and optically controlled. In a subsequent work, a UV laser and XY scanning stages have been used to expose a photoalignment layer and fabricate several alignment patterns, including phase gratings.^[96] The procedure enables highly precise and efficient gratings that can be fabricated with the same periodicity over a large area, solving a great difficulty in fabricating such devices.

Although many different ways of fabricating nematic gratings have been published, very few display 2D diffraction pattern, an essential requirement in many applications. It is worth noting that, by using a high symmetry LC such as the nematic, one can fabricate such grating by manipulating the surface anchoring condition only. A photosensitive alignment layer was spin coated on both substrates limiting a nematic sample and illuminated with interfering UV light of right and left handed polarizations.^[97] The patterns are the same for each substrate but they are rotated over 90° compared to each other. Upon filling E7 (an eutectic mixture of several alkyl and alkoxy cyanobiphenyls and cyanoterphenyl derivative) material into the cell, a complex 3D pattern with double periodicity is observed, and, when a probe laser is used, a 2D diffraction pattern appears, being field controllable with high efficiency, thanks to the overall quality of the structure. Very recently, even surface induced zigzag patterns in the newly discovered twist-bend nematic (Ntb) phase have been proposed as a route for diffraction gratings.^[98–100]

3.1.2. Optically Driven Gratings

Another approach is to fabricate optically driven gratings using nematic LCs. One such way is to use nonlinear effects of LCs. Indeed, LCs are highly nonlinear optical media. This nonlinearity is responsible for some interesting properties of light when passing through nematics, including four wave mixing.^[101] In fact, in the initial studies, it was demonstrated that a nematic cell under magnetic field (to induce a specific orientation) subjected to two laser beams yielded wave mixing,^[102,103] which is produced by a sinusoidal reorientation of the director at the interference spots between the two beams,^[104] which means a grating is formed. The diffraction efficiency, that is, the ratio of the generated beam to the input beam, in these preliminary studies ranged around 0.01%. This optically driven grating was shown to diffract light into various orders and proven to be highly controllable. Later, the

response time of such gratings used for four wave mixing was explored. The response time for optical molecular reorientation in a 50 μm thick cell is in the order of seconds.^[105] The variation of thermal index associated with laser absorption has been used to create a diffraction grating with sub-milliseconds response time.^[106] However, such phenomenon occurs in materials with high absorbance of light, such as the well-known MBBA nematic LC. In a later publication, Khoo and coauthors have also studied the grating generation under nanosecond pulsed laser, resulting in an index grating that can be associated with changes in the density and in the order parameter, a unique feature of LCs.^[107] The induced grating in LCs has been later shown to determine molecular dynamics aspects of nematics. The holographic grating technique has also been used with picosecond lasers,^[108] showing two kinds of gratings: one due to the optical Kerr effect and another to a standing longitudinal acoustic wave. The rotational reorientation time is readily calculated from the diffracted beam of the Kerr effect induced grating, demonstrating nonexponential decay times, a feature not previously observed when using nanosecond excitation. Further insights on the mechanisms acting during short pulse excitation, including the coupling between density, temperature, flow, and reorientation have been described.^[109,110]

Over the years, more and more applications of LC diffraction gratings started to arise, forcing researchers to develop ingenious designs capable of fulfilling these applications. It is well known that conformational changes that azo-dyes undergo upon irradiation promote molecular reorientation of the LC director. Accordingly, holographic gratings were recorded in azo-dye doped systems,^[111] in which conformational change (*cis*–*trans*) of the dye molecules cause director reorientation in the interference pattern of two recording Ar lasers at 514 nm wavelength. The diffraction efficiency is strongly polarization dependent (probing beam at 633 nm) and has a response time in the order of 100 ms. Such system has also been shown to be stabilized by surface treatments.^[112] Another interesting effect that can be used for fabricating LC gratings is the adsorption of dyes doped in the nematic material.^[113,114] The interference pattern of two laser beams (UV) was shone on a nematic sample with azodye methyl red (MR),^[115,116] which is phototransformed at the constructive interference areas. These molecules are adsorbed to the surfaces and induce local easy axis change, therefore, creating a grating with 1000 lines mm^{-1} and diffraction efficiency of up to 8%, demonstrating an easy to make data storage device. Fabrication of gratings with adsorbed dye molecules on a previously patterned surface relief substrate has also been reported for twisted nematics.^[117] For a nematic LC doped with azo-dye MR sandwiched between periodically structured polydimethylsiloxane (PDMS) that favors homeotropic alignment and a substrate inducing planar alignment, a polarization sensitive grating is formed.^[118] The grating exhibits Raman–Nath diffraction and, upon shining a pump laser (532 nm), *cis*–*trans* isomerization takes place, changing the refractive index of the medium and thus tuning the diffraction intensity. Holography patterning of surfaces has also been used for recording phase gratings on photosensitive Langmuir–Blodgett films which orients a nematic LC,^[119] yielding other promising grating technologies.

Another ingenious way of making LC gratings has been demonstrated.^[120] The grating is made of a nematic cell sandwiched with poly(*N*-vinylcarbazole) (PVK), a photoconductive polymer films across insulated polymer films. If the film is nonuniformly illuminated, charges migrate out of the illuminated areas and get trapped in the dark areas on the surface polymer. Upon holographic writing (two lasers interfering) periodic illuminated areas form and thus, periodic charge distribution arises when the cell is subjected to a DC applied field, which consequently cause director reorientation and forms the diffraction grating. Similar method was applied by the authors to PDLC for forming Raman–Nath-type gratings.^[121] Such photorefractive effect has also been explored in PDLC (see the next section) gratings.^[122] Photorefractive nematic gratings were later studied where it was shown that the effect was caused by surface charges rather than bulk charges and that the grating can be hidden or revealed by tuning a DC electric field.^[123]

Other ways of controlling LC gratings can be achieved through phototuning the alignment layer. Following a previously developed principle,^[93] a phototunable grating working under alternating parallel and twist nematic regions by using photosensitive alignment layer sulfonic azo dye (SD1) was designed,^[124] which can be optically tuned, erased, and rewritten with the polarized light. In a more recent publication, some of the authors reported that this dye can be patterned through interference by using a Lloyd's mirror, yielding high precision gratings with sub-micron scale periodicity.^[125] The photosensitive surface is first aligned by a laser beam and then mutually perpendicular domains are created with the interfering beams produced by the mirror. This alignment layer then is used for orienting a nematic grating. Figure 9A shows the scheme of the mirror in action and Figure 9B shows a photomicrograph of the grating. A nanosecond optically switchable grating has been fabricated and studied.^[126] In order to make the grating, a polymer matrix with grating template was made by holographic photopatterning and filled with a mixture of mesogenic azo dye mixture and E7 nematic LC and exposed to green laser. The grating, which can be tuned once the dye suffers conformation change, switches diffraction efficiency from 87% to 17% in just 4 ns and can be restored in microseconds. The optical anisotropy induces strong polarization dependence, strongly diffracting p-polarized light and weakly diffracting s-polarized light. Figure 9C shows a picture of the grating under POM and the inset shows the scheme of the grating. The s and p arrows represent two impinging probe light polarization.

3.1.3. Polymer-Based Nematic Gratings

The nematic LC has, however, its drawbacks to be used as gratings. Since it is the more symmetric LC, it is somehow challenging to impose, maintain and even tune the grating structure. A great aid to impose the periodic structure on the nematic organization is by using polymer network and LC mixtures. One of the first gratings fabricated with such materials was made of polymer-dispersed LCs (PDLC), which consist of nematic droplets dispersed in a continuous polymer binder.^[127] In general, a PDLC is fabricated by polymerizing monomers dispersed in an LC media. Such polymerization might happen

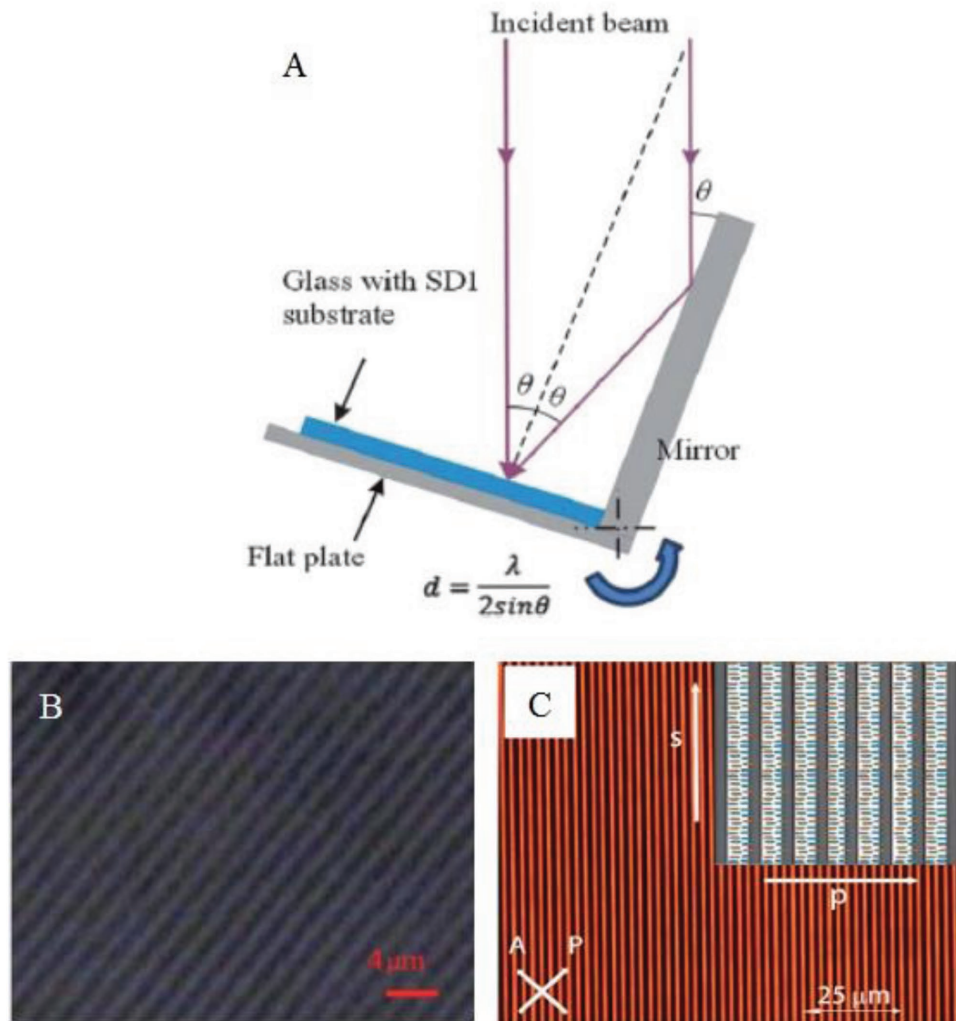


Figure 9. A) Lloyd's mirror is used for photopatterning a substrate to generate a nematic grating (B). Adapted with permission.^[125] Copyright 2013, The Royal Society of Chemistry. C) Grating and scheme of nematic grating doped with dye, strongly sensitive to polarization of impinging beam and nanosecond switching. Adapted with permission.^[126] Copyright 2014, The Royal Society of Chemistry.

through several different methods, including UV exposure of the mixture containing monomer, photoinitiator and LC. In 1989, two groups performed experiments with PDLC gratings. Sutherland analyzed filter and switchers made of PDLCs and designed a grating through a standard holographic method during polymerization, in which LC droplets are favored in high intensity regions.^[128] This caused a coarse periodic distribution of sizes. Up to second order, diffraction through laser transmission was observed and the field effect as well as polarization dependence was studied. A correlation between droplet size and (UV) exposure intensity, LC concentration and photoinitiator concentration has been established.^[129] During polymerization, a photomask with 25 μm periodicity, partially transparent ruling, was used to yield a grating pattern. Up to fifth order diffraction, 0.72° diffraction angle and diffraction intensity control under field was reported.

A few years later, Bragg-type grating was also realized with PDLCs,^[130] with high diffraction efficiency and narrow angular selectivity. In such devices, the rapid photopolymerization and

anisotropic curing does not allow the droplets to grow to a micrometer size ($\sim 0.5 \mu\text{m}$), thus allowing the Bragg-type diffraction. In a subsequent work,^[131] the authors reported how to control and electrically switch the transmission grating, with diffraction efficiency ranging from nearly 50% to zero as the field increased and the PDLC droplets reoriented. A complete morphology study, as well as the dynamics of diffraction during the curing process was later published with more details.^[132,133] PDLCs doped with guest-host dyes have also been reported^[134,135] and azo LC dyes capable of switching Bragg gratings with UV radiation has been demonstrated.^[136] A review on holographic PDLCs has been documented.^[137] The process of writing and erasing a grating in LCs may be used for data storage. It was demonstrated that a side-chain liquid crystalline polyesters can be used to fabricate gratings with standard holographic method aiming data storage.^[138] This polymer nematic LC is easy to cast, does not require preorientation and can be erased by heating the sample. The idea was further demonstrated when a hologram was recorded in a PDLC

volume grating^[139] produced in similar manner as described previously.^[130] The hologram, which consists of a superposition of multiple diffraction gratings, was easily erased and restored by electric field. Such holographic PDLC (H-PDLC) rapidly matured as a main technology for switchable Bragg gratings.^[140] Other uses of H-PDLCs for data storage and large-angle beam steering were later shown.^[141–144] In a more recent work, Bunning and co-workers used six lasers to create 3D beam interfering pattern thus enabling three mutually orthogonal diffraction gratings in photopolymerizable monomer and LC mixture.^[145] LC droplets of approximately 50 nm form in the null regions resulting in a periodic structure that can be manipulated with electrical field (by reorienting the LC droplet), present photonic bandgap (Bragg diffraction) and can be fabricated in different kinds of lattice size. **Figure 10A–C** presents images of an orthorhombic LC-filled photonic crystal. Figure 10A shows atomic force microscope (AFM) image while Figure 10B,C is SEM images at different scales. In a very recent publication,^[146] Bunning and co-workers fabricated a reverse, or hidden, holographic PDLC grating. The HPDLC gratings discussed so far have the disadvantage of presenting the nondiffractive state

only when field is applied, which is not always desired. After polymerization, periodic walls of LC polymer alternated with LC polymer and nematic domains exist.^[146] Since there is a match between the refractive index of the two materials, under zero field the material is transparent. However, as a small electric field is applied, the grating structure appears, resulting in high diffraction efficiency, with fast response time.

The use of PDLCs however imposes some difficulties depending on the type of application. For instance, PDLCs need relatively high fields to switch and present quite large light scattering. Similar hologram techniques have been applied to produce surface relief gratings in a side-chain azobenzene polyester LC, demonstrating that the anisotropy and the surface relief appear simultaneously during the recording process.^[147] Dynamical control using holographic method was also demonstrated with polymer LCs containing azobenzene derivatives capable of *cis-trans* isomerization,^[148] switching on and off the grating by turning on and off the writing beam. The authors later demonstrated the mechanism behind the formation of holographic gratings in polymer azobenzene LCs.^[149] Accordingly, the photoisomerization of the azo moieties is different depending on the

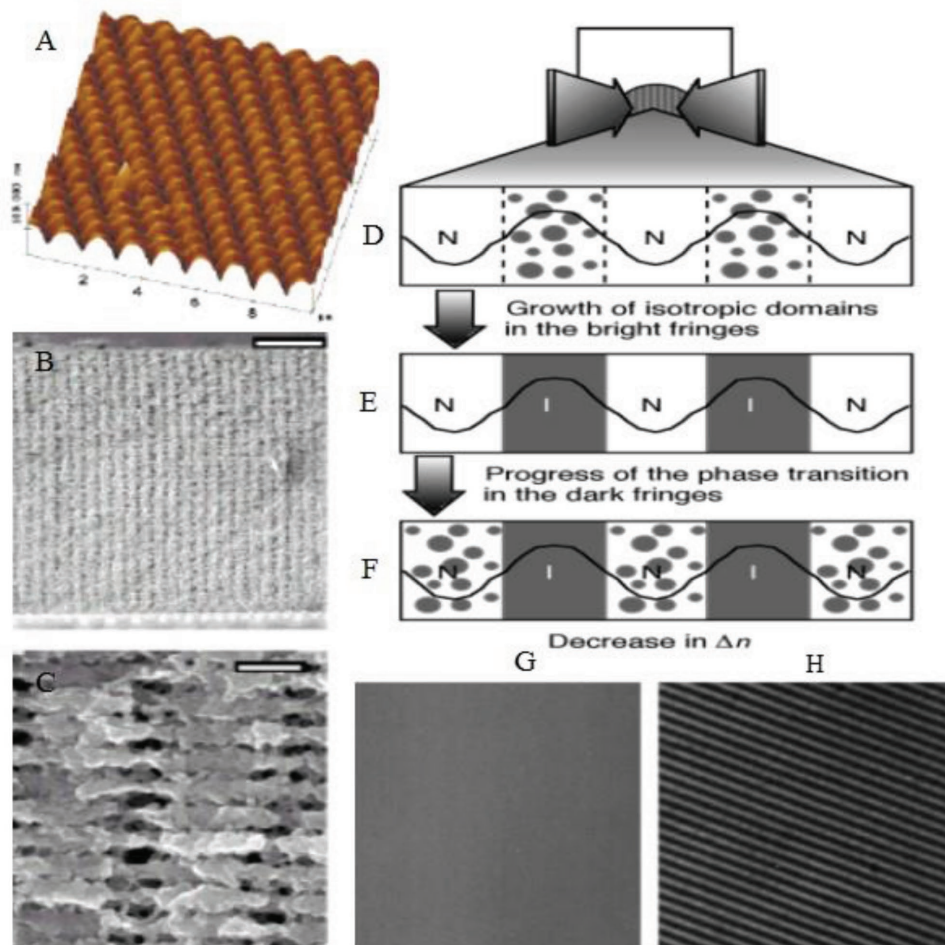


Figure 10. A–C) Images of an orthorhombic p nematic LC-filled photonic crystal. Panel (A) shows AFM while panels (B) and (C) are SEM images at different scales. Adapted with permission.^[145] Copyright 2002, Wiley-VCH. D–F) The holographic switching of polymer LCs containing azobenzene derivatives; the sample G) before and H) after illumination by the interfering beams. Adapted with permission.^[149] Copyright 2000, The Royal Society of Chemistry.

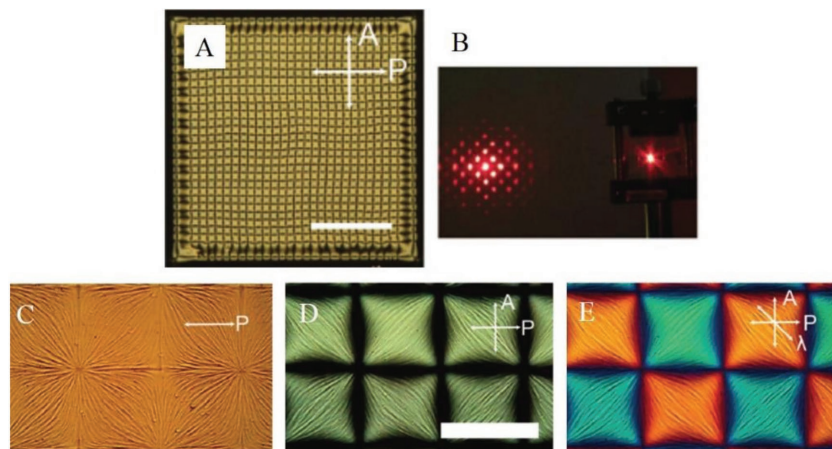


Figure 11. Micropixelated array of defects in a nematic cell used as a diffraction grating. A) Array of defects; B) 2D diffraction pattern generated by the array of defects; and C-E) different closed-up views of the polymer stabilized array, under plane polarized light, crossed polarizers, and with full wave plate, respectively. Adapted with permission.^[156] Copyright 2017, Wiley-VCH.

region of bright interfering fringes or dark interfering fringes, as shown in Figure 10D–F. The trans-cis photoisomerization leads to isotropic islands in the bright regions. In Figure 10E, there is clear separation of isotropic and nematic regions leading to maximum diffraction efficiency. Further exposition leads to phase transition in the low intensity regions too, as shown in Figure 10F. Figure 10G,H shows the film before and after the grating is recorded, respectively. This leads to a control below 1 μm and more than 1000 lines mm⁻¹. Surface relief gratings have also been demonstrated in a hybrid system with a polymer containing azobenzene in the side chain and 5CB under holographic grating^[150] and in polyurethane elastomers.^[151]

A liquid crystalline azobenzene dimethacrylate monomer mixed with a nematic phase has also been used to fabricate gratings that could be switched simultaneously by electric field and UV radiation,^[152] thus these can be operated as dual-mode LC gratings. A holographic grating is demonstrated with nematic LC films separated with polymer slices,^[153,154] presenting a great reduction of scattered light and increased diffraction efficiency. A remarkable approach for producing interference-based electro-optic phase gratings has been shown.^[155] The working principle of this grating is the use of a close packed array of monodispersed emulsion drops of nematic LC in a polymer matrix. The droplets were fabricated by extrusion through a capillary, the droplets arranged in a hexagonal array and stabilized by a thin polymer film. These droplets, which arrange internally in a bipolar fashion, act as a periodically distributed refractive index, whose periodicity is governed by the droplet size. The droplets can be readily tuned by relatively low electric field with short response times, acting similarly to an H-PDLC.

New ways of generating periodic structures capable of serving as diffraction grating, is a current challenge in the LC field. A great example of periodic structure to this end has been recently published,^[156] where a micropixelated LC structure made of a square array of topological defects was fabricated and polymer stabilized in a nematic sample. The method used to fabricate the square array was published in 2016,^[157] where the array of defects arise when a nematic sample is

doped with ionic impurities and subjected to an AC field. The polymer stabilization process allows for electric-field controllable, 2D gratings. Figure 11A shows the defect array while Figure 11B shows the 2D diffracted pattern. Figure 11C–E shows a close look of the polymerized area under three different modes of a POM: panel (C) shows the structure under plane polarized light, panel (D) shows the same area under crossed polarizers and E with a full-wave plate. A similar structure was also recently demonstrated with photoresponsive LC networks that are able to change shape upon light irradiation.^[158]

3.2. Smectic LCs

Among the three most common LC phases known in thermotropics (nematic, CLCs, and smectic LCs), the smectic (Sm) LC phase is the least explored one as diffraction grating. This is in part due to its complex hierarchical organization, which is more difficult to align and switch, resulting in poor tunability and low diffraction efficiency. As previously discussed, the molecules in Sm LC phases organize themselves in layers, possessing at least 1D positional order. The most common Sm LC phase is SmA, in which the molecules are organized in layers and orient along a common direction, perpendicular to the layer planes. Within each layer, no positional order among the molecules is encountered, so there is liquid-like behavior but flowing across the layers requires permeation, so the material can be thought of as 1D crystals. In certain materials, there is a special organization in which the molecules make an angle ϕ with the layer normal. This Sm LC phase with tilted molecular organization is referred to as SmC phase. The SmC phase has lower symmetry than the SmA phase. There are a number of other Sm LC phases, depending on the molecular arrangements.^[159] There is, however, a special Sm LC phase that has attracted more attention for diffraction gratings, i.e., the chiral SmC phase, often denoted as SmC*. If the material is chiral, it forms a helix in which the molecules are still tilted with respect to the layer normal but a small rotation of the director's projection on the layer occurs from one layer to the other. The repetition occurs every P (pitch) length rather than $P/2$ as in the chiral nematic phases, and the pitch length comprises many layers. The combination of molecular tilt and chirality opens the possibility for ferroelectricity since the only symmetry left is a two-fold rotation axis perpendicular to the director and parallel to the layers. In general, this polarization is averaged out as the medium spirals along the helical axis, however, in thin SmC* samples, where the helix is suppressed, the ferroelectric nature can be used in applications with very fast response time, a configuration usually achieved through surface designs, as first pointed out by Clark and Lagerwall.^[160] Most of the diffraction gratings made with Sm LCs make use of the ferroelectric phase. For this reason, we will divide this section into two subsections: one for SmA, chiral smectic A (SmA*), and smectic C (SmC) LC phases, and another just devoted to SmC* phase.

3.2.1. Smetic A, Chiral Smectic A, and Smectic C LCs

The Sm phase, with exception of the SmC* phase, have not been extensively used in the fabrication of diffraction gratings. Although they can be used for forming complex periodic patterns, they are somehow difficult to achieve and are not easily tunable. Nonetheless, such periodic structures are being developed more and more, so in the near future diffraction gratings using Sm LCs may proliferate. The first uses of Sm phase as diffraction gratings occurred as electroconvection studies took place. Similar to the nematic phase, upon changing applied voltage and frequency, several electroconvective states might occur in Sm LCs. Such patterns are, in some cases, periodic structures that develop over time and have several shapes, including cylindrical lense-like and domain lines. Simova et al. noticed that when a SmC LC subjected to an AC field acts as a 2D diffraction grating.^[161] There is one modulation along the rubbing direction and another modulation perpendicular to the rubbing direction, resulting in a 2D grating. These diffraction patterns have been recently explored.^[162] Fluctuations of the diffracted intensities were later explained by periodical alternation of the amplitudes of the angular distortions of the director.^[163] A few years later, Khoo and Normandin showed that in a homoerotropically aligned SmA sample doped with a small amount of dye, thermal and density grating through photoabsorption occurs when two pulsed lasers interfere inside the sample.^[164] Noticeably, if the pulsed laser energy is about 25 mJ, the grating written is permanent. That is because in the region of maximum interference, the sample is superheated during irradiation and then supercooled when the illumination was over, keeping the sample in a state of disorder while the regions of minimum interference remain ordered. Diffraction efficiency for the first-order spot was about 0.9%. Other studies on such nonlinear effects were later published.^[165] Electrically and surface induced array of focal conics were demonstrated in SmA samples,^[166] opening the possibility for another kind of Sm diffraction grating. Sm gratings were also successfully demonstrated in grating coupled waveguides.^[65] Very recently, bistable operation of a SmA grating was demonstrated by means of interdigitated electrodes.^[167] The device, which relies on dielectric switching, results in 2D patterns that can be electrically controlled with high efficiency and low power consumption.

Chiral SmA phase has been used to fabricate gratings by using photorefractive effect.^[168] The photorefractive effect, which consists of electric field induced space-modulation of the refractive index due to the presence of photogenerated charges, was created by using a layer of a photoconductive material (PVK) coated at both substrates of a slab cell. The SmA* LC was injected into the cell and two laser beams were superimposed on the sample, thus creating charge separation on the interfering beams. Under a DC electric field application, grating with periodicity of 21 μm were created due to the electroclinic effect (rather than the dielectric anisotropy of nematics), a reorientation of the director that is linear with the applied field. The authors, in a subsequent publication, demonstrated the same effect in polymer dispersed SmA* phase.^[169] The Sm LC has attracted a great deal of attention because their defects can be self-assembled into periodic arrays. Such arrays

may, in principle, be used as diffraction grating, although it has not been extensively studied to this end.^[170] Here we discuss the few studies where the optical grating property was explored. The deformation of the layers of a SmA phase was studied in frustrated films between two interfaces that induce opposite anchoring (hybrid alignment).^[171] A thin 8CB LC film was used between a planar favoring alignment layer and air (which favors homeotropic alignment). Under such constraints, the Sm layers are stacked into flattened hemicylinders that are 1D focal-conic domains that form a grating-like structure with period ranging from 1 to 2.5 μm. Figure 12A shows the scheme of the hemicylinders of Sm layers concentrically stacked lying on a flat substrate while Figure 12B shows an AFM image of the grating whose period is about 1.8 μm. It was recently shown that oriented striped pattern is formed in thin samples while hexagonal lattices of focal conic domains appear for thicker samples in hybrid aligned cells.^[172] Therefore, depending on the thickness of the sample, 1D diffraction grating or 2D (hexagonal) gratings are fabricated. The samples were confined between substrates treated to align the director homeotropically at one end and planar at the other one. Figure 12C shows the striped pattern formed for cell thickness 1.2 μm and period 2.6 μm. The inset shows the diffraction pattern under green light illumination. Figure 12D shows the close-packed lattice of focal conic domains in a 2.7 μm sample with period 4.6 μm. The inset shows the hexagonal diffraction pattern resulting from green laser illumination. It is important to mention here that holographic recording and LC to isotropic phase transition, as discussed here, has also been used to fabricate gratings in LC polymers presenting Sm phases, yielding refractive index and surface relief gratings.^[173–176]

3.2.2. Chiral Smectic C LCs

It took quite a while, in comparison to the nematic LC, for the SmC* phase to be used as diffraction gratings. Initially, the SmC* LC attracted attention in the Bragg mode,^[177] or in the Raman–Nath mode (perpendicular to the helical axis) just for determining the pitch length^[178] or in ferroelectric spatial light modulators, where the pixels are addressed to form a grating.^[179] The first time SmC* LCs were treated as phase gratings were in the calculation to attempt to model the medium^[180] based on the Raman–Nath theory, which was proven incomplete a few years later since the internal diffractions were ignored. The first complete study of SmC* gratings working in the Raman–Nath mode has been performed in 1994.^[181] There, Suresh and co-workers observed unusual features and strong polarization dependence of the diffraction pattern. The grating was obtained by applying a magnetic field to the sample while still in the SmA* phase, then the field was removed and the sample slowly cooled to the SmC*, forming a uniform grating. In a range of cell thickness, the diffracted light was polarized parallel to the helical axis while for thicker gratings and high temperatures the polarization was nearly perpendicular to the helical axis. Up to seven diffraction orders were reported and it was shown that the diffracted intensity, as a function of thickness, has modulations at different length scales. Later, the authors showed that this modulation was due to the coupling between different

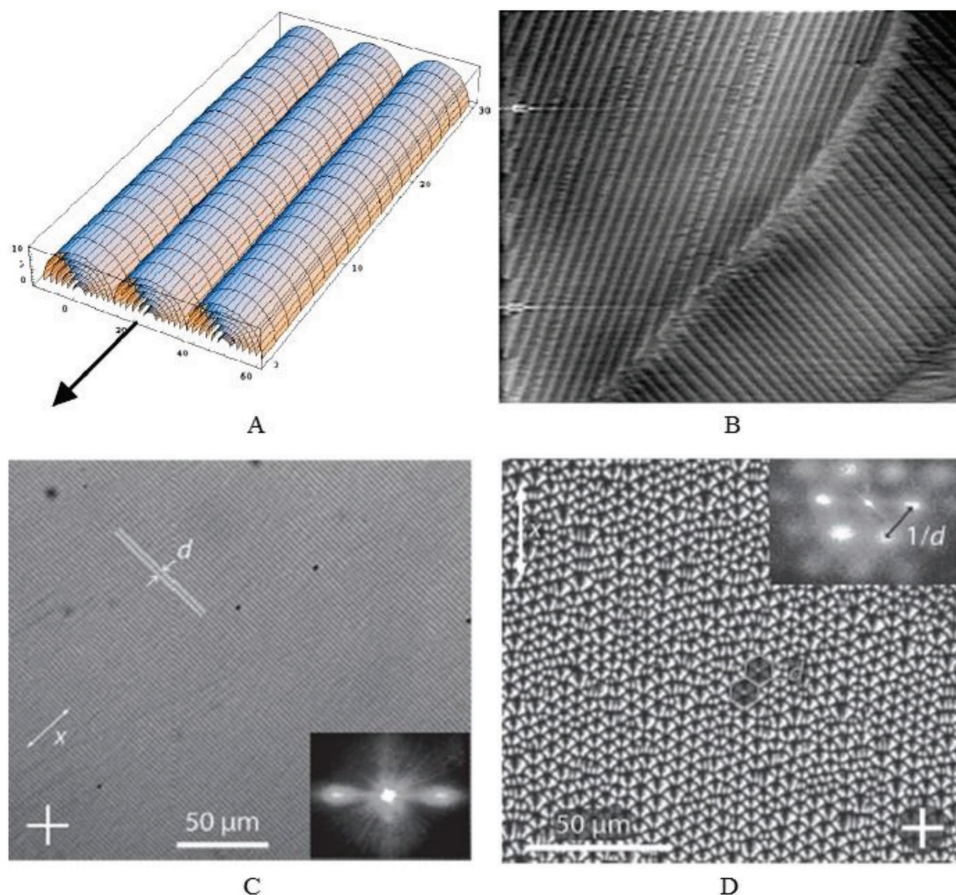


Figure 12. A) Hemicylinders of SmA layers concentrically stacked lying on a flat substrate; B) an AFM image of the grating whose period is about $1.8\text{ }\mu\text{m}$. Reproduced with permission.^[171] Copyright 2004, American Physical Society. C,D) Striped and hexagonal arrangement of focal conic in 1.2 and $2.7\text{ }\mu\text{m}$ thick samples under hybrid alignment. The insets show the corresponding diffraction pattern. Adapted with permission.^[172] Copyright 2015, Wiley-VCH.

orders of scattering.^[182] Beam steering with two ferroelectric SLMs has been reported about the same time.^[183]

Photoinduced gratings were subsequently reported in SmC* systems doped with a photochromic dye.^[184] The mixture was filled into a $4\text{ }\mu\text{m}$, planar rubbed cell and a setup to simultaneously apply DC voltage, probe the diffracted beam and two interfering continuous wave laser (pump) at 514.5 nm was built. Initially, spatially uniform irradiation was used and photoinduced spontaneous polarization demonstrated. When the interfering beams were used, a grating was created whose diffraction efficiency could be controlled by field since it has the effect of unwinding the helix. Diffraction efficiency of up to 0.56% and response time of a few seconds was reported. Nonmonotone dynamics is observed for step-like voltage changes under continuous light illumination, as has been demonstrated.^[185] A similar approach has been employed where a surface stabilized ferroelectric cell doped with MR dye was fabricated.^[186] Two coherent laser beams were used to write a grating formed due to the reorientation of the LC molecules caused the interaction with the photoinduced adsorption of dye molecules. The written grating was permanent and electrically switchable. Calculations of the first-order diffraction efficiency for short pitch surface stabilized ferroelectric LCs showed that for as the pitch gets shorter, the efficiency's peak value

decreases becomes increasingly dependent on the incoming light polarization.^[187] The photorefractive properties of a chiral smectic C* phase of cyclopalladated complexes were demonstrated a few years later by writing a diffraction grating the two beam-coupling technique.^[188] Remarkably, hologram writing was used in an advanced prototype device using field deformed-helix of SmC* phase to enable high diffraction efficiency (30%) and high resolution.^[189]

The development of SmC* gratings took a step forward with the introduction of polymer stabilization. A mixture of SmC* phase (R0623) containing a photocurable LC (UCL001) was filled into a thin, $2\text{ }\mu\text{m}$, coated with polyimide and rubbed, cell.^[190] A monodomain structure was obtained by cooling the sample to room temperature with a 15 V DC voltage on. Then, the samples were photopolymerized with a grating photomask that allowed polymerization only to the exposed, transparent areas, resulting in an alternating stripes configuration. The polymerized zones did not switch under an applied field while the nonpolymerized zones switched the cone angle as a field was gradually increased from 0° to $\approx 80^\circ$, so the grating goes from off (no diffraction) at zero field to on at 11 V . The grating is polarization independent in the full switched state and has fast response time, in the μs range, for switching toward stable state. Figure 13A shows the POM pictures of the grating at 3

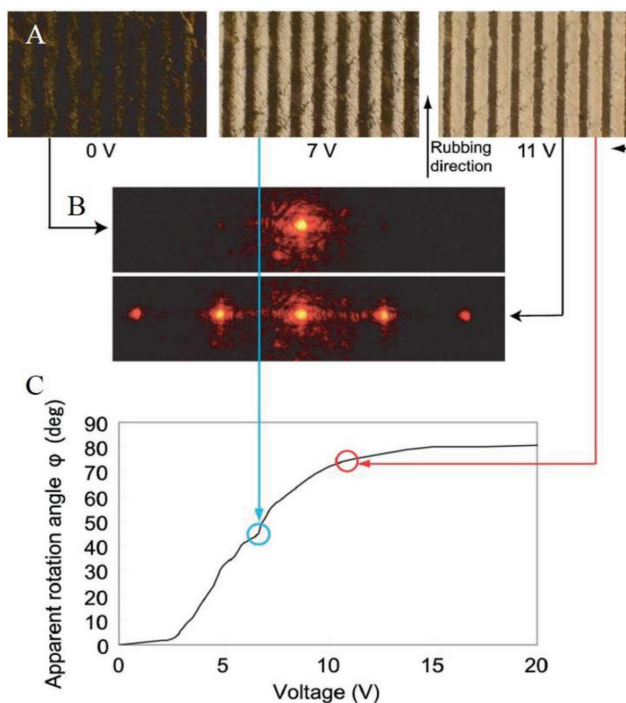


Figure 13. A) Photopolymerized SmC* LC grating at three different applied voltages; B) their two corresponding diffraction patterns; C) angle rotation versus applied voltage and its corresponding texture. Adapted with permission.^[190] Copyright 2006, American Institute of Physics.

different voltages. Figure 13B shows the diffraction pattern at 0 and 11 V while Figure 13C shows the rotation angle versus applied voltage and its corresponding texture. For fabricating gratings with three different periodicities: 3.32, 7.40, and 11.3 μm , two beam interference was used to cure a mixture of a chiral smectic C* LC and a photocurable monomer (in a 5 μm cell).^[191] When looked through a POM, the gratings present low contrast if oriented at 0° with the polarizer and high contrast if oriented 45° with the polarizer, suggesting different domains between polymer walls. The grating could be switched under field and diffraction efficiency of up to 12% with switching times between 20 and 50 μs are reported.

An impressive approach has been reported by Srivastava et al.^[192] As previously seen, SmC* phase suffer of some issues, which include low diffraction efficiency, since it is still challenging to obtain a uniformly aligned SmC* texture.^[193] The nematic gratings have much better efficiency but lack switching speed whereas blue phase gratings (as we shall see later) have fast response time but need high driving voltages to work. The proposed SmC* grating improves almost all the aforementioned qualities.^[192] It consists of a ferroelectric material that is well aligned, provided that some criteria are met such as pitch length shorter than the cell thickness of the slab it is filled into. The inner substrates are coated with sulfonic dye SD1, a photoalignment layer whose easy axis direction orients perpendicular to the polarization plane of the incident light (UV). A two-step exposition procedure with a photomask is used to generate mutually perpendicular alignment zones, so 1D and 2D gratings are fabricated. When the alignment is parallel to either the polarizer or analyzer, no diffraction occurs, however,

upon applying an electric field, the material is switched and diffraction occurs. The 1D and 2D diffraction gratings fabricated viewed under POM are shown in Figure 14A,B, and their corresponding diffraction pattern of both gratings are shown in Figure 14C,D. The grating has high contrast for the first-order diffraction, high diffraction efficiency, low driving voltage, and response time faster than 20 μs . In a subsequent publication, the authors demonstrated similar grating by patterning only one substrate that could be written and erased in simple steps.^[194] A more detailed exploration of such grating, including improvements and a mathematical model has been discussed.^[195] Recently, another design has been proposed to optically control a SmC* diffraction grating.^[196] The grating consists of a ferroelectric LC doped with MR dye that suffers conformational change upon light irradiation. The sample was filled into 5 μm slabs (to suppress the helical pitch) that had already been prepared to have alternated regions without and with polymer network (previously photopolymerized with a nematic material that was later washed out). When a pump laser (544 nm) was used to induce conformational change of the dye, the diffraction efficiency of the zeroth order increased up to 62% while the first order decreased slightly, from 8% to 7%. The response time is faster than most optically driven nematic gratings. Fork gratings for optical vortices generation using SmC* phase have also been recently demonstrated.^[197]

3.3. Cholesteric LCs

The CLC phase is prominent for light manipulation. This comes from the fact that it presents, depending on the texture and pitch length, several optical states. CLCs have no mirror symmetry, which is a consequence of spontaneous rotation of the director along a direction called helical axis. For each plane perpendicular to this axis the material is essentially a nematic, however, any other cross section perpendicular to the helix is slightly rotated with respect to each other, completing a full 360° rotation within a length called pitch (P).

The view of a well-oriented helix is, in general, not true. This is because CLCs are always bounded by the limiting glass substrates of the cell and this helix is hardly ever well compatible with the boundary conditions, resulting in deformation and frustration of the helix that, depending on the sample structure, yields several different textures (organizations) and, therefore, several optical states, see for example refs. [198,199]. In fact, CLCs are soft materials so the helix can be compressed, stretched, rotated and distorted. It is therefore common to encounter CLCs in several different ways depending on the confinement characteristics,^[200,201] including if other external agents are at play (such as an applied field for example). The most straightforward arrangement is the Grandjean texture, which consists of planar aligned molecules at the bounding walls, thus orienting the helical axis perpendicularly to the substrates.^[12] Depending on the pitch length, the CLC phase may rotate linearly polarized light (Mauguin regime), make the incident light more and more circularly polarized as the pitch gets shorter (from the Mauguin regime) or Bragg reflect circularly polarized light with same handedness as the helix for pitch lengths comparable to the wavelength of light. If a sufficiently

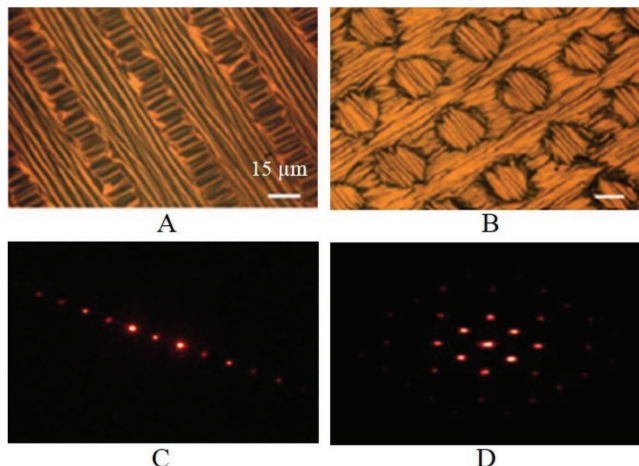


Figure 14. A) 1D and B) 2D gratings fabricated with SmC* viewed under POM and their corresponding C) 1D and D) 2D diffraction patterns. Adapted with permission.^[192] Copyright 2012, American Institute of Physics.

high electric field is applied (for positive dielectric anisotropy) on the Grandjean texture, the helix is unwound and the material becomes essentially a homeotropically aligned nematic. Nonetheless, the transition from the Grandjean to the homeotropic texture, a few states are possible. The process of unwinding the helix may take two paths: a nucleation of defects process takes place, breaking the Grandjean texture in domains with the same pitch length, but with helical axis randomly oriented from one domain to the other.^[12] This texture is called focal-conic and it scatters light. On the other hand, if there are few nucleation sites, the CLC film may adopt a periodic organization in the plane perpendicular to the helical axis, commonly known as the Helfrich deformation.^[202] As we will show later, this texture can be used as diffraction grating. Figure 15A shows an illustration of the Helfrich structure while Figure 15B shows the corresponding POM image. If the field is further raised from the Helfrich texture (or conversely from the focal-conic texture), the helical axis is switched and lies parallel to the substrates, hence twisting in a direction perpendicular to the field of view when observed under a microscope. If the pitch is short, the optical resolution does not allow visualization, even though this arrangement is often used in flexoelectric devices.^[203] Nonetheless, for larger pitch lengths, the periodicity can be realized under microscope, which appears as randomly oriented stripes, resembling a fingerprint. It is worth mentioning that although we used field as examples to achieve such textures, they may be achieved by other stimuli like temperature, light irradiation, confinement etc. A special situation occurs when the aforementioned stripes are aligned along a certain direction. This configuration, called lying helix (LH) configuration, resembles a diffraction grating and is obtained under special situations such as when the cells are treated for planar alignment and an electric or magnetic field is applied. The important point here is that the LH configuration is a periodically varying refractive index media that can be readily applied as diffractive elements. Figure 15C shows the illustration of the LH scheme while Figure 15D shows the POM picture. As reported for nematics, CLCs can be used for phase gratings and present

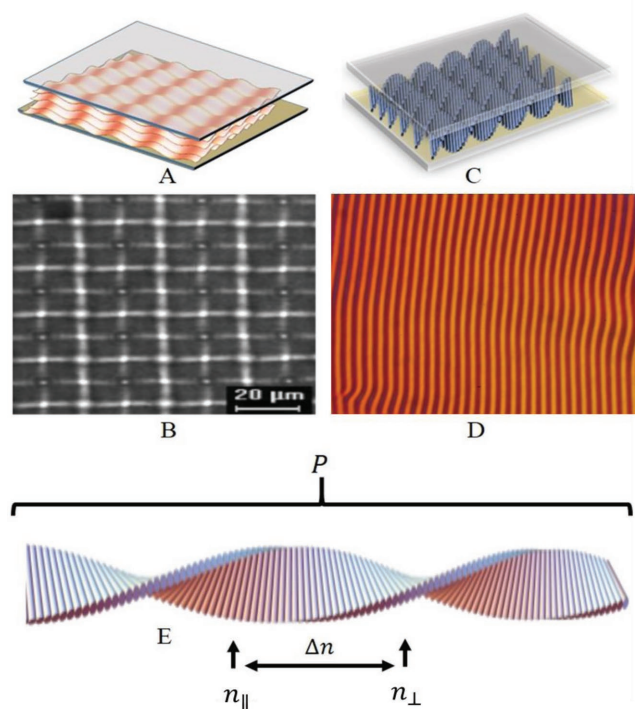


Figure 15. A) A schematic illustration and B) its corresponding POM image of the Helfrich deformation; C) schematic illustration and D) its corresponding POM image of LH configuration; E) refractive index modulation that occurs naturally in a CLC material. B) Adapted with permission.^[202] Copyright 2006, American Physical Society.

several different diffraction patterns that range from 1D to 2D, arc shaped, integer and half integer diffraction points and many others.^[204] Figure 15E shows the natural refractive index modulation that occurs in CLCs, where n_{\parallel} and n_{\perp} are the refractive index for light propagating parallel and perpendicular to the director, respectively, thus making it suitable to be used as diffraction gratings.

CLCs are currently one of the most used LC phases for several applications. This is because they possess a self-organized helical structure that can be controlled and switched by many stimuli.^[100,201,205–212] These controllable actions enable CLCs to be used in ground-breaking devices and application. In general, most of the applications come from the fact that external stimuli cause pitch changes^[213–217] and helical axis switching,^[33,35] both resulting in remarkable mesoscopic changes that qualify incredibly well as diffraction gratings. CLCs in both the LH configuration and Helfrich deformed states have been shown to diffract light. The periodic structure of CLCs has long been recognized for its potential to behave as Raman–Nath diffraction gratings. Such realization, which shall be discussed here later, has opened many doors in basic and applied sciences for the use of CLCs. The diffraction profile, for example, has been calculated almost 30 years ago,^[180] and more recently for nonuniform CLCs.^[215] Diffraction grating-like behavior is found in naturally occurring materials that resemble CLCs.^[216,218] The CLC grating has a great potential for nonmechanical beam-steering devices, phased arrays, as masks for lithography^[219] and even for generating optical vortices.^[220] However, what makes CLCs special

is the fact that one can switch the grating by many different stimuli and in many different ways, which, without doubt, make them unique when compared to commonly found static diffraction gratings. In the next section, we will discuss some examples reported in the literature where diffraction gratings have been fabricated and controlled by different stimuli, such as by applied field, photostimulation, temperature, polymer stabilization and dual-stimuli.

3.3.1. Applied Bias

It is usually referred in the literature that the first work reporting CLCs as diffraction gratings was the pioneer work of Sackman et al. who used a magnetic field to orient the helical axis parallel to the substrates of a mixture of cholesteryl chloride and cholesteryl myristate.^[221] Then, a He–Ne laser was used to probe the sample and diffraction patterns that varied with temperature, as the cell passed through different twist regimes (pitch length), were reported, including the nematic LC where no diffraction orders are observed. Although no microscope images are given, the diffraction patterns indicate that the magnetic field has induced a fingerprint-like arrangement. As mentioned earlier, we here focus on the switchable (controlled) nature of the gratings, although it is worth mentioning that other studies reported diffraction patterns in static finger print structures.^[222] It was only in 1997 that CLCs were studied for, as clearly stated, switchable Raman–Nath diffraction gratings.^[223] The design of such device is quite simple: a planar oriented CLC is subjected to an electric field. For low field amplitude, the material remains in the planar state. For high values of field, the helix is unwound and the homeotropic state occurs. For intermediate values of field, the LH structure is observed, where the alignment of the modulations is set by the unidirectional orientation at the surfaces. The diffraction pattern is polarization dependent and has the second order spots with higher intensity. First orders also are observed but are much weaker. Therefore, upon increasing the field, the grating may be written and erased with field. The authors also showed that,^[224,225] by carefully designing the pitch to cell thickness ratio, the applied field could be used to form the LH configuration and to change the periodicity of the modulation (grating) for cell whose ratio of thickness to pitch (d/P) is larger than 1, and thus, create a beam steering effect. This change in periodicity with applied field is shown in **Figure 16A,B**.

Two different mechanisms for grating formation in CLCs have been reported.^[227,228] Accordingly, for $0.5 < d/P < 1.0$, the stripes appear everywhere simultaneously across the sample like the development of a photography which is referred to as developable modulation (DM). On the other hand, for $d/P > 1.5$, the stripes grow from the edges, spacers and dust particles and slowly cover the whole sample area. This second type is called growing modulation (GM). Surprisingly, it was noticed that only the GM type can steer light electrically and its efficiency is maximized if the polarization of the incident beam is parallel to the grating stripes. On the other hand, the efficiency of DM type shows a dependence on polarization that changes as the d/P ratio changes. In fact, the overall direction of the stripes also is highly dependent on the d/P ratio, for both DM

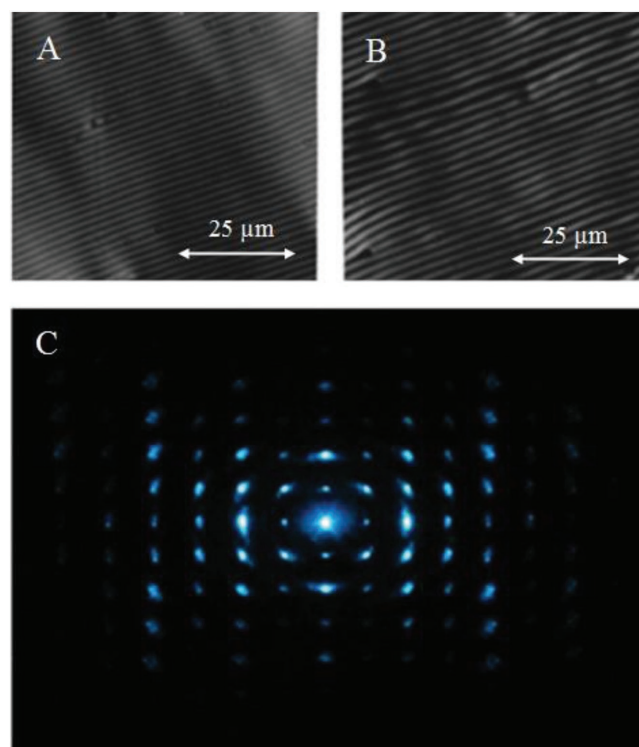


Figure 16. A,B) Pitch modulation by applying different values of field to CLC sample at A) $U = 1.1$ V and B) $U = 1.75$ V. Adapted with permission.^[224] Copyright 1997, American Institute of Physics; C) diffracted pattern from undulated state when 6 V is applied. Adapted with permission.^[226] Copyright 2005, International Society for Optics and Photonics.

and GM types.^[229] It was later demonstrated that the diffraction efficiency can be enhanced by the surface plasmon effect that occurs when silver nanoparticles are deposited at one of the limiting substrates of the CLC grating.^[230]

The above reported results however describe only static gratings, whose periodicity can be switched on demand by field but the stripe direction is fixed, depending on the d/P ratio. The first direction tunable grating was reported by Yao et al.^[231] It is well known that the least energetic way of anchoring CLCs under homeotropic alignment layers is by forming fingerprint textures. The authors observed that for a rubbed cell the stripes change orientation as the amplitude of an applied field increases, which is caused by the drift of the structure center due to the rubbing process.

A very interesting approach toward CLC grating has been reported.^[226,232] Instead of using the LH structure, the undulation of the CLC layers was used as the repeating refractive index media required for the grating. The undulation, previously discussed as Helfrich deformations, occur in order to reduce the elastic energy build up when an electric field is applied. Usually, instead of the undulations, the fingerprint or focal-conic texture is preferable since it possesses slightly lower critical field. Nonetheless, the fingerprint is a nucleation structure, meaning it needs seeds and surface irregularities to develop.^[233] Through careful cell design, the fingerprints were avoided and the 2D undulation pattern was created. The periodicity and intensities of the diffraction maxima can be field tuned and 2D

diffraction patterns are observed. Figure 16C shows an example of diffraction pattern. The diffraction patterns are polarization independent and can be used for many applications, including beam steering devices, optical waveguides, devices for splitting monochromatic beams and beam multiplexing. A few years later, similar approach was employed in polymer stabilized CLCs yielding tunable and stable 2D gratings with up to 84% diffraction efficiency.^[234] 2D diffraction patterns have also been reported by stacking two CLC cells and electrically controlling them to create 2D gratings.^[235]

The LH configuration was reported in 2010.^[236] If a CLC material is filled into a hybrid aligned cell (one substrate promotes homeotropic alignment while the opposite substrate promotes planar direction), a well-oriented LH structure is observed. The stripes continuously rotate under thickness change and application of an electric field, both very important for grating switching applications such as beam steering. Rotations of up to 90° are reported.

CLCs have also been reported to produce gratings based on slit electrodes,^[237] where the top substrate has a whole electrode while the bottom substrate has slit electrodes with chosen gap. Both substrates are treated for planar alignment. When a field is applied, the CLC material in the area under the electrodes is switched whereas the zones without electrode (from the bottom electrode) do not change. For medium fields, the grating has alternating planar and fingerprint textures while for high fields it has alternating planar and homeotropic alignment. Therefore, the grating works in two modes: electrically swept, presenting high second order diffraction efficiency for medium voltage amplitudes and first-order efficiency of up to 32% for high voltages.

3.3.2. Polymer Mediated

As previously seen for the case of nematic phase, the use of polymer networks is quite desirable depending on the kind of grating needed, and solid structure is often required for diffraction gratings. Thus, we now review some cases where the polymer network is used as the key element for CLC gratings.

In one of the first studies of using polymer stabilization of CLC gratings, the sample consisted of a commercially available nematic doped with low amount of chiral dopant to form CLCs with pitch length in the few microns range.^[238] A small amount of reactive monomer (5%) and a photoinitiator was added to the CLC mixture. The mixture was filled into a planar rubbed cell and, before photopolymerization, an electric field used to drive the planar oriented CLC to the LH configuration. Upon polymerization, the grating was stable at zero fields since the polymer network stabilized the CLC structure and could be switched “off” by applying moderate values of field. Another advantage of polymerization is the fact that it considerably improves the diffraction efficiency, the authors reporting up to 75% efficiency. When studying the polymer morphology by SEM measurements of such gratings,^[239] the authors discovered that the network is anchored at the substrates and connected to a less dense sawtooth structure alternating between substrates. The morphology consists of regions in the cell interior with periodicity equal the pitch (P) length and twisted

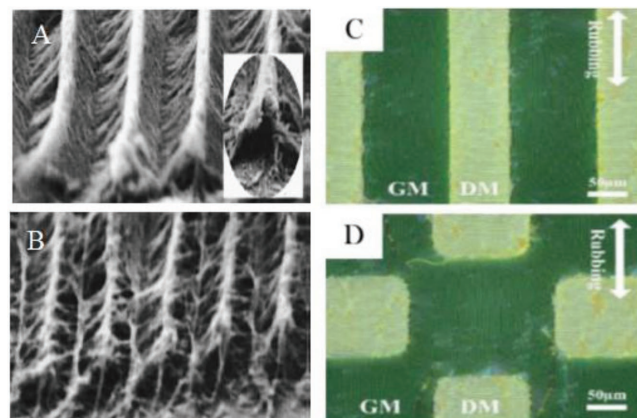


Figure 17. A,B) SEM views of CLC gratings UV cured with polarization parallel or perpendicular to the helical axis. Adapted with permission.^[239] Copyright 2000, American Institute of Physics. C,D) Gratings patterned with two different structures of DM- and GM-type modulations. Adapted with permission.^[249] Copyright 2016, Optical Society of America.

surface regions of period $2P$, explaining the appearance of integer and half integer peaks in the diffraction pattern. The SEM images are shown in Figure 17A,B. Thus, it is proposed that two grating vectors are present in the cell. The concentration of monomer effect on the diffraction orders has also been studied where multiple order diffraction patterns were obtained by varying the monomer concentration.^[240] Polymer templating was also demonstrated in Bragg gratings,^[241] in polymer stabilized phase gratings,^[242] and in microgratings, which were fabricated by exposing the CLC material under an electric field to a Gaussian UV laser of desirable size.^[243] Dual recording of CLC polymer films made with photosensitive chiral dopant were also shown by holographic recording and phototuning the photosensitive chiral dopant used to fabricate the material.^[244] New insights about diffraction efficiency and the mechanism of grating formation under the dual stimuli use to create the gratings are demonstrated.

The possibility of using polymer to template CLC structures, including to fabricate gratings, has been demonstrated.^[245] The polymerization of the CLC and monomer mixture was done in two different UV wavelengths, 322 and 365 nm.^[246] In the shorter wavelength, there is high absorption and the polymer network forms on the surface while for the longer wavelengths the absorption is slower so the network is distributed in the bulk. The surface grating yields lower threshold voltages and shorter transition times while the bulk grating reduces the contrast between on and off state and both arrangements create robust switchable gratings.

Other kind of polymeric structure has been demonstrated by fabricating a CLC gel grating.^[247] In an LC gel, the LC material is contained by a network of fibrous aggregates of a compound called gelator. The CLC gel is composed of 1% gelator and a mixture of nematic host and chiral dopant. The mixture is filled into an ITO coated cell and cooled from 130 °C to room temperature, where tiny fibrous aggregates form. If the sample is heated above the aggregates melting point and exposed to UV light with a stripe photomask, a grating structure appears (when temperature is lowered) since the aggregates form outside the exposed area. The grating can be erased by heating it

to the isotropic phase and can be switched on and off by an applied electric field, thus the grating efficiency can be tuned.

The possibility of using short pitch CLCs with sub-millisecond switching time as diffraction grating has been demonstrated.^[248] A CLC sample was made by mixing a commercially available nematic and high twisting power chiral dopant to induce short pitch (<250 nm). To this mixture, 7% of a reactive mesogen and photoinitiator was added and later polymerized. This mixture was then filled into interdigitated electrodes and planar alignment. When an electric field is applied, a refractive index modulation is induced in the cell, thus behaving as a grating. Up to third order diffraction, spots are observed as the field is applied and the “on” and “off” switching occurs in less than 1 ms.

Another interesting way of using polymer stabilization of CLCs to obtain gratings is by patterning the sample through a sequence of polymerization. Chen and co-workers used the fact that, under the right conditions, both the GM and the DM type can be obtained in a single cell.^[249] For the d/P configuration used ($d/P \approx 1.45$), the DM type aligns parallel to the rubbing direction and occurs at 4.7 V when applying the field from the planar texture while the GM type aligns perpendicular to the rubbing direction and form at 3.6 V after decreasing the field from the homeotropic state. The authors went through different sequence of photomasks that yielded alternating DM and GM regions (stripe pattern) or square regions (checker pattern). Some of these patterns are shown in Figure 17C,D. Distinct diffraction pattern with circular shaped spots is found when using a He-Ne laser probe with high dependence on the polarization of the beam and high efficiency of the zeroth order spots.

3.3.3. Light-Switched Cholesteric LC Grating

There is a recurring desire in the scientific community for light controllable devices, since they represent the true meaning of the word “remote” control, so such device could be started, switched, and terminated with no wires or physical contact whatsoever. In general, photocontrolled CLCs require either photo induced reorientation, caused by light’s electric field or the use of photosensitive materials such as dyes. In general, three manners of fabricating such photocontrolled materials are possible: first, a chiral mesogens with photosensitive groups, second by doping a CLC system with a photosensitive material and third, a chiral dopant with a photosensitive group is used to dope the nematic host.^[33] In practice, the third approach is the most frequently used since it tunes the pitch length resulting in the necessary actions for switching, for example, the diffraction grating.

One of the first CLC grating generated by light was reported by Zolot’ko et al.^[250] A CLC mixture was illuminated at different wavelengths by a laser light source. For 647 nm wavelength, a diffraction pattern appeared resembling a 2D grating. Irradiation with 515 and 488 nm did not produce the diffraction pattern which was compatible with a grating spacing expected to happen when the CLC assumes a wrinkled state. The possible mechanism for driving the system to this state was associated with the reorientation of the director due to light’s electric field or the stress caused by the pitch change during the heating of

the LC material by the laser beam. Other gratings in CLCs have been reported using nonlinear effects through the interference of a laser; similar to what was shown previously for nematic phases, however, with little potential for applications in beam steering devices. The reader interested in these situations may refer to some of the pioneer studies.^[251,252]

The 2D, electrically induced undulated pattern previously discussed^[232] was also obtained under photoexcitation for low power during the initial application of UV light.^[253] To this end, a CLC material was doped with an azobenzene material that suffers conformation change under UV irradiation. The sample, a CLC material doped with low concentration of azo NLC 1005, was filled into a planar aligned cell and displayed the 2D undulated pattern as a consequence to the strain of the CLC layers caused by the elastic response of the material to the change in pitch length. 2D diffraction patterns are reported for focused and unfocused beams of 633 nm laser, which were used to confirm the periodicity of the grating. Figure 18A,B shows the diffraction pattern of unfocused and focused laser beam, respectively.

Optically induced Freédericksz transition may also be used for driving the formation of CLC gratings. This phenomenon occurs when the electric field of light causes reorientation of the director. Although this effect is often used in nematic phases, the order from the substrates reappears right after the illumination is ceased. However, frustrated CLCs can be used in such a way that the information written is stable after the field is shut off. The frustration occurs, for example, when a CLC is filled into a homeotropic alignment cell, where depending on the d/P ratio the helix unwinds in order to satisfy the surface imposition. Typically, such effect happens for $d/P < 1$. If $d/P \approx 1$, the fingerprint organization is still suppressed, but it can be induced by any external stimuli, including light. If the stimulus acts locally, as it happens under computer controlled laser light, the helix is induced at a tiny spot or along a line where the laser is applied. Finely built CLC grating was shown with high diffraction orders and defect mode (dislocation) was used for optical vortices generation.^[254] A similar setup was used but Gaussian beams were used to generate stripe twisted torons, i.e., structures containing two point singularities and a ring of twist-escaped disclination.^[255] By computer controlling the fabrication of an array of torons, 2D diffraction patterns with high order diffraction that can be electric field erased is demonstrated. The array may be square or hexagonal, as observed in the 2D diffracted pattern, shown in Figure 18C,D, respectively. Figure 18E shows the intensity profile in the horizontal direction in Figure 18C while Figure 18F shows the intensity versus voltage behavior of the zeroth-, first-, second-, and third-order diffraction spots for the square array. Recently, field-induced, bubble domains^[256] and polymer-stabilized bubble domains have also been used as diffraction gratings.^[257]

Most applications of CLCs as diffraction gratings rely on the fingerprint or the LH configuration to act as the diffractive element. The advantage of such gratings is that in general, some degree of tunability is possible. For CLCs, in general, the tunability is a consequence of the pitch change induced by some external stimuli such as light. A nematic host was doped with two chiral dopants: one is photosensitive and the other one is not and they induce CLCs of opposite handedness.^[258]

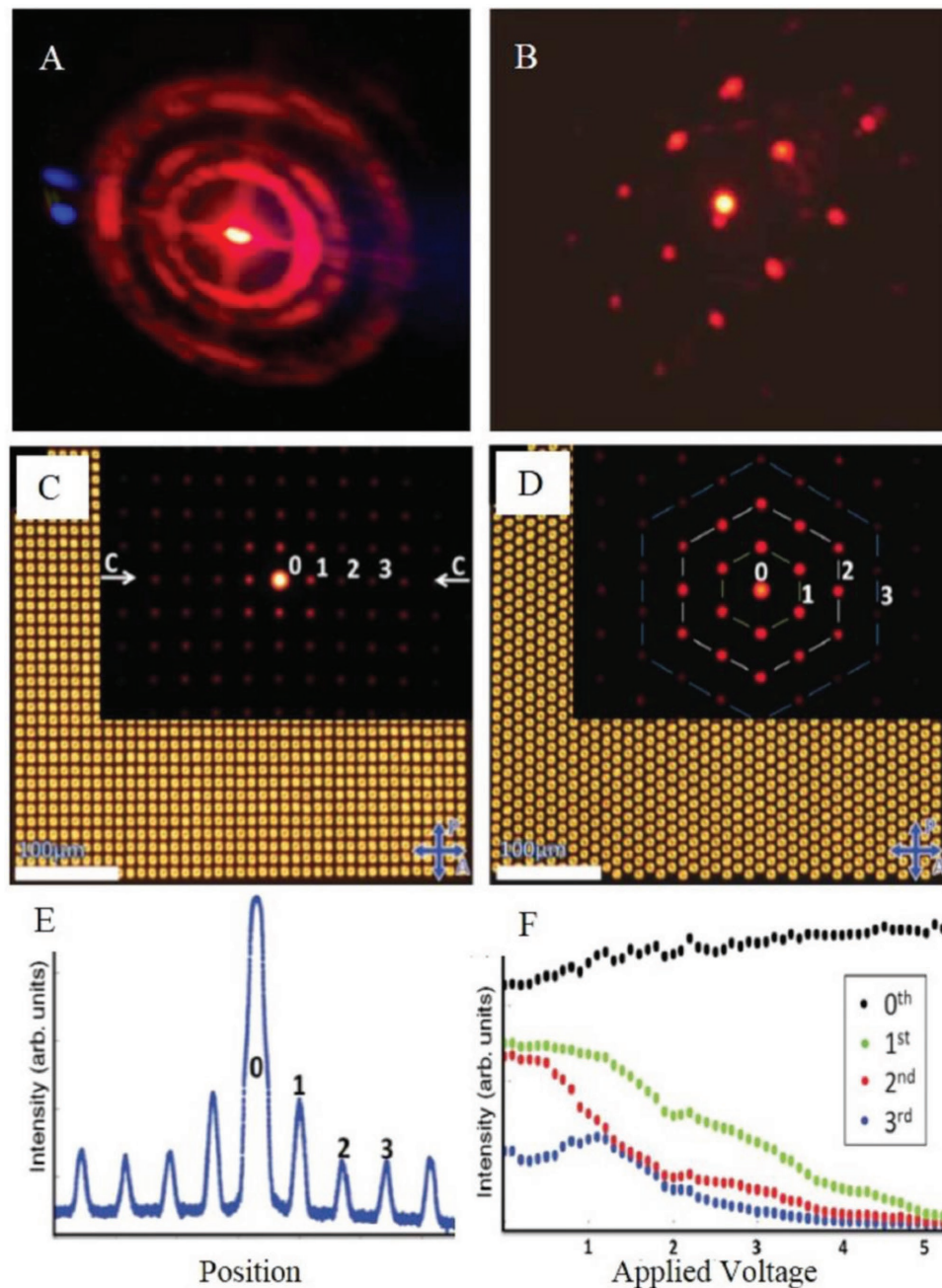


Figure 18. A,B) Diffraction pattern formed by a laser light passing through light-induced undulation in CLCs with the A) unfocused and B) focused probe beams. Adapted with permission.^[253] Copyright 2007, Optical Society of America. The array and its diffraction pattern of the C) square array and D) hexagonal array of laser-generated torons in CLCs; E) the intensity profile along the CC line in (C); F) intensity versus voltage behavior of the zeroth-, first-, second-, and third-order diffraction spots for the square array. Adapted with permission.^[255] Copyright 2012, American Physical Society.

The mixture initially twists in the sense of the photosensitive dopant. Under UV irradiation, the twisting power of the tunable dopant weakens and the mixture goes through the nematic LC and then to the CLC with opposite handedness. The sample is filled into a rubbed homeotropic alignment cell, thus the fingerprint texture. By shinning a probe laser, diffraction patterns are observed through the whole process. This dynamic process allows diffraction angle switching and diffraction efficiency tuning of about 30%. A similar approach has also been

employed,^[259] but with far reaching outcome. The mixture, composed of a nematic host, a nonphotochromic chiral dopant and a photochromic chiral dopant was filled into a hybrid aligned cell. CLCs are known to form well-aligned stripes in the hybrid cell since at the homeotropic side the layers try to align vertically but the opposite planar surface does not allow, causing a sinusoidal arrangement so the CLC becomes spontaneously periodic distorted. The orientation of the stripes depends strongly on the d/P ratio, so the UV radiation, which

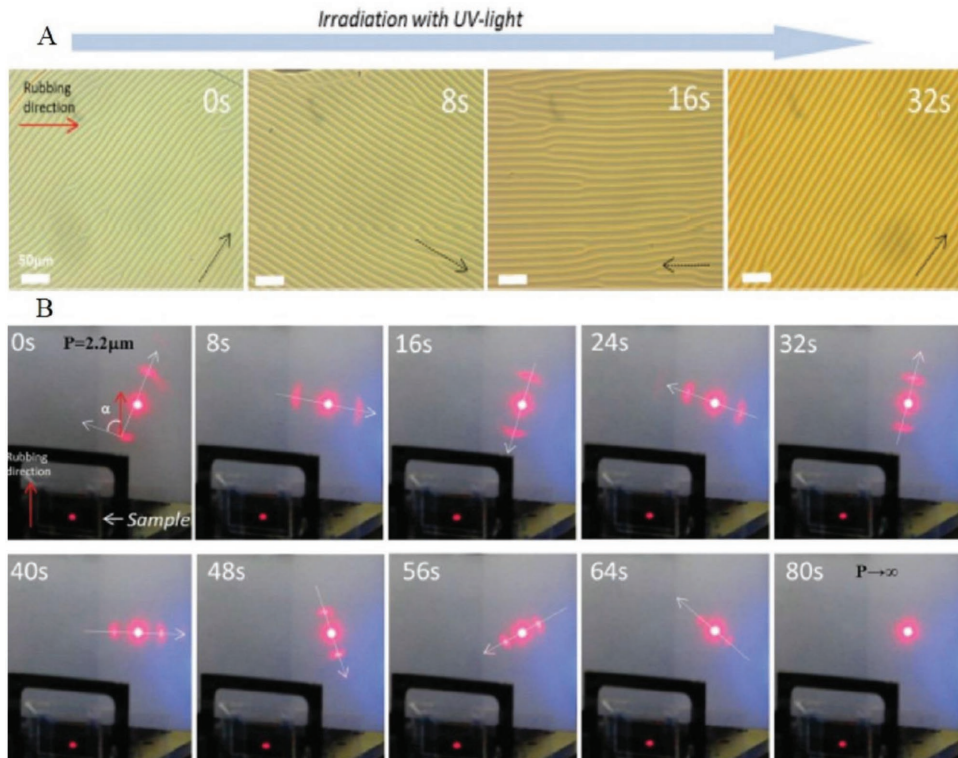


Figure 19. The evolution of the stripe direction in a photosensitive CLC cell (A: POM images) and diffraction pattern (B: diffraction vector) of a photosensitive CLC grating. Adapted with permission.^[259] Copyright 2015, Wiley-VCH.

causes the CLC to unwind, makes the stripes rotate continuously. Continuous rotation of up to 690° is reported under UV radiation. POM images of the stripes and the diffraction pattern rotation with time is shown in Figure 19A (POM) and Figure 19B (diffraction pattern). Since the CLC grating is a phase grating, the beam is circularly polarized in order to avoid maximum/minimum efficiency when the linear polarization is perpendicular/parallel to the grating vector. Recently, light-driven rotation exceeding one or two circles was used for fabricating diffraction gratings in semifree films (CLC anchored at the bottom substrate and in contact with air on the top),^[260] demonstrating analogue rotation of the diffraction pattern as in Figure 19B.

Photoalignment has also been shown to enable the generation of gratings in CLCs. A polarization sensitive sulfonic azo dye was used as the alignment layer and, by using a photolithography method, highly aligned stripes were obtained.^[261] The diffraction pattern presents high integer and half-integer orders. Furthermore, the pattern is the same no matter where the cell is illuminated, indicating the cell is uniformly oriented. The authors also demonstrated circular diffraction pattern from a circularly aligned grating. Surface photopatterning was also employed,^[262] where a holographic method was used to record a periodic design on a photoreactive LC polymer that oriented the director in a planar fashion but with controlled direction of the azimuthal direction. The complex director distribution formed a diffraction grating whose pattern and efficiency depend on the pitch length. Recently, preprogrammed photoalignments films were used to encode information onto a planar oriented CLC

material.^[263] Gratings were thus fabricated by directing the surface alignment to specific patterns, including the generation of Dammann vortex grating. In just 116 nm wavelength interval, up to twenty-five different optical vortex were shown. Such easy yet powerful method demonstrates high precision and reproducibility for CLC grating fabrication with tailored control.

A remarkable advance in the field of remotely controlled gratings was reported by Li and co-workers, where 3D control of the helical axis solely by light stimuli has been achieved.^[264] A dithienylcyclopentene-based, axially chiral molecular switch was used with the nematic host E7 to fabricate a CLC and the mixture was filled into a $3.7\ \mu\text{m}$ homogeneous alignment cell. Upon 310 nm illumination, the chiral dopant switches from an open ring structure to a closed ring one, leading to the inversion of helix sense from right handed to left-handed which is reversible upon 550 nm light irradiation. When UV light is irradiated in the initially planar, right-handed organization, the unwinding process takes place. After the left-handed helix forms, in a few seconds, it disappears and the LH texture is observed. The reverse process, when visible light is used, the left-handed texture turns into the right handed configuration, however, the LH texture remains rotating clockwise by about 40° , until eventually the Grandjean texture is formed again. The balance of cell thickness, surface anchoring, pitch length and external stimuli creates oblique orientation of the director due to interactions of the LC molecules and the rapidly changing chiral switch. 2D beam steering controlled by light is demonstrated along with 1D to 2D diffraction pattern switching through a succession of different array of intensity maxima.

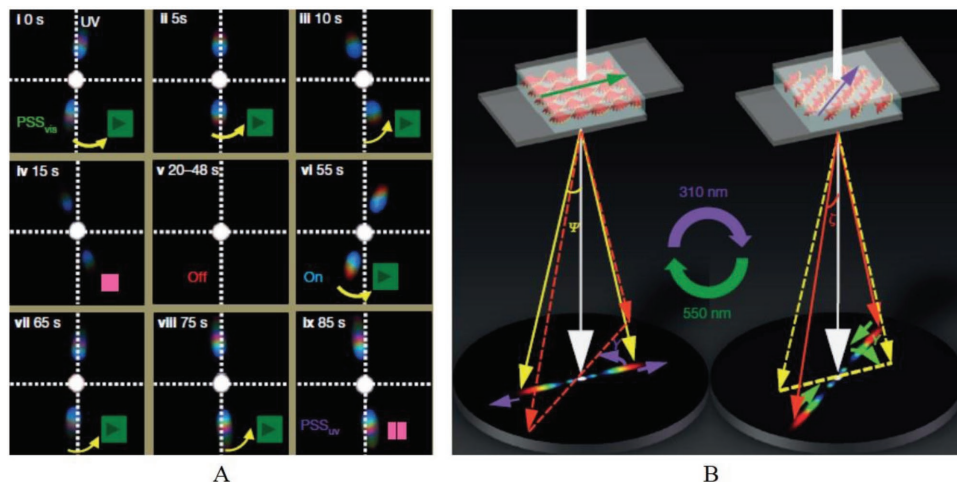


Figure 20. 2D beam steering effect in a light-driven CLC cell. A) The helical axis change and pitch modulation combinedly produce the 2D beam steering effect solely by light irradiation; B) the diagram shows the scheme behind 2D beam steering. Adapted with permission.^[264] Copyright 2016. Macmillan Publishers Limited.

Figure 20A shows the 2D beam steering process governed solely by light irradiation. Figure 20B shows a diagram illustrating this effect.

A distinct CLC grating was fabricated by polymer stabilization of a photoresponsive CLC sample.^[265] The sample, which was mixed with a small amount of a reactive monomer, was photopolymerized prior to being exposed to a 532 nm laser through a periodic photomask. The nonexposed area maintains the pitch length of the original sample, which presents a photonic bandgap. The exposed area has the pitch enlarged, thus changing the photonic properties of these areas. Consequently, a diffraction grating is formed for which the polymer network is used to sharpen the boundaries between adjacent domains. Interestingly, this grating diffracts light on both the transmissive and reflective sides of the sample. The diffracted light can be modulated through application of an electric field and the grating can be erased under uniform light exposure.

In another study, a CLC mixture was doped with an azobenzene derivative and the sample was filled into a homogeneous alignment cell, where the initial d/P ratio was ≈ 2 .^[266] When an electric field is applied, the LH structure is formed. For fields above the critical field for the appearance of the LH structure but lower than the critical field for complete helix unwinding, the pitch length is tuned, increasing as the field increases and consequently decreasing the diffraction angle. On the other hand, UV illumination causes the *trans* isomer to switch to the *cis* isomer, disorganizing the molecular arrangement and decreasing the pitch length, thus increasing the diffraction angle. Simultaneous application and control of both stimuli therefore results in controllable and reversible diffraction angles of up to 19° . In a similar experimental situation, another azobenzene material was used for tuning the CLC grating by electric field and UV radiation.^[267] Since the LH orientation depends on the d/P ratio, the grating could be oriented parallel or perpendicular to the rubbing direction depending on whether developed from the Grandjean texture or from the homeotropic state, since the transient planar texture (when the homeotropic texture is allowed to form the helix again) have

different pitch length. Furthermore, in each configuration UV light tunes the pitch leading to diffraction angle change. An important step was taken when a nematic host was doped with axially chiral molecular switch containing two azo linkages.^[268] Such dopant has very high helical twisting power and the azo groups make it sensitive (change the twisting power) to violet and green light for each isomer, thus the grating is switched by visible light. A small amount of the chiral switch (0.8 wt%) was added to the nematic host E48 and filled into a homogeneous alignment cell. When 3.4 V is applied to the cell, the LH helix structure develops, as shown in Figure 21A. By increasing the field, the observed first-order diffraction angle reduces from 54° to 41° as the pitch elongates. By illuminating the sample with violet light, further decrease of the diffraction angle is observed, within 33° - 54° under continuous illumination. Cycling through violet and green light allows further diffraction angle switching, demonstrating therefore a wide angle beam steering device. The beam steering effect for several illumination times is shown in Figure 21B.

Sun et al. have fabricated a light-driven CLC using a chiral molecular motor.^[269] They have developed a periodic pattern via photopolymerization using photomask technique. This periodic pattern involving alternating planar and focal conic domains of cholesteric liquid crystals causes diffraction of light so they were able to demonstrate light-driven reversible nonmechanical beam steering.

3.3.4. Thermally Switched Cholesteric LC Gratings

Tunability is a key point of LC gratings, since it allows nonmechanical applications, as discussed previously. An important way of controlling gratings is via thermal stimulus, especially for those applications involving change of temperature of the system. Nonetheless, is quite astonishing that very few of such gratings have been reported so far. To this end, CLCs are remarkable candidates since it might, depending on the material used, have a temperature dependent pitch. It is therefore

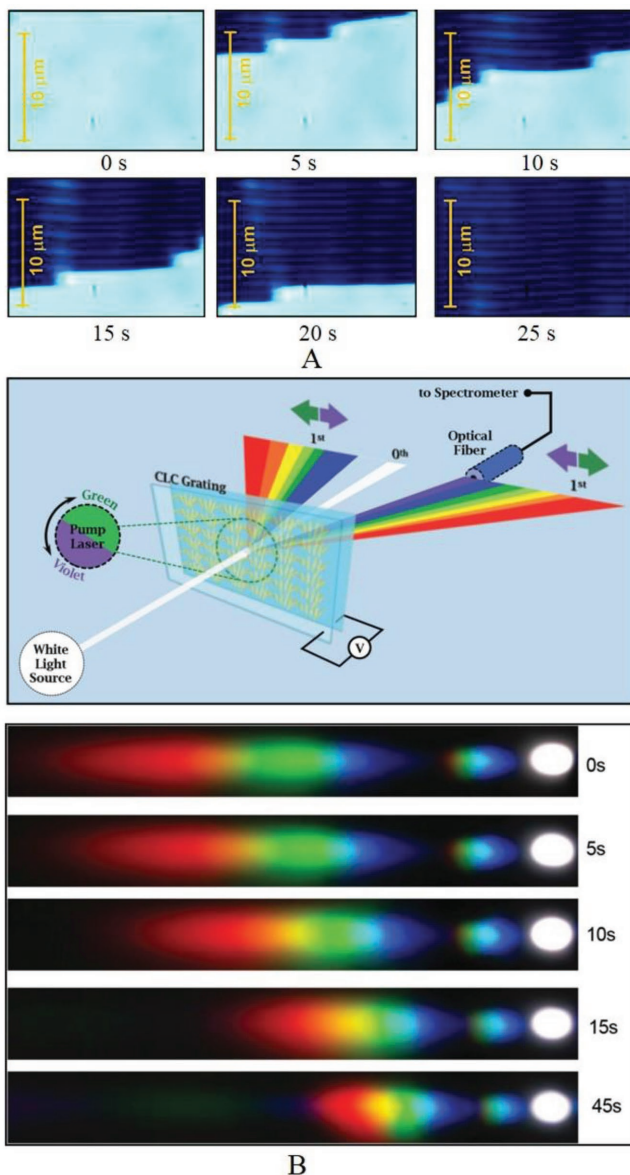


Figure 21. A) The formation process of the cholesteric LC grating with 3.4 V applied voltage; B) light diffraction in a cholesteric LC cell under electric field and light irradiation for different visible light exposition times. Adapted with permission.^[268] Copyright 2014, Wiley-VCH.

expected that some of the techniques described so far can be used with temperature sensitive CLC materials.

Lin et al. designed a rotatable grating^[270] whose working principle is similar to the light-driven rotatable grating,^[259] but the driving stimulus was heat. The authors used two commercially available components, namely, E7 (nematic host) and 4-(2-methylbutyl)-4-cyanobiphenyl (CB15) chiral dopant, to produce CLCs with the d/P ratio ranging from 2.2 to 3.0 and filled the mixtures in hybrid aligned cells. As previously discussed, the CLC under such constraint forms a striped texture. From 25 to 49 °C, the stripes rotate since the pitch length decreases with increasing temperature. The higher the value of d/P is, the larger the angle is rotated, reaching values larger than 100° rotation

during the temperature interval. Similar behavior is possible by changing the thickness of the cell rather than the pitch.^[271,272] The diffraction pattern of this grating therefore continuously rotates under temperature change. The process is reversible as temperature is cooled down. Recently, holographically regulated photoalignment were used to fabricate thermal driven gratings.^[273] A CLC composed of 5CB and CB15 was filled into a cell whose one substrate was coated with such photosurface that had been previously patterned through the interference of two laser beams in a periodic fashion. The top substrate was coated with polyvinyl alcohol (PVA) to induce planar anchoring. Under these circumstances, the CLC material forms periodic structures separated by line defects that form due to the twisted alignment and the alignment layers. Under temperature change, the defect position shifts and this causes a change in the gratings diffractive properties. Diffraction efficiency of roughly 40% for the first-order maxima that can be tuned under temperature change is reported. Other CLC gratings that are temperature sensitive have also been recently reported in the literature but the temperature is not the only driving stimuli for its formation/switching and are discussed below.

Very recently, a thermoresponsive chiral switch was used to dope a nematic host and form a CLC mixture.^[274] The chiral switch possesses high change in helical twisting power under temperature variation, presenting handedness inversion at a certain temperature. Such mixture was added to a planar aligned cell and a low voltage field of 1.25 V was applied to the sample at 22 °C. Under these circumstances, the LH helix structure appears perpendicular to the rubbing direction. As temperature is raised, the pitch elongates, leading to a decrease in the diffraction angle, until at 38 °C where the stripe pattern disappears. Remarkably, further increasing of temperature results in the formation of helix along the opposite direction if the voltage is reduced to 0.75 V where the stripe pattern is again observed, but this time they orient parallel to the rubbing direction. The reduction of the applied field is understood because the pitch gets longer so the critical field for the LH formation decreases. The switching in the grating direction is caused by the orientation of the director in the middle layer of the cell at each temperature. Under further temperature rising, the pitch continuously increases, further reducing diffraction angle but now in the orthogonal direction. The POM images and the schematic illustrations are given in Figure 22. Therefore, the grating switches 90° in direction, enabling nonmechanical beam steering along two orthogonal directions.

3.3.5. Dual Stimuli-Driven Cholesteric LC Gratings

In certain situations, more than one simultaneous stimulus might be needed to drive the formation and/or switching of the grating. Although this adds a certain degree of complexity in the operation, it also improves the controllability, precision and overall usefulness of the grating. In fact, this is a quite common strategy when driving LCs for several different applications. As previously seen, diffraction gratings based on azobenzene polymer stabilized LCs have already been reported.^[152]

The use of dual stimuli in general means one of them is used to generate the grating and the other one is to manipulate

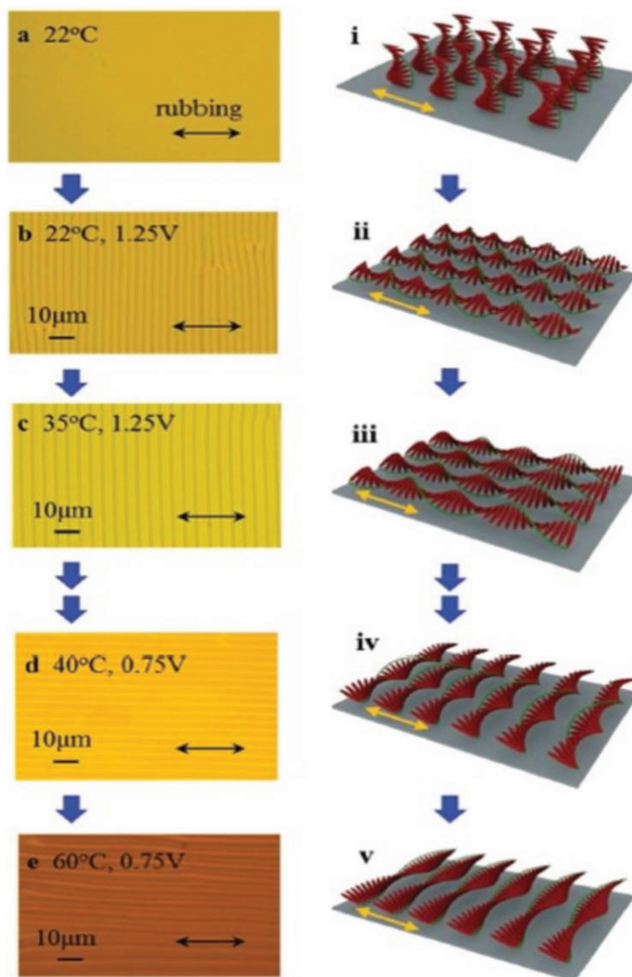


Figure 22. Thermally sensitive CLC grating. POM images and the corresponding schemes of the helix in the planar orientation b–ii) and in the lying helix configuration with different pitch lengths and orthogonal orientation (compare iv) and (v)). Adapted with permission.^[274] Copyright 2017, Wiley-VCH.

and switch the stripes. One of the first examples of dual stimuli CLC gratings was reported by Fuh et al.^[275] A CLC mixture was doped with a dichroic guest-host dye (2 wt%) and the sample was filled into a slab cell previously treated for inducing planar alignment. The dye absorbs the light of a pump beam and consequently induces temperature change. The sample, with a pitch of approximately 2.2 μm , is subjected first to an external AC voltage of 2.3 V and the fingerprint texture is formed. Upon changing the pump laser (Ar^+) power, the diffraction pattern of a He-Ne probe beam changed its efficiency of the first (decreased) and second order (increased). Second order diffraction angle also was observed to change. It was attributed to the heat generated by the pump beam that weakens the surface anchoring. The heat thus broadens the grating spacing in the interior of the cell (where the spacing is $P/2$). Moreover, it causes a narrow surface twist region with spacing P .

A controllable zigzag grating was recently reported under the dual stimuli of electric field and light irradiation.^[276] A photo-sensitive chiral switch was used to form a CLC material. The

switch promotes helix inversion under continuous UV irradiation, going from right handed to left handed during the exposition. The material, filled into a planar alignment cell, has $d/P = 1$ initially when a voltage of 1.0 V is applied, thus forming the LH texture perpendicular to the rubbing direction. Upon UV irradiation, with the field maintained, the helix unwinds, passing through the nematic LC until it forms the LH texture with left handedness. As the d/P ratio grows, caused by the decreasing of pitch in the left-handed configuration, the straight stripes start to bend, forming a zigzag pattern that lasts from $|d/P| = 1.2$ until $|d/P| = 1.8$. The zigzag pattern is caused by the orientation coupling of the LH structure, since it may orient perpendicular or parallel to the rubbing direction and as the d/P ratio changes, the system reaches an intermediate point where both orientations can be energetically favorable. Such zigzag texture was used as a CLC grating, and yielded distinct diffraction patterns, as shown in Figure 23A,B. Initially, a 1D pattern is observed, where the diffraction angle of the first-order spot quickly changes as the pitch is tuned under UV exposition. When the zigzag appears, a bracket shaped pattern that increases and decreases as the zigzag angle changes is observed, opening up new possibilities for photonic devices, and fabricate variable photomask methodologies and surfaces with distinct topologies. MR doped CLCs were used to fabricate controllable gratings. The CLC mixture, which due to MR molecules is photosensitive, has different initial organization in a twisted planar geometry upon light illumination, which allows for multivariant control of electric field-controlled stripes, resulting in dynamical diffraction gratings.^[277] Recently, even light-controlled electroconvection patterns on CLCs doped with photosensitive materials under AC fields were demonstrated to be a route for controllable gratings.^[278]

3.4. Blue Phase LC Gratings

Blue phases are a group of remarkable chiral LC phases with fascinating optical properties. BPs are observed in highly chiral LCs and are basically composed of double twist cylinders that form a defect lattice and arrange themselves in symmetric structures, such as simple cubic (BPII) or body-centered cubic (BPI) lattices. The BPs with cubic lattices exhibit Bragg reflection and have attracted considerable attention in the past decade due to their potential applications.^[279,280] Similar to the CLC phases, BPs may also be used as diffraction gratings. In the past years, LCs exhibiting BPs have attracted a lot of attention due to their potential applications in several areas ranging from displays to photonic applications.^[280–285] The BPs are isotropic Kerr medium, but under an electric field they become anisotropic. There are certain advantages of using BPs in a given application, especially for diffraction gratings: they do not require an alignment layer, which simplifies fabrication process; they present very fast response time, in the order of microseconds and, because of the medium's optical properties, the grating is polarization independent. These features come from the fact that, in many applications, the desired response comes from the distortion of the crystal lattice structure, which restores much quicker than the reorientation process of nematics and does not require alignment.

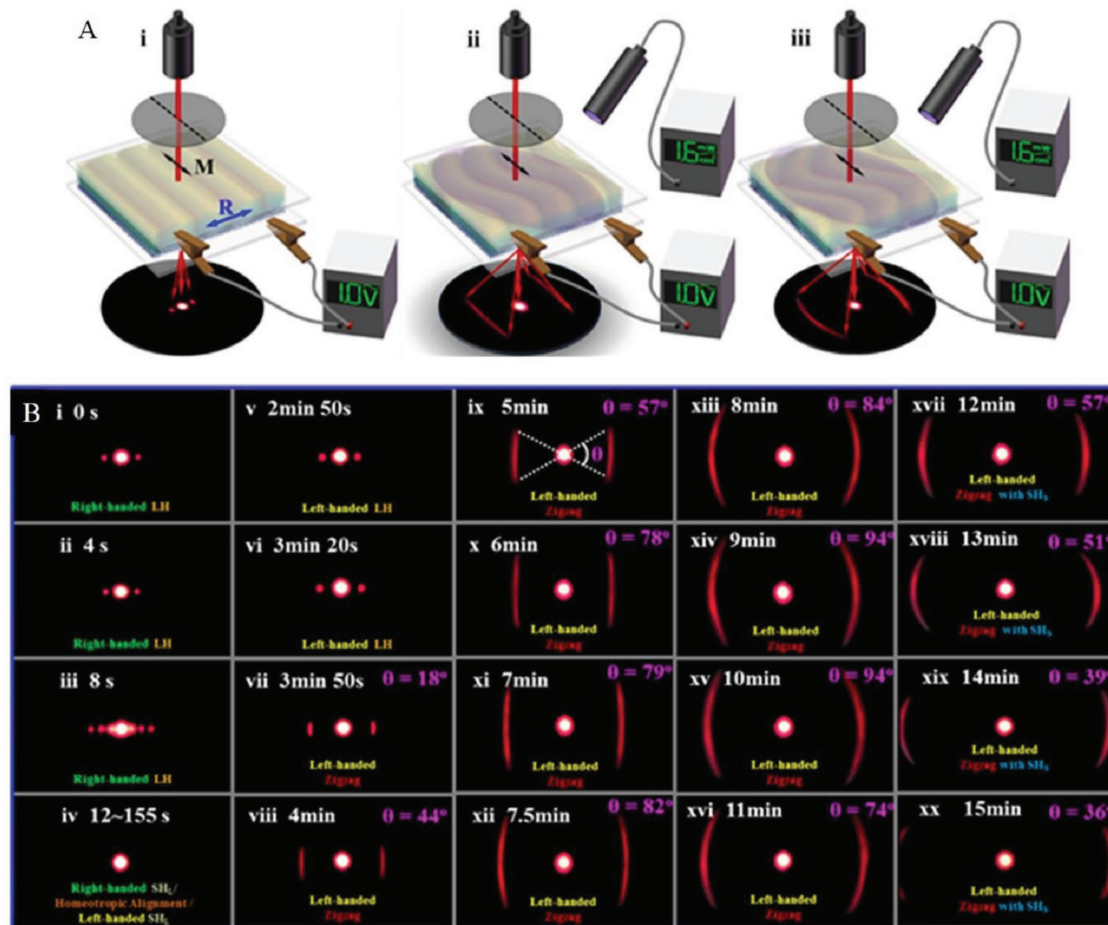


Figure 23. A) Dual stimuli (electric field and light irradiation) driven CLC cell that produces the zigzag pattern; B) diffraction pattern of a probe beam while the stripes change from straight to zigzag. As the zigzag angle increases, the well-defined nonzero spots become arc shaped. The arc angle grows initially and then decreases, while the arc distance from zeroth order continuously increases. Adapted with permission.^[276] Copyright 2017, Wiley-VCH.

Unfortunately, there are not many reports of BP LC gratings in the literature. In fact, one of the first reports occurred as recently as 2011.^[286] This grating takes advantage of polymer stabilization in order to function. BP LCs are incredible delicate mesophases that usually appear in a temperature interval of just about 1 °C. Furthermore, BP LCs do not have a natural grating architecture as CLCs have, so they need some kind of patterning to behave as a grating. To this end, Kikuchi et al. demonstrated that BP LCs can be polymer stabilized (PSBP), thus stabilizing in a temperature interval of up to 60 K.^[279] It also allows pattern stabilization of the phase once an external stimulus is used to fabricate the grating. Wu and co-workers reported that when a BP LC mixed with monomer and photoinitiator was injected into an IPS (in-plane switching) cell and then UV photopolymerized, weak diffraction is observed at zero fields from the striped electrodes.^[286] Nonetheless, during field on state, birefringence is induced in the field zone, causing a periodic distribution of refractive index and, therefore, a diffraction pattern with several orders is observed and up to 40% diffraction efficiency is reported. Furthermore, sub-millisecond switching for all the diffraction orders occurs. Nonlinear optical diffraction gratings were shown recently in dye doped BP LCs

caused by two interfering continuous wave lasers.^[287] Undoped samples showed small optical nonlinearities but the samples doped with MR dye produce strong nonlinear self-diffraction effects. The self-diffracted pattern is polarization independent and is attributed to director axis reorientation, disorder, and lattice distortion by the laser-excited dye molecules. Photoinduced phase transition in BPs doped with azobenzene bent shaped molecules were recently demonstrated.^[288] By UV illuminating the sample through a photomask, isotropic domains are induced in the illuminated areas. Striped patterns are demonstrated with potential for fabrication of gratings and applications in data storage systems.

Another BP LC was photopolymerized after being filled into a cell with stripe electrodes, however, both substrates were patterned in an orthogonal manner.^[289] As a result, whenever both substrates were set for voltage on, the BP could be switched in a 2D fashion, thus yielding 2D diffraction patterns, as shown in **Figure 24A**. When used in the 1D mode, 37% efficiency is achieved while up to 90% efficiency is reported for 2D patterns. Along with sub-millisecond switching, and lower driving voltage (due to larger Kerr constant) when compared to the previously reported work. A similar study was focused on the

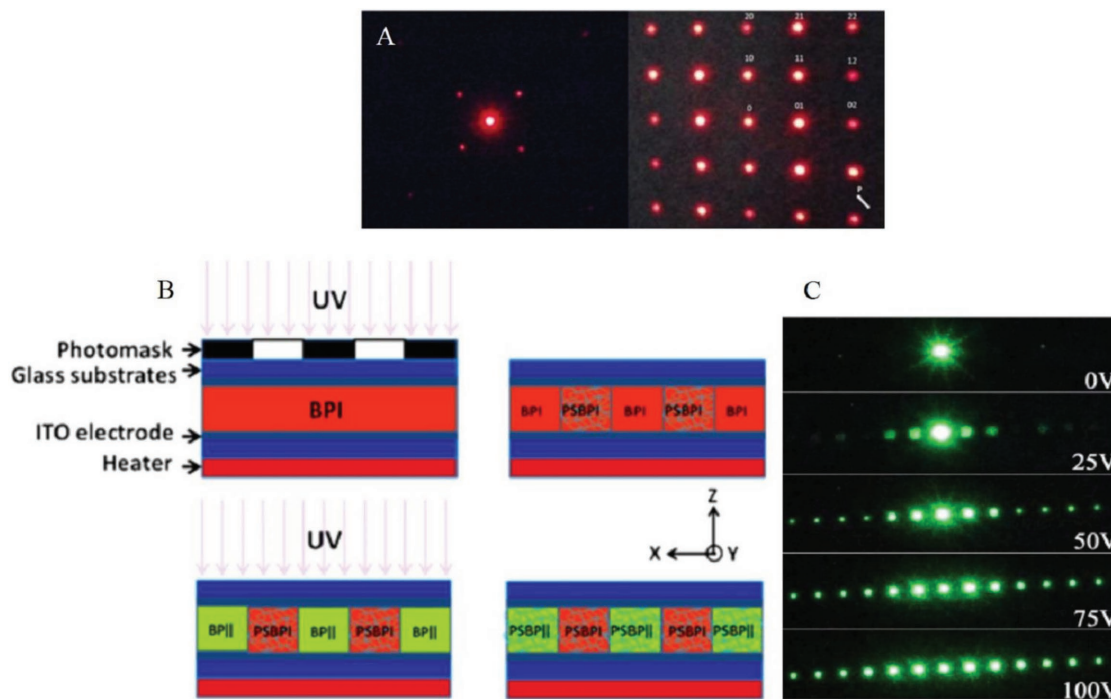


Figure 24. A) 2D diffraction pattern of BP LC grating working with striped electrodes. Adapted with permission.^[289] Copyright 2012, American Institute of Physics; B) fabrication of the hybrid BP LC grating with two Kerr constants. Adapted with permission.^[293] Copyright 2013, American Institute of Applied Physics; C) examples of diffraction patterns for the dual-period BP grating for several applied voltages (large period). Adapted with permission.^[294] Copyright 2015, Optical Society of America.

polarization independence caused by the vertically applied field on the two patterned, orthogonal substrates.^[290] A few years later, fork-like electrodes were patterned on one of the substrates (while the other was coated with ITO) to induce fork phase profile. The PSBP was then successfully used for creating fast beam vortex.^[291]

As previously discussed for the case of nematic phase, a polymer slice structure has been used to fabricate a BP grating with high efficiency.^[292] A photoresist was spin-coated on an ITO covered glass and exposed through a photomask to collimated UV light. The exposed zones are removed after developing the photoresist, so the unexposed areas form a periodic structure with depth equal to the resist thickness. Then, it is assembled with another ITO glass on top and the LC material is filled in. The grating can be field controlled and responds in sub-millisecond manner. The sharp phase profile yields high efficiency, polarization independence and tunability of several diffraction spots with electric field. The dependence of the Kerr constant on curing temperature was used to fabricate a diffraction grating.^[293] A BP LC material was mixed with monomer and photoinitiator and the sample was injected into an ITO coated cell. The sample was exposed to UV light in order to cure the polymer with a patterned photomask first at 34 °C, where the material is in the BP I. Then, the sample is heated to 38 °C, when it transits to the BP II, the photomask removed and again exposed to UV light. As a result, two periodically repeating zones were formed: one with polymer stabilized BP I and the other with polymer stabilized BP II. The resulting grating is polarization independent and fast, although the

efficiency is low due to the small phase difference between BP I and BP II. The fabrication process and the grating are shown in Figure 24B.

The pursuit for advanced gratings using BPs is still under way. A polymer stabilized BP LC was filled into a slab cell at which the top substrate had an electrode without pattern while the bottom substrate had two pairs of interdigitated electrodes, called Comb A and Comb B.^[294] The field can be applied from Comb A to Comb B or between the fingers of a given comb, without using the other one. As a result, two different gratings are available within the same sample. High efficiency, polarization independence and fast response time is achieved in both configurations. Figure 24C shows examples of diffraction patterns under different applied voltages.

More recently, another kind of dual stimuli tunable grating was proposed.^[295] The grating uses just one set of interdigitated electrodes on the bottom substrate and a plain electrode on the top to drive the change in refractive index. Nonetheless, the authors simultaneously applied a DC field with the AC signal changing the component of the field in the vertical direction with respect to the horizontal direction. Consequently, the grating period was tuned as the magnitude of the AC and DC fields were switched. By using a polymer stabilized BP LC, the diffraction angle could be varied, maintaining high efficiency, polarization independence and fast response time reported before. In a recent work, a 2D switchable polymer stabilized BP grating was fabricated by nanosphere lithography.^[296] Besides interdigitated electrodes, regular ITO coated electrodes have been used to drive a polymer stabilized BP LC grating.^[297] To

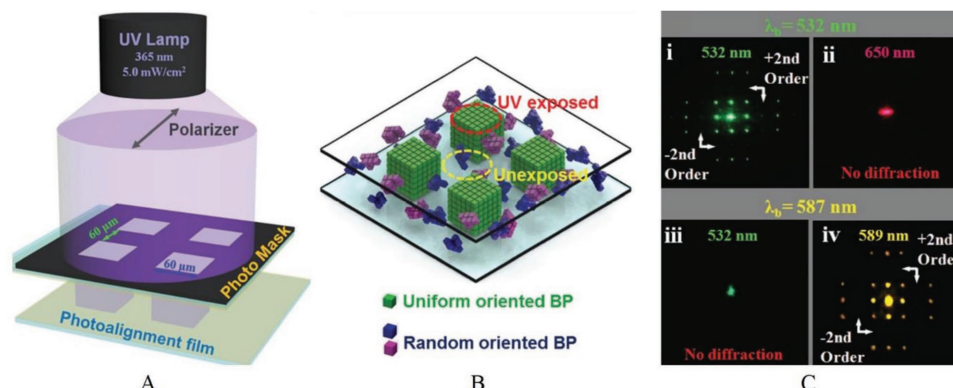


Figure 25. A,B) Photopolymerization of blue phase material with designed photomask, yielding uniform oriented BP regions (exposed area) and random orientated regions (not exposed areas); C) 2D diffracted pattern that is wavelength dependent. Adapted with permission.^[299] Copyright 2017, Wiley-VCH.

accomplish this, the photopolymerization process was carried out by exposing the cell to two interfering visible laser beams. The bright regions result in higher polymer concentration than the dark region, so the electric field, when applied, has different effects on the director switching process, thus resulting in a periodic arrangement. Several diffraction spots are realized depending on the voltage applied, with high efficiency, sub-millisecond response time and polarization independence. Ultra-fast switching was also recently observed in a BP grating thanks to the use of chiral polymer stabilization.^[298]

A clever design has been recently used by Li and co-workers.^[299] By using a photomask, a BP was polymer stabilized according to desired patterns, resulting in uniformly oriented regions that were exposed to UV light and other regions with random oriented BP, as shown in Figure 25A,B. Beautiful 2D patterns were demonstrated, including 2D lattice and grating shaped designs that are thermally and electric field driven. The patterns can be used, as 2D diffraction gratings that are wavelength dependent, as demonstrated in Figure 25C. Zhou et al. disclosed a reversible transformation between BP II and CLC driven by light that is enabled by a molecular switch functionalized nanocage.^[300] Using a photomask technique, they fabricated a pattern with alternating BP regions and cholesteric regions that yields a diffraction pattern. This diffraction can be switched off by driving the entire LC film to either the CLC phase or BP II.

All the described BP gratings show their great potential they possess. Although they have not been extensively explored, it is expected that in the near future more BP gratings with high efficiency would be realized.

4. Summary and Perspective

Nature is full of examples of periodic structures that give rise to unique properties. From periodic molecular arrangements, genetic codification of living organisms, to periodic distribution of sand dunes and fingerprints, periodic disposition of components is a clever way to emulate nature to design smart and functional structures. Scientists and engineers do not hesitate in “borrowing” ideas from nature, as nature has had plenty of time to perfect them. In fact, this is “required”

when designing synthetic versions of natural materials toward the fabrication of smart materials to advance state-of-the-art devices. Controlled periodic structures are, therefore, an important step when fabricating smart materials, especially those designed for a specific function, such as in diffraction gratings. Next-generation devices require nonmechanical capabilities and easy tunability for adapting to the most varied situations, including, but not limited to, beam steering and quick sample spectroscopy. LCs are suitable candidates for fulfilling these needs since they have the right structure and switching characteristics for stimuli directed, nonmechanical tunable gratings. During the past few years, significant advances in the LC grating field have been made. Herein, we have summarized the development, material designs, capabilities, and the several kinds of LC gratings reported in the literature, and especially the methods of fabricating and controlling such gratings. It is evident that LC gratings are emerging as a new class of stimuli controlled optical devices for applications that range from basic material characterization to astronomy. In this review, we focused on the nematic, smectic, chiral nematic phases, and blue phases used for the fabrication of diffraction gratings. From the pioneer works that used electroconvective patterns in the nematic LC, interesting grating behavior of well-known patterns such as Williams and Chevron domains, including 2D diffraction patterns, were discovered. New cell designs in combination with specially designed materials for the bounding surfaces (as in the use of photoconductive layers) including photolithography process for designing special electrodes pushed the development of nematic gratings even further. Impressive results, including blazed gratings with high diffraction efficiency and phased arrays that are applicable for small and large-angle beam steering devices, have been reported. Many of the gratings are surface relief structures that produce high efficiency diffraction. Needless to say that, in all these cases, the grating is electrically switchable. The development of materials with improved capabilities has allowed optically switchable nematic gratings through nonlinear effects and holographically writable gratings, including those doped with photosensitive materials. Mixtures with polymer networks have also been extensively used for structure and high diffraction efficiency switchable gratings either by applying an electric field or light irradiation.

Specially designed cells with hybrid alignment have been used for SmA gratings, for which the periodic arrangement of helicylinders in thin cells or the periodic array of focal conics formed in thicker cells has been explored for switchable gratings. Nonetheless, the surface stabilized SmC*, thus in the ferroelectric mode, has been the main focus in several contexts, including the cases of dye-doped systems and polymer stabilization. When photosensitive alignment layers are used, in combination with periodic photomasks, optical gratings that can be switched with field, fast response time, high diffraction efficiency, and 2D diffraction capabilities have been demonstrated.

CLCs have been extensively studied in recent years and are emerging as new technologies for nonmechanical beam steering and as switchable gratings. CLCs have the advantage that, under appropriate situation, their structure naturally forms a grating. Under an applied electric field, the pitch can be reversibly tuned and the helical axis direction can be reversibly switched, resulting in change of the diffracted angle and the diffraction pattern direction. Undulations of the CLC layers also result in 2D diffraction gratings. Remarkably, if the CLC material is filled into a hybrid aligned cell, the lowest free energy organization is the stripe pattern. Such pattern continuously rotates under electric field, allowing grating vector control. Through polymer templating, improved diffraction efficiency, sub-millisecond switching time, and interesting patterns can be designed resulting in distinct diffraction patterns. Light-driven CLC gratings are especially important toward the fabrication of nonmechanical beam steering devices. Specially designed chiral molecular switches or motors have been explored recently toward light irradiation control of gratings. Optically induced Freédericksz transition is also a possibility for locally writing information in a CLC cell. The use of photosensitive chiral dopants, whose HTP value changes under light irradiation, permits the creation of gratings that rotate continuously as the sample is irradiated by light. Azobenzene derivatives have been extensively employed as the photochromic moiety, but recently other photochromic groups have been explored, such as dithienylcyclopentene-based, axially chiral molecular switch. Up to 690° rotation of the grating vector, surface photopatterning and remarkable 3D control of the helical axis have also been demonstrated with promising outcomes, including 1D to 2D diffraction patterns under light illumination only. Thermoresponsive materials and gratings working under dual stimuli are other fascinating examples of responsive gratings. Recently, polymer stabilized BPs have begun to draw attention. Although a few examples have been demonstrated in the literature so far, BPs are highly promising since they allow sub-millisecond switching, polarization independence, and high diffraction efficiency.

The possibility of using synthetic materials to fabricate and mimic naturally occurring systems is an exciting idea since it helps to elucidate the key aspects of the natural patterns. The functionalization of such synthetic patterns has, therefore, dual advantage since it can both help advance understanding natural phenomena and it is readily applied in smart devices, which is the case in LC diffraction grating. The future seems bright for the development of new materials, i.e., mesogens

and dopants, for LC gratings. In the nematic LC, functionalized surface anchoring layers are expected to play a major role, especially the light-driven anchoring layers capable of switching and controlling the diffractive characteristics of the gratings. Smectic LCs, on the other hand, have great potential since they can be used to construct interesting periodic structures. Currently, it seems only the “tip of the iceberg” has been touched for most of the smectic phases, although surface stabilized ferroelectric LCs are evolving for robust and fast switchable gratings. Newly synthesized dopants, including chiral switches and functionalized nanoparticles, appear as very promising technologies when combined with CLC materials. The synthesis and development of functionalized dopants with intense response to a given stimulus seem to be an important area of study toward full control and wide beam steering devices that shall soon become a reality with nonmechanical switching capabilities. It is worth mentioning that BPs are just starting to be used as gratings. New materials that enable lower driving voltages (high Kerr constant) and photoresponsivity appear to be the route these gratings will follow. George R. Harrison, one of the former heads of the MIT’s Spectroscopy Laboratory, accurately summarized the importance of diffraction gratings: *It is difficult to point to another single device that has brought more important experimental information to every field of science than the diffraction grating. The physicist, the astronomer, the chemist, the biologist, the metallurgist, all use it as a routine tool of unsurpassed accuracy and precision, as a detector of atomic species to determine the characteristics of heavenly bodies and the presence of atmospheres in the planets, to study the structures of molecules and atoms, and to obtain a thousand and one items of information without which modern science would be greatly handicapped.*^[4] LCs are now one of the systems responsible for continuing this revolution, which can march forward quickly if the grating becomes lighter, more agile, flexible, nonmechanically and remotely controlled, and capable of switching on and off as desired. For about 50 years, scientists around the globe have been working toward making this vision a reality. LCs, in fact, are fascinating materials that surprise us every day with the great number of ways they can be used in state-of-the-art devices. As diffraction gratings, although there is plenty of room for improvements, they have already proven to be one of the routes for controlling light with the right characteristics that future devices shall require.

Acknowledgements

R.S.Z. and H.K.B. contributed equally to this work. We are thankful for the support from the Air Force Office of Scientific Research (AFOSR), the Air Force Research Laboratory (AFRL), the Department of Defense (DoD) Multidisciplinary University Research Initiative, the National Science Foundation, DoD-Army, the National Aeronautics and Space Administration (NASA), and the Ohio Third Frontier. R.S.Z. thanks the National Institute of Science and Technology Complex Fluids (INCT-FCx, Brazil).

Conflict of Interest

The authors declare no conflict of interest.

Keywords

diffraction, grating, light direction, liquid crystals, stimuli-responsive

Received: September 23, 2018

Revised: October 22, 2018

Published online:

- [1] A. Ashkin, J. M. Dziedzic, J. E. Bjorkholm, S. Chu, *Opt. Lett.* **1986**, 11, 288.
- [2] D. G. Grier, *Nature* **2003**, 424, 810.
- [3] J. R. Moffitt, Y. R. Chemla, S. B. Smith, C. Bustamante, *Annu. Rev. Biochem.* **2008**, 77, 205.
- [4] E. G. Loewel, E. Popov, *Diffraction Gratings and Applications*, Marcel Dekker Inc., New York **1997**.
- [5] C. Palmer, *Diffraction Grating Handbook*, Newport Corporation, New York **2005**.
- [6] D. Rittenhouse, *J. Am. Philos. Soc.* **1786**, 201, 202.
- [7] J. M. Cowley, *Diffraction Physics*, Elsevier B.V., Amsterdam **1995**.
- [8] T. Young, *Philos. Trans. R. Soc. London* **1802**, 92, 12.
- [9] J. V. Fraunhofer, *Ann. Phys. Phys. Chem.* **1823**, 74, 337.
- [10] G. R. Harrison, E. G. Loewen, *Appl. Opt.* **1976**, 15, 1744.
- [11] M. G. Moharam, L. Young, *Appl. Opt.* **1978**, 17, 1757.
- [12] D. Yang, S. Wu, *Fundamentals of Liquid Crystal Devices*, Wiley & Sons, Chichester **2006**.
- [13] H. Nematic, D.-K. Yang, K.-L. Cheng, C.-C. Liang, J.-W. Shiu, C.-C. Tsai, R. S. Zola, *J. Appl. Phys.* **2012**, 112, 124513.
- [14] N. Bonod, J. Neauport, *Adv. Opt. Photonics* **2016**, 8, 156.
- [15] G. Qin, P. B. Dennis, Y. Zhang, X. Hu, J. E. Bressner, Z. Sun, W. J. Crookes-Goodson, R. R. Naik, F. G. Omenetto, D. L. Kaplan, *J. Polym. Sci., Part B: Polym. Phys.* **2013**, 51, 254.
- [16] R. J. Baskin, K. P. Roos, Y. Yeh, *Biophys. J.* **1979**, 28, 45.
- [17] S. Kinoshita, S. Yoshioka, J. Miyazaki, *Rep. Prog. Phys.* **2008**, 71, 076401.
- [18] H. M. Whitney, M. Kolle, P. Andrew, L. Chittka, U. Steiner, B. J. Glover, *Science* **2009**, 323, 130.
- [19] A. R. Parker, *Philos. Trans. R. Soc., A* **2004**, 362, 2709.
- [20] Y. Liu, J. Shigley, K. Hurwit, *Opt. Express* **1999**, 4, 177.
- [21] B. K. Hsiung, R. H. Siddique, D. G. Stavenga, J. C. Otto, M. C. Allen, Y. Liu, Y. F. Lu, D. D. Deheyn, M. D. Shawkey, T. A. Blackledge, *Nat. Commun.* **2017**, 8, 2278.
- [22] H.-Z. Yu, *Chem. Commun.* **2004**, 2633.
- [23] K. Van Acoleyen, W. Bogaerts, J. Jágerská, N. Le Thomas, R. Houdré, R. Baets, *Opt. Lett.* **2009**, 34, 1477.
- [24] K. Van Acoleyen, H. Rogier, R. Baets, *Opt. Express* **2010**, 18, 13655.
- [25] D. Kwong, A. Hosseini, Y. Zhang, R. T. Chen, *Appl. Phys. Lett.* **2011**, 99, 051104.
- [26] J. C. Hulme, J. K. Doylend, M. J. R. Heck, J. D. Peters, M. L. Davenport, J. T. Bovington, L. A. Coldren, J. E. Bowers, *Opt. Express* **2015**, 23, 5861.
- [27] *Liquid Crystals beyond Displays: Chemistry, Physics, and Applications* (Ed: Q. Li), John Wiley & Sons, Hoboken, NJ **2012**.
- [28] L. Wang, Q. Li, *Adv. Funct. Mater.* **2016**, 26, 10.
- [29] L. Wang, A. M. Urbas, Q. Li, *Adv. Mater.* **2018**, 30, 1801335.
- [30] L. S. Hirst, G. Charra, *Nature* **2017**, 544, 164.
- [31] H. K. Bisoyi, Q. Li, *Acc. Chem. Res.* **2014**, 47, 3184.
- [32] Y. Li, C. Xue, M. Wang, A. Urbas, Q. Li, *Angew. Chem., Int. Ed.* **2013**, 52, 13703.
- [33] Y. Wang, Q. Li, *Adv. Mater.* **2012**, 24, 1926.
- [34] *Nanoscience with Liquid Crystals: From Self-Organized Nanostructures to Applications* (Ed: Q. Li), Springer, Heidelberg **2014**.
- [35] *Functional Organic and Hybrid Nanostructured Materials: Fabrication, Properties, and Applications* (Ed: Q. Li), Wiley-VCH, Weinheim **2017**.
- [36] H. K. Bisoyi, Q. Li, *Chem. Rev.* **2016**, 116, 15089.
- [37] A. M. Figueiredo Neto, S. R. A. Salinas, *The Physics of Lyotropic Liquid Crystals: Phase Transitions and Structural Properties*, Oxford University Press, New York **2005**.
- [38] H. K. Bisoyi, Q. Li, *Kirk-Othmer Encyclopedia of Chemical Technology*, Wiley, New York **2014**.
- [39] *Pattern Formation in Liquid Crystals* (Eds: A. Buka, L. Kramer) Springer, New York **1996**.
- [40] I. Dierking, *Textures of Liquid Crystals*, Wiley-VCH, Weinheim **2003**.
- [41] W. Helfrich, *J. Chem. Phys.* **1969**, 51, 4092.
- [42] P. A. Penz, *Phys. Rev. Lett.* **1970**, 24, 1405.
- [43] R. Williams, *J. Chem. Phys.* **1963**, 39, 384.
- [44] C. Deutsch, P. N. Keating, *J. Appl. Phys.* **1969**, 40, 4049.
- [45] S. Lu, D. Jones, *J. Appl. Phys.* **1971**, 42, 2138.
- [46] P.-G. de Gennes, *The Physics of Liquid Crystals*, Clarendon Press, Oxford **1974**.
- [47] E. W. Aslaksen, B. Ineichen, *J. Appl. Phys.* **1971**, 42, 882.
- [48] W. Greubel, U. Wolff, *Appl. Phys. Lett.* **1971**, 19, 213.
- [49] T. O. Carroll, *J. Appl. Phys.* **1972**, 43, 767.
- [50] R. A. Kashnow, J. E. Bigelow, *Appl. Opt.* **1973**, 12, 2302.
- [51] E. Guyon, I. Janossy, P. Pieranski, J. M. Jonathan, *J. Opt.* **1977**, 8, 357.
- [52] A. Takase, S. Sakagami, M. Nakamizo, *Jpn. J. Appl. Phys.* **1975**, 14, 228.
- [53] W. S. Quon, E. Wiener-Avnea, *Solid State Commun.* **1974**, 15, 1761.
- [54] M.-Y. Xu, M. Zhou, Y. Xiang, P. Salamon, N. Éber, Á. Buka, *Opt. Express* **2015**, 23, 15224.
- [55] H.-Z. Jing, Y. Xiang, M.-Y. Xu, Z.-D. Zhang, Z. Cheng, D. Shen, Z.-G. Zheng, J.-L. Li, M.-J. Zhou, E. Wang, Y.-Q. Wang, Y.-H. Cai, *Opt. Mater. Express* **2016**, 6, 2584.
- [56] R. Yuan, W.-J. Ye, H.-Y. Xing, Z.-J. Li, T.-T. Sun, Y.-B. Sun, J.-L. Zhu, Y. Xiang, Z.-Y. Zhang, M.-L. Cai, *Opt. Express* **2018**, 26, 4288.
- [57] N. Éber, Y. Xiang, Á. Buka, *J. Mol. Liq.* **2018**, 267, 436.
- [58] Y. Hori, K. Asai, M. Fukai, *IEEE Trans. Electron Devices* **1979**, 26, 1734.
- [59] B. H. Soffer, J. D. Margerum, A. M. Lackner, D. Boswell, A. R. Tanguay, T. C. Strand, A. A. Sawchuk, P. Chavel, *Mol. Cryst. Liq. Cryst.* **1981**, 70, 145.
- [60] A. R. J. Tanguay, W. C. S. P. Chavel, T. C. Strand, A. A. Sawchuk, *Opt. Eng.* **1983**, 22, 687.
- [61] A. R. Tanguay, P. Chavel, T. C. Strand, C. S. Wu, B. H. Soffer, *Opt. Lett.* **1984**, 9, 174.
- [62] K. Knop, *Appl. Opt.* **1978**, 17, 3598.
- [63] H. Murai, T. Gotoh, M. Suzuki, E. Hasegawa, K. Mizoguchi, *F. Devices*, *Proc. SPIE* **1992**, 1665, 230.
- [64] G. P. Bryan-Brown, J. R. Sambles, K. R. Welford, *Liq. Cryst.* **1993**, 13, 615.
- [65] G. P. Bryan-Brown, J. R. Sambles, K. R. Welford, *J. Appl. Phys.* **1993**, 73, 3603.
- [66] J. Prost, P. S. Pershan, *J. Appl. Phys.* **1976**, 47, 2298.
- [67] R. G. Lindquist, J. H. Kulick, G. P. Nordin, J. M. Jarem, S. T. Kowal, M. Friends, T. M. Leslie, *Opt. Lett.* **1994**, 19, 670.
- [68] Z. He, T. Nose, S. Sato, *Jpn. J. Appl. Phys.* **1996**, 35, 3529.
- [69] P. F. McManamon, E. A. Watson, T. A. Dorschner, L. J. Barnes, *Opt. Eng.* **1993**, 32, 2657.
- [70] A. Tanone, Z. Zhang, C.-M. Uang, F. T. S. Yu, *Microwave Opt Technol. Lett.* **1994**, 7, 285.
- [71] P. F. McManamon, T. A. Dorschner, D. L. Corkum, L. J. Friedman, D. S. Hobbs, M. Holz, S. Liberman, H. Q. Nguyen, D. P. Resler, R. C. Sharp, E. A. Watson, *Proc. IEEE* **1996**, 84, 268.
- [72] X. Wang, B. Wang, P. J. Bos, P. F. McManamon, J. J. Pouch, F. A. Miranda, J. E. Anderson, *J. Appl. Phys.* **2005**, 98, 073101.
- [73] W. Klaus, M. Ide, S. Morokawa, M. Tsuchiya, T. Kamiya, *Opt. Commun.* **1997**, 138, 151.
- [74] X. Wang, D. Wilson, R. Muller, P. Maker, D. Psaltis, *Appl. Opt.* **2000**, 39, 6545.

- [75] C. M. Titus, J. R. Kelly, E. C. Gartland, S. V. Shiyanovskii, J. A. Anderson, P. J. Bos, *Opt. Lett.* **2001**, *26*, 1188.
- [76] P. F. McManamon, P. J. Bos, M. J. Escutie, J. Heikenfeld, S. Serati, H. Xie, E. A. Watson, *Proc. IEEE* **2009**, *97*, 1078.
- [77] J. Beeckman, K. Neyts, P. J. M. Vanbrabant, *Opt. Eng.* **2011**, *50*, 081202.
- [78] X. Wang, Q. Tan, Z. Huang, Z. Tang, *Opt. Commun.* **2014**, *313*, 360.
- [79] D. Xu, G. Tan, S.-T. Wu, *Opt. Express* **2015**, *23*, 12274.
- [80] H. Chen, G. Tan, Y. Huang, Y. Weng, T.-H. Choi, T.-H. Yoon, S.-T. Wu, *Sci. Rep.* **2017**, *7*, 39923.
- [81] W. M. Gibbons, P. J. Shannon, S.-T. Sun, B. J. Swetlin, *Nature* **1991**, *351*, 49.
- [82] W. M. Gibbons, S. T. Sun, *Appl. Phys. Lett.* **1994**, *65*, 2542.
- [83] J. Chen, P. J. Bos, H. Vithana, D. L. Johnson, *Appl. Phys. Lett.* **1995**, *67*, 2588.
- [84] C. M. Titus, P. J. Bos, *Appl. Phys. Lett.* **1997**, *71*, 2239.
- [85] V. K. Gupta, N. L. Abbott, *Science* **1997**, *276*, 1533.
- [86] D. Dantsker, J. Kumar, S. K. Tripathy, *J. Appl. Phys.* **2001**, *89*, 4318.
- [87] M. Ibn-Elhaj, M. Schadt, *Nature* **2001**, *410*, 796.
- [88] B. Wen, R. G. Petschek, C. Rosenblatt, *Appl. Opt.* **2002**, *41*, 1246.
- [89] G. P. Crawford, J. N. Eakin, M. D. Radcliffe, A. Callan-Jones, R. A. Pelcovits, *J. Appl. Phys.* **2005**, *98*, 123102.
- [90] C. Provenzano, P. Pagliusi, G. Cipparrone, *Appl. Phys. Lett.* **2006**, *89*, 121105.
- [91] J. Kim, J.-H. Na, S.-D. Lee, *Opt. Express* **2012**, *20*, 3034.
- [92] M. Horina, T. Nose, *Appl. Phys. Lett.* **2012**, *101*, 041107.
- [93] W. Hu, A. Srivastava, F. Xu, J.-T. Sun, X.-W. Lin, H.-Q. Cui, V. Chigrinov, Y.-Q. Lu, *Opt. Express* **2012**, *20*, 5384.
- [94] K. Won, A. Palani, H. Butt, P. J. W. Hands, R. Rajeskharan, Q. Dai, A. A. Khan, G. A. J. Amarantunga, H. J. Coles, T. D. Wilkinson, *Adv. Opt. Mater.* **2013**, *1*, 368.
- [95] C. Provenzano, P. Pagliusi, G. Cipparrone, *Opt. Express* **2007**, *15*, 5872.
- [96] M. N. Miskiewicz, M. J. Escutie, *Opt. Express* **2014**, *22*, 12691.
- [97] I. Nys, J. Beeckman, K. Neyts, *Soft Matter* **2015**, *11*, 7802.
- [98] R. You, D. A. Paterson, J. M. D. Storey, C. T. Imrie, D. K. Yoon, *Liq. Cryst.* **2017**, *44*, 168.
- [99] Y. Wang, G. Singh, D. M. Agra-Kooijman, M. Gao, H. K. Bisoyi, C. Xue, M. R. Fisch, S. Kumar, Q. Li, *CrystEngComm* **2015**, *17*, 2778.
- [100] Y. Wang, Z.-G. Zheng, H. K. Bisoyi, K. G. Gutierrez-Cuevas, L. Wang, R. S. Zola, Q. Li, *Mater. Horiz.* **2016**, *3*, 442.
- [101] I.-C. Khoo, S.-T. Wu, *Optics and Nonlinear Optics of Liquid Crystals*, World Scientific Publishing, London **1993**.
- [102] I. C. Khoo, *Phys. Rev. A* **1982**, *25*, 1040.
- [103] I. C. Khoo, *Phys. Rev. A* **1982**, *25*, 1636.
- [104] S. D. Durbin, S. M. Arakelian, Y. R. Shen, *Opt. Lett.* **1982**, *7*, 145.
- [105] Y. G. Fuh, R. F. Code, G. X. Xu, *J. Appl. Phys.* **1983**, *54*, 6368.
- [106] I. C. Khoo, S. Shepard, *J. Appl. Phys.* **1983**, *54*, 5491.
- [107] I. C. Khoo, R. Normandin, *IEEE J. Quantum Electron.* **1985**, *21*, 329.
- [108] G. Eyring, M. D. Fayer, *J. Chem. Phys.* **1984**, *81*, 4314.
- [109] I. C. Khoo, R. G. Lindquist, R. R. Michael, R. J. Mansfield, P. LoPresti, *J. Appl. Phys.* **1991**, *69*, 3853.
- [110] H. J. Eichler, R. Macdonald, *Phys. Rev. Lett.* **1991**, *67*, 2666.
- [111] A. G. Chen, D. J. Brady, *Opt. Lett.* **1992**, *17*, 441.
- [112] A. G. Chen, D. J. Brady, *Opt. Lett.* **1992**, *17*, 1231.
- [113] V. G. Guimaraes, H. V. Ribeiro, Q. Li, L. R. Evangelista, E. K. Lenzi, R. S. Zola, *Soft Matter* **2015**, *11*, 1658.
- [114] R. S. Zola, F. C. M. Freire, E. K. Lenzi, L. R. Evangelista, G. Barbero, *Chem. Phys. Lett.* **2007**, *438*, 144.
- [115] F. Simoni, O. Francescangeli, Y. Reznikov, S. Slussarenko, *Opt. Lett.* **1997**, *22*, 937.
- [116] S. Slussarenko, O. Francescangeli, F. Simoni, Y. Reznikov, *Appl. Phys. Lett.* **1997**, *71*, 3613.
- [117] S. Y. Huang, S. T. Wu, A. Y. G. Fuh, *Appl. Phys. Lett.* **2006**, *88*, 041104.
- [118] L. De Sio, J. G. Cuennet, A. E. Vasdekis, D. Psaltis, *Appl. Phys. Lett.* **2010**, *96*, 131112.
- [119] L. M. Blinov, R. Barberi, G. Cipparrone, M. Iovane, A. Checco, V. V. Lazarev, S. P. Palto, *Liq. Cryst.* **1999**, *26*, 427.
- [120] H. Ono, N. Kawatsuki, *Appl. Phys. Lett.* **1997**, *71*, 1162.
- [121] H. Ono, N. Kawatsuki, *Jpn. J. Appl. Phys.* **1997**, *36*, 6444.
- [122] G. Cipparrone, A. Mazzulla, F. Simoni, *Opt. Lett.* **1998**, *23*, 1505.
- [123] J. Zhang, V. Ostroverkhov, K. D. Singer, V. Reshetnyak, Y. Reznikov, *Opt. Lett.* **2000**, *25*, 414.
- [124] J. Sun, A. K. Srivastava, L. Wang, V. G. Chigrinov, H. S. Kwok, *Opt. Lett.* **2013**, *38*, 2342.
- [125] E. A. Shteyner, A. K. Srivastava, V. G. Chigrinov, H.-S. Kwok, A. D. Afanasyev, *Soft Matter* **2013**, *9*, 5160.
- [126] L. De Sio, S. Serak, N. Tabiryan, T. Bunning, *J. Mater. Chem. C* **2014**, *2*, 3532.
- [127] J. W. Doane, N. A. Vaz, B. G. Wu, S. Žumer, *Appl. Phys. Lett.* **1986**, *48*, 269.
- [128] R. L. Sutherland, *Proc. SPIE* **1989**, *1080*, 83.
- [129] A. M. Lackner, J. D. Margerum, E. Ramos, K.-C. Lim, *Proc. SPIE* **1989**, *1080*, 53.
- [130] R. L. Sutherland, L. V. Natarajan, V. P. Tondiglia, T. J. Bunning, *Chem. Mater.* **1993**, *5*, 1533.
- [131] R. L. Sutherland, V. P. Tondiglia, L. V. Natarajan, T. J. Bunning, W. W. Adams, *Appl. Phys. Lett.* **1994**, *64*, 1074.
- [132] T. J. Bunning, L. V. Natarajan, V. Tondiglia, R. L. Sutherland, D. L. Vezie, W. W. Adams, *Polymer* **1995**, *36*, 2699.
- [133] M. Jazbiršek, I. D. Olerik, M. Zgonik, A. K. Fontecchio, G. P. Crawford, *J. Appl. Phys.* **2001**, *90*, 3831.
- [134] A. Y.-G. Fuh, M.-S. Tsai, L.-J. Huang, T.-C. Liu, *Appl. Phys. Lett.* **1999**, *74*, 2572.
- [135] A. Y. G. Fuh, M. S. Tsai, C. R. Lee, Y. H. Fan, *Phys. Rev. E* **2000**, *62*, 3702.
- [136] A. Urbas, J. Klosterman, V. Tondiglia, L. Natarajan, R. Sutherland, O. Tsutsumi, T. Ikeda, T. Bunning, *Adv. Mater.* **2004**, *16*, 1453.
- [137] T. J. Bunning, L. V. Natarajan, V. P. Tondiglia, R. L. Sutherland, *Annu. Rev. Mater. Sci.* **2000**, *30*, 83.
- [138] S. Hvilsted, F. Andruzzi, P. S. Ramanujam, *Opt. Lett.* **1992**, *17*, 1234.
- [139] V. P. Tondiglia, L. V. Natarajan, R. L. Sutherland, T. J. Bunning, W. W. Adams, *Opt. Lett.* **1995**, *20*, 1325.
- [140] L. Domash, G. P. Crawford, A. Ashmead, R. Smith, M. Popovich, J. Storey, *Proc. SPIE* **2000**, *4107*, 46.
- [141] A. Y. G. Fuh, M. S. Tsai, C. Y. Huang, T. C. Ko, L. C. Chien, *Opt. Quantum Electron.* **1996**, *28*, 1535.
- [142] Z. Zheng, L. Yao, L. Xuan, D. Shen, *Liq. Cryst.* **2011**, *38*, 17.
- [143] Z. Zheng, L. Zhou, D. Shen, L. Xuan, *Liq. Cryst.* **2012**, *39*, 387.
- [144] M. Liua, Z. Diao, L. Xuan, Z. Peng, L. Yao, Q. Wang, Z. Cao, Y. Liu, *J. Phys. D: Appl. Phys.* **2018**, *51*, 385103.
- [145] V. P. Tondiglia, L. V. Natarajan, R. L. Sutherland, D. Tomlin, T. J. Bunning, *Adv. Mater.* **2002**, *14*, 187.
- [146] L. De Sio, P. F. Lloyd, N. V. Tabiryan, T. J. Bunning, *ACS Appl. Mater. Interfaces* **2018**, *10*, 13107.
- [147] N. C. R. Holme, L. Nikolova, P. S. Ramanujam, S. Hvilsted, *Appl. Phys. Lett.* **1997**, *70*, 1518.
- [148] M. Hasegawa, T. Yamamoto, A. Kanazawa, T. Shiono, T. Ikeda, *Adv. Mater.* **1999**, *11*, 675.
- [149] T. Yamamoto, M. Hasegawa, A. Kanazawa, T. Shiono, T. Ikeda, *J. Mater. Chem.* **2000**, *10*, 337.
- [150] T. Ubukata, T. Seki, K. Ichimura, *Adv. Mater.* **2000**, *12*, 1675.
- [151] Y. Wu, A. Natansohn, P. Rochon, *Macromolecules* **2004**, *37*, 6090.
- [152] X. Tong, G. Wang, A. Yavrian, T. Galstian, Y. Zhao, *Adv. Mater.* **2005**, *17*, 370.
- [153] R. Caputo, L. De Sio, A. Veltri, C. Umeton, A. V. Sukhov, *Opt. Lett.* **2004**, *29*, 1261.
- [154] A. d'Alessandro, R. Asquini, C. Gizzi, R. Caputo, C. Umeton, A. Veltri, A. V. Sukhov, *Opt. Lett.* **2004**, *29*, 1405.

- [155] D. Rudhardt, A. Fernández-Nieves, D. R. Link, D. A. Weitz, *Appl. Phys. Lett.* **2003**, *82*, 2610.
- [156] Y. Sasaki, M. Ueda, K. V. Le, R. Amano, S. Sakane, S. Fujii, F. Araoka, H. Orihara, *Adv. Mater.* **2017**, *29*, 1703054.
- [157] Y. Sasaki, V. S. R. Jampani, C. Tanaka, N. Sakurai, S. Sakane, K. V. Le, F. Araoka, H. Orihara, *Nat. Commun.* **2016**, *7*, 13238.
- [158] S. Nocentini, D. Martella, C. Parmeggiani, S. Zanotto, D. S. Wiersma, *Adv. Opt. Mater.* **2018**, *6*, 1800167.
- [159] A. Jakli, A. Saupe, *One- and Two-Dimensional Fluids*, CRC Press, Boca Raton **2006**.
- [160] N. A. Clark, S. T. Lagerwall, *Ferroelectrics* **1984**, *59*, 25.
- [161] P. Simova, M. Petrov, N. Kirov, *Mol. Cryst. Liq. Cryst.* **1977**, *42*, 295.
- [162] M. Petrov, E. Keskinova, H. Haradikian, B. Katranchev, *J. Optoelectron. Adv. Mater.* **2008**, *11*, 1226.
- [163] P. Simova, M. Petrov, *J. Phys. D: Appl. Phys.* **1977**, *10*, 2439.
- [164] I. C. Khoo, R. Normandin, *J. Appl. Phys.* **1984**, *55*, 1416.
- [165] R. Macdonald, H. J. Eichler, *Appl. Phys. B: Lasers Opt.* **1995**, *60*, 543.
- [166] H. P. Hinov, N. Shonova, K. Avramova, *Mol. Cryst. Liq. Cryst.* **1983**, *97*, 297.
- [167] J. W. Huh, T. H. Choi, J. H. Kim, J. H. Woo, J. H. Seo, T. H. Yoon, *ACS Photonics* **2018**, *5*, 3152.
- [168] R. Termine, B. C. de Simone, A. Golemme, *Appl. Phys. Lett.* **2001**, *78*, 688.
- [169] R. Termine, A. Golemme, *Opt. Lett.* **2001**, *26*, 1001.
- [170] Y. H. Kim, D. K. Yoon, H. S. Jeong, O. D. Lavrentovich, H. T. Jung, *Adv. Funct. Mater.* **2011**, *21*, 610.
- [171] J. P. Michel, E. Lacaze, M. Alba, M. de Boissieu, M. Gailhanou, M. Goldmann, *Phys. Rev. E* **2004**, *70*, 1.
- [172] I. Gryn, E. Lacaze, R. Bartolino, B. Zappone, *Adv. Funct. Mater.* **2015**, *25*, 142.
- [173] H. Yu, K. Okano, A. Shishido, T. Ikeda, K. Kamata, M. Komura, T. Iyoda, *Adv. Mater.* **2005**, *17*, 2184.
- [174] H. Yu, A. Shishido, T. Ikeda, *Appl. Phys. Lett.* **2008**, *92*, 103117.
- [175] H. Yu, Y. Naka, A. Shishido, T. Ikeda, *Macromolecules* **2008**, *41*, 7959.
- [176] X. Zhang, J. Zhang, Y. Sun, H. Yang, H. Yu, *Nanoscale* **2014**, *6*, 3854.
- [177] C. Oldano, *Phys. Rev. Lett.* **1984**, *53*, 2413.
- [178] K. Kondo, F. Kobayashi, H. Takezoe, A. Fukuda, E. Kuze, *Jpn. J. Appl. Phys.* **1980**, *19*, 2293.
- [179] S. E. Broomfield, M. A. A. Neil, E. G. S. Paige, G. G. Yang, *Electron. Lett.* **1992**, *28*, 26.
- [180] K. A. Suresh, P. B. S. Kumar, G. S. Ranganath, *Liq. Cryst.* **1992**, *11*, 73.
- [181] K. A. Suresh, S. Yuvaraji, P. B. S. Kumar, G. S. Ranganath, *Phys. Rev. Lett.* **1994**, *72*, 2863.
- [182] Y. Sah, P. B. S. Kumar, K. A. Suresh, *Phys. Rev. E* **1996**, *54*, 3025.
- [183] B. Lofving, S. Hard, *Opt. Lett.* **1998**, *23*, 1541.
- [184] B. Saad, L. Dinescu, R. P. Lemieux, T. V. Galstyan, *Appl. Phys. Lett.* **1998**, *73*, 279.
- [185] B. Saad, T. V. Galstyan, L. Dinescu, R. P. Lemieux, *Chem. Phys.* **1999**, *245*, 395.
- [186] A. Y.-G. Fuh, T.-S. Mo, *Jpn. J. Appl. Phys.* **2002**, *41*, 2122.
- [187] C. V. Brown, E. E. Kriegis, *Appl. Opt.* **2004**, *43*, 5287.
- [188] M. Talarico, R. Termine, P. Prus, G. Barberio, D. Pucci, M. Ghedini, A. Golemme, *Mol. Cryst. Liq. Cryst.* **2005**, *429*, 65.
- [189] D. V. Wick, T. Martinez, M. V. Wood, J. M. Wilkes, M. T. Gruneisen, V. A. Berenberg, M. V. Vasil'ev, A. P. Onokhov, L. A. Beresnev, *Appl. Opt.* **1999**, *38*, 3798.
- [190] S. Matsumoto, M. Goto, S. Choi, Y. Takanishi, K. Ishikawa, H. Takezoe, G. Kawamura, I. Nishiyama, H. Takada, *J. Appl. Phys.* **2006**, *99*, 113709.
- [191] S. J. Wolzman, J. N. Eakin, G. P. Crawford, S. Žumer, *Opt. Lett.* **2006**, *31*, 3273.
- [192] A. K. Srivastava, W. Hu, V. G. Chigrinov, A. D. Kiselev, Y. Q. Lu, *Appl. Phys. Lett.* **2012**, *101*, 031112.
- [193] V. G. Chigrinov, V. M. Kozenkov, H. S. Kwok, *Photoalignment of Liquid Crystalline Materials: Physics and Applications, Series in Display Technology*, Wiley, Chichester **2008**.
- [194] Y. Ma, J. Sun, A. K. Srivastava, Q. Guo, V. G. Chigrinov, H. S. Kwok, *EPL* **2013**, *102*, 24005.
- [195] Y. Ma, X. Wang, A. K. Srivastava, V. G. Chigrinov, H. S. Kwok, *AIP Adv.* **2016**, *6*, 035207.
- [196] J. Kim, J.-H. Suh, B.-Y. Lee, S.-U. Kim, S.-D. Lee, *Opt. Express* **2015**, *23*, 12619.
- [197] Y. Ma, B. Y. Wei, L. Y. Shi, A. K. Srivastava, V. G. Chigrinov, H. Kwok, W. Hu, Y. Q. Lu, *Opt. Express* **2016**, *24*, 5822.
- [198] K. G. Gutierrez-Cuevas, L. Wang, Z. G. Zheng, H. K. Bisoyi, G. Li, L. S. Tan, R. A. Vaia, Q. Li, *Angew. Chem., Int. Ed.* **2016**, *55*, 13090.
- [199] D.-K. Yang, X.-Y. Huang, Y.-M. Zhu, *Annu. Rev. Mater. Sci.* **1997**, *27*, 117.
- [200] L. Wang, D. Chen, K. G. Gutierrez-Cuevas, H. K. Bisoyi, J. Fan, R. S. Zola, G. Li, A. M. Urbas, T. J. Bunning, D. A. Weitz, Q. Li, *Mater. Horiz.* **2017**, *4*, 1190.
- [201] J. Fan, Y. Li, H. K. Bisoyi, R. S. Zola, D.-K. Yang, T. J. Bunning, D. A. Weitz, Q. Li, *Angew. Chem., Int. Ed.* **2015**, *54*, 2160.
- [202] B. I. Senyuk, I. I. Smalyukh, O. D. Lavrentovich, *Phys. Rev. E* **2006**, *74*, 11712.
- [203] F. Castles, S. M. Morris, D. J. Gardiner, Q. M. Malik, H. J. Coles, *J. Soc. Inf. Disp.* **2010**, *18*, 128.
- [204] A. Ryabchun, A. Bobrovsky, *Adv. Opt. Mater.* **2018**, *6*, 1800335.
- [205] Y. Li, M. Wang, A. Urbas, Q. Li, *J. Mater. Chem. C* **2013**, *1*, 3917.
- [206] Y. Li, A. Urbas, Q. Li, *J. Am. Chem. Soc.* **2012**, *134*, 9573.
- [207] L. Chen, Y. Li, J. Fan, H. K. Bisoyi, D. A. Weitz, Q. Li, *Adv. Opt. Mater.* **2014**, *2*, 845.
- [208] H. Nemati, S. Liu, R. S. Zola, V. P. Tondiglia, K. M. Lee, T. White, T. Bunning, D.-K. Yang, *Soft Matter* **2015**, *11*, 1208.
- [209] W. Huang, C. Yuan, D. Shen, Z. Zheng, *J. Mater. Chem. C* **2017**, *5*, 6923.
- [210] M. Mathews, R. S. Zola, S. Hurley, D.-K. Yang, T. J. White, T. J. Bunning, Q. Li, *J. Am. Chem. Soc.* **2010**, *132*, 18361.
- [211] L. Wang, A. Urbas, K. G. Gutierrez-Cuevas, Q. Li, *Adv. Opt. Mater.* **2016**, *4*, 247.
- [212] W. Hu, H. Zhao, L. Song, Z. Yang, H. Cao, Z. Cheng, Q. Liu, H. Yang, *Adv. Mater.* **2010**, *22*, 468.
- [213] L. Wang, H. Dong, Y. Li, R. Liu, Y.-F. Wang, H. K. Bisoyi, L.-D. Sun, C.-H. Yan, Q. Li, *Adv. Mater.* **2015**, *27*, 2065.
- [214] L. Wang, H. Dong, Y. Li, C. Xue, L. D. Sun, C. H. Yan, Q. Li, *J. Am. Chem. Soc.* **2014**, *136*, 4480.
- [215] H. K. Bisoyi, T. J. Bunning, Q. Li, *Adv. Mater.* **2018**, *30*, 1706512.
- [216] S. N. Fernandes, Y. Geng, S. Vignolini, B. J. Glover, A. C. Trindade, J. P. Canejo, P. L. Almeida, P. Brogueira, M. H. Godinho, *Macromol. Chem. Phys.* **2013**, *214*, 25.
- [217] J. Sun, L. Yu, L. Wang, C. Li, Z. Yang, W. He, C. Zhang, L. Zhang, J. Xiao, X. Yuan, F. Li, H. Yang, *J. Mater. Chem. C* **2017**, *5*, 3678.
- [218] P. Rofouie, D. Pasini, A. D. Rey, *J. Chem. Phys.* **2015**, *143*, 114701.
- [219] H. S. Jeong, Y. H. Kim, J. S. Lee, J. H. Kim, M. Srinivasarao, H. T. Jung, *Adv. Mater.* **2012**, *24*, 381.
- [220] D. Voloschenko, O. D. Lavrentovich, *Opt. Lett.* **2000**, *25*, 317.
- [221] E. Sackmann, S. Meiboom, L. C. Snyder, A. E. Meixner, R. E. Dietz, *J. Am. Chem. Soc.* **1968**, *90*, 3567.
- [222] M. Kawachi, K. Kato, O. Kogure, *Jpn. J. Appl. Phys.* **1978**, *17*, 1245.
- [223] D. Subacius, P. J. Bos, O. D. Lavrentovich, *Appl. Phys. Lett.* **1997**, *71*, 1350.
- [224] D. Subacius, S. V. Shiyanovskii, P. Bos, O. D. Lavrentovich, *Appl. Phys. Lett.* **1997**, *71*, 3323.
- [225] S. V. Shiyanovskii, D. Subacius, D. Voloschenko, P. J. Bos, O. D. Lavrentovich, *Proc. SPIE* **1998**, *3475*, 56.
- [226] B. Senyuk, I. Smalyukh, O. Lavrentovich, *Proc. SPIE* **2005**, *5936*, 59360W.

- [227] O. D. Lavrentovich, S. V. Shiyanovskii, D. Voloschenko, *Proc. SPIE* **1999**, 3787, 149.
- [228] A. Y.-G. Fuh, C.-H. Lin, C.-Y. Huang, *Jpn. J. Appl. Phys.* **2002**, 41, 211.
- [229] J. J. Wu, Y. S. Wu, F. C. Chen, S. H. Chen, *Jpn. J. Appl. Phys.* **2002**, 41, L1318.
- [230] W.-C. Hung, W.-H. Cheng, M.-S. Tsai, Y.-C. Juan, I.-M. Jiang, P. Yeh, *Appl. Phys. Lett.* **2007**, 90, 183115.
- [231] I.-A. Yao, C.-H. Liaw, S.-H. Chen, J.-J. Wu, *J. Appl. Phys.* **2004**, 96, 1760.
- [232] B. I. Senyuk, I. I. Smalyukh, O. D. Lavrentovich, *Opt. Lett.* **2005**, 30, 349.
- [233] R. S. Zola, H. Nematici, Y.-C. Yang, D.-K. Yang, C.-C. Liang, K.-L. Cheng, F. Shiu, C.-C. Tsai, *J. Soc. Inf. Disp.* **2013**, 21, 22.
- [234] S. W. Kang, L. C. Chien, *Appl. Phys. Lett.* **2007**, 90, 221110.
- [235] R. Hamdi, G. Petriashvili, M. P. De Santo, G. Lombardo, R. Barberi, *Mol. Cryst. Liq. Cryst.* **2012**, 553, 97.
- [236] T. Nose, T. Miyanishi, Y. Aizawa, R. Ito, M. Honma, *Jpn. J. Appl. Phys.* **2010**, 49, 051701.
- [237] C.-T. Kuo, R.-H. Chiang, C.-Y. Wang, P.-H. Hsieh, Y.-T. Lin, C.-H. Lin, C.-Y. Huang, *Opt. Express* **2014**, 22, 9759.
- [238] S. N. Lee, L. C. Chien, S. Sprunt, *Appl. Phys. Lett.* **1998**, 72, 885.
- [239] S. W. Kang, S. Sprunt, L. C. Chien, *Appl. Phys. Lett.* **2000**, 76, 3516.
- [240] S. N. Lee, S. Sprunt, L.-C. Chien, *Liq. Cryst.* **2001**, 28, 637.
- [241] X. Xiang, J. Kim, M. J. Escutie, *Sci. Rep.* **2018**, 8, 7202.
- [242] X. Li, X. Du, P. Guo, J. Zhu, W. Ye, Q. Xu, Y. Sun, *Polymers* **2018**, 10, 884.
- [243] K. Kang, L. C. Chien, S. Sprunt, *Liq. Cryst.* **2002**, 29, 9.
- [244] A. Ryabchun, A. Bobrovsky, A. Sobolewska, V. Shibaev, J. Stumpe, *J. Mater. Chem.* **2012**, 22, 6245.
- [245] S. W. Kang, S. Sprunt, L. C. Chien, *Adv. Mater.* **2001**, 13, 1179.
- [246] S. W. Kang, S. Sprunt, L. C. Chien, *Chem. Mater.* **2006**, 18, 4436.
- [247] Y. Zhao, X. Tong, *Adv. Mater.* **2003**, 15, 1431.
- [248] S. M. Morris, D. J. Gardiner, F. Castles, P. J. W. Hands, T. D. Wilkinson, H. J. Coles, *Appl. Phys. Lett.* **2011**, 99, 253502.
- [249] W.-S. Li, L.-L. Ma, L.-L. Gong, S.-S. Li, C. Yang, B. Luo, W. Hu, L.-J. Chen, *Opt. Mater. Express* **2016**, 6, 19.
- [250] S. A. Zolot'ko, V. F. Kitaeva, N. N. Sobolev, V. Y. Fedorovich, N. M. Shtykov, *JETP Lett.* **1986**, 43, 614.
- [251] H. Espinet, M. Lesiecki, M. Ramsburg, *Appl. Phys. Lett.* **1987**, 50, 1924.
- [252] H. J. Eichler, G. Heppke, R. Macdonald, H. Schmid, *Mol. Cryst. Liq. Cryst. Sci. Technol., Sect. A* **1992**, 223, 159.
- [253] U. A. Hrozyk, S. V. Serak, N. V. Tabiryan, T. J. Bunning, A. Force, W. A. Force, *Opt. Express* **2007**, 15, 9273.
- [254] P. J. Ackerman, Z. Qi, Y. Lin, C. W. Twombly, M. J. Laviada, Y. Lansac, I. I. Smalyukh, *Sci. Rep.* **2012**, 2, 414.
- [255] P. J. Ackerman, Z. Qi, I. I. Smalyukh, *Phys. Rev. E* **2012**, 86, 21703.
- [256] A. Varanytsia, G. Posnjak, U. Mur, V. Joshi, K. Darrah, I. Mušević, S. Čopar, L. C. Chien, *Sci. Rep.* **2017**, 7, 16149.
- [257] A. Varanytsia, L.-C. Chien, *Proc. SPIE* **2015**, 9384, 93840J.
- [258] I. Gvozdovskyy, O. Yaroshchuk, M. Serbina, R. Yamaguchi, *Opt. Express* **2012**, 20, 3499.
- [259] A. Ryabchun, A. Bobrovsky, J. Stumpe, V. Shibaev, *Adv. Opt. Mater.* **2015**, 3, 1273.
- [260] L.-L. Ma, W. Duan, M.-J. Tang, L.-J. Chen, X. Liang, Y.-Q. Lu, W. Hu, *Polymers* **2017**, 9, 295.
- [261] L.-L. Ma, S.-S. Li, W.-S. Li, B. L. Wei Ji, Z.-G. Zheng, Z.-P. Cai, V. Chigrinov, Y.-Q. Lu, W. Hu, L.-J. Chen, *Adv. Opt. Mater.* **2015**, 3, 1691.
- [262] T. Sasaki, R. Shimura, K. Kawai, K. Noda, M. Sakamoto, N. Kawatsuki, H. Ono, *Jpn. J. Appl. Phys.* **2016**, 55, 012001.
- [263] P. Chen, L. L. Ma, W. Duan, J. Chen, S. J. Ge, Z. H. Zhu, M. J. Tang, R. Xu, W. Gao, T. Li, W. Hu, Y. Q. Lu, *Adv. Mater.* **2018**, 30, 1705865.
- [264] Z. Zheng, Y. Li, H. K. Bisoyi, L. Wang, T. J. Bunning, Q. Li, *Nature* **2016**, 531, 352.
- [265] P. Sun, Z. Liu, W. Wang, L. Ma, D. Shen, W. Hu, Y. Lu, L. Chen, Z. Zheng, *J. Mater. Chem. C* **2016**, 4, 9325.
- [266] H.-C. Jau, T.-H. Lin, R.-X. Fung, S.-Y. Huang, J.-H. Liu, A. Y.-G. Fuh, *Opt. Express* **2010**, 18, 17498.
- [267] H. C. Jau, T. H. Lin, Y. Y. Chen, C. W. Chen, J. H. Liu, A. Y. G. Fuh, *Appl. Phys. Lett.* **2012**, 100, 131909.
- [268] H.-C. Jau, Y. Li, C.-C. Li, C.-W. Chen, C.-T. Wang, H. K. Bisoyi, T.-H. Lin, T. J. Bunning, Q. Li, *Adv. Opt. Mater.* **2015**, 3, 166.
- [269] J. Sun, R. Lan, Y. Gao, M. Wang, W. Zhang, L. Wang, L. Zhang, Z. Yang, H. Yang, *Adv. Sci.* **2018**, 5, 1700613.
- [270] C.-H. Lin, R.-H. Chiang, S.-H. Liu, C.-T. Kuo, C.-Y. Huang, *Opt. Express* **2012**, 20, 26837.
- [271] R. S. Zola, L. R. Evangelista, Y.-C. Yang, D.-K. Yang, *Phys. Rev. Lett.* **2013**, 110, 57801.
- [272] R. L. Biagio, R. T. De Souza, L. R. Evangelista, R. R. R. de Almeida, R. S. Zola, *J. Mol. Liq.* **2018**, 269, 703.
- [273] T. Sasaki, R. Shimura, K. Kawai, M. Sakamoto, K. Noda, N. Kawatsuki, H. Ono, *Appl. Phys. B* **2016**, 122, 276.
- [274] L. Zhang, L. Wang, U. S. Hiremath, H. K. Bisoyi, G. G. Nair, C. V. Yelamaggad, A. M. Urbas, T. J. Bunning, Q. Li, *Adv. Mater.* **2017**, 29, 1700676.
- [275] A. Y. Fuh, C. Lin, M. Hsieh, C. Huang, *Jpn. J. Appl. Phys.* **2001**, 40, 1334.
- [276] Z. Zheng, R. S. Zola, H. K. Bisoyi, L. Wang, Y. Li, T. J. Bunning, Q. Li, *Adv. Mater.* **2017**, 29, 1701903.
- [277] S. Sen Li, Y. Shen, Z. N. Chang, W. S. Li, Y. C. Xu, X. Y. Fan, L. J. Chen, *Appl. Phys. Lett.* **2017**, 111, 231109.
- [278] H. Jing, Y. Xiang, M. Xu, E. Wang, J. Wang, N. Éber, Á. Buka, *Phys. Rev. Appl.* **2018**, 10, 14028.
- [279] H. Kikuchi, M. Yokota, Y. Hisakado, H. Yang, T. Kajiyama, *Nat. Mater.* **2002**, 1, 64.
- [280] L. Wang, K. G. Gutierrez-Cuevas, H. K. Bisoyi, J. Xiang, G. Singh, R. S. Zola, S. Kumar, O. D. Lavrentovich, A. Urbas, Q. Li, *Chem. Commun.* **2015**, 51, 15039.
- [281] H. J. Coles, M. N. Pivnenko, *Nature* **2005**, 436, 997.
- [282] T. H. Lin, Y. Li, C. T. Wang, H. C. Jau, C. W. Chen, C. C. Li, H. K. Bisoyi, T. J. Bunning, Q. Li, *Adv. Mater.* **2013**, 25, 5050.
- [283] M. Wang, C. Zou, J. Sun, L. Zhang, L. Wang, J. Xiao, F. Li, P. Song, H. Yang, *Adv. Funct. Mater.* **2017**, 27, 1702261.
- [284] W. He, G. Pan, Z. Yang, D. Zhao, C. Niu, W. Huang, X. Yuan, J. Cuo, H. Cao, H. Yang, *Adv. Mater.* **2009**, 21, 2050.
- [285] T.-H. Lin, C.-W. Chen, Q. Li, in *Anisotropic Nanomaterials: Preparation, Properties, Applications* (Ed: Q. Li), Springer, Heidelberg **2015**, Chap. 9.
- [286] J. Yan, Y. Li, S.-T. Wu, *Opt. Lett.* **2011**, 36, 1404.
- [287] I. C. Khoo, T.-H. Lin, *Opt. Lett.* **2012**, 37, 3225.
- [288] Y. Wen, Z. Zheng, H. Wang, D. Shen, *Liq. Cryst.* **2012**, 39, 509.
- [289] J. L. Zhu, J. G. Lu, J. Qiang, E. W. Zhong, Z. C. Ye, Z. He, X. Guo, C. Y. Dong, Y. Su, H. P. D. Shieh, *J. Appl. Phys.* **2012**, 111, 033101.
- [290] G. Zhu, J. Li, X. Lin, H. Wang, W. Hu, Z. Zheng, H. Cui, D. Shen, Y. Lu, *J. Soc. Inf. Disp.* **2012**, 20/6, 341.
- [291] S.-J. Ge, W. Ji, G.-X. Cui, B.-Y. Wei, W. Hu, Y.-Q. Lu, *Opt. Mater. Express* **2014**, 4, 2535.
- [292] J. Yan, Q. Li, K. Hu, *J. Appl. Phys.* **2013**, 114, 3.
- [293] Y. T. Lin, H. C. Jau, T. H. Lin, *J. Appl. Phys.* **2013**, 113, 1.
- [294] J. Yan, Y. Xing, Q. Li, *Opt. Lett.* **2015**, 40, 4520.
- [295] L. Gao, Z.-Z. Zheng, J.-L. Zhu, W.-M. Han, Y.-B. Sun, *Opt. Lett.* **2016**, 41, 3775.
- [296] M. Wahle, K. Brassat, J. Ebel, J. Bürger, J. K. N. Lindner, H.-S. Kitzerow, *Opt. Express* **2017**, 25, 22608.
- [297] Y. Yuan, Y. Li, C. P. Chen, S. Liu, N. Rong, W. Li, X. Li, P. Zhou, J. Lu, R. Liu, Y. Su, *Opt. Express* **2015**, 23, 20007.
- [298] R. Manda, S. Pagidi, S. S. Bhattacharya, H. Yoo, A. Kumar, Y. J. Lim, S. H. Lee, *J. Phys. D: Appl. Phys.* **2018**, 51, 185103.
- [299] Z. G. Zheng, C. L. Yuan, W. Hu, H. K. Bisoyi, M. J. Tang, Z. Liu, P. Z. Sun, W. Q. Yang, X. Q. Wang, D. Shen, Y. Li, F. Ye, Y. Q. Lu, G. Li, Q. Li, *Adv. Mater.* **2017**, 29, 1703165.
- [300] K. Zhou, H. K. Bisoyi, J. Q. Jin, C. L. Yuan, Z. Liu, D. Shen, Y. Q. Lu, Z. G. Zheng, W. Zhang, Q. Li, *Adv. Mater.* **2018**, 30, 1800237.